JGED

JOURNAL OF GRAPHIC ENGINEERING AND DESIGN

Cultural authenticity and purchase intention of Chinese luxury brand logo
Wang Zheng, Louis Ringah Kanyan, Musdi Bin Shanat

Enhancing accessibility of Thai government mobile applications through effective use of typefaces, type sizes, and colour contrast: A technical review
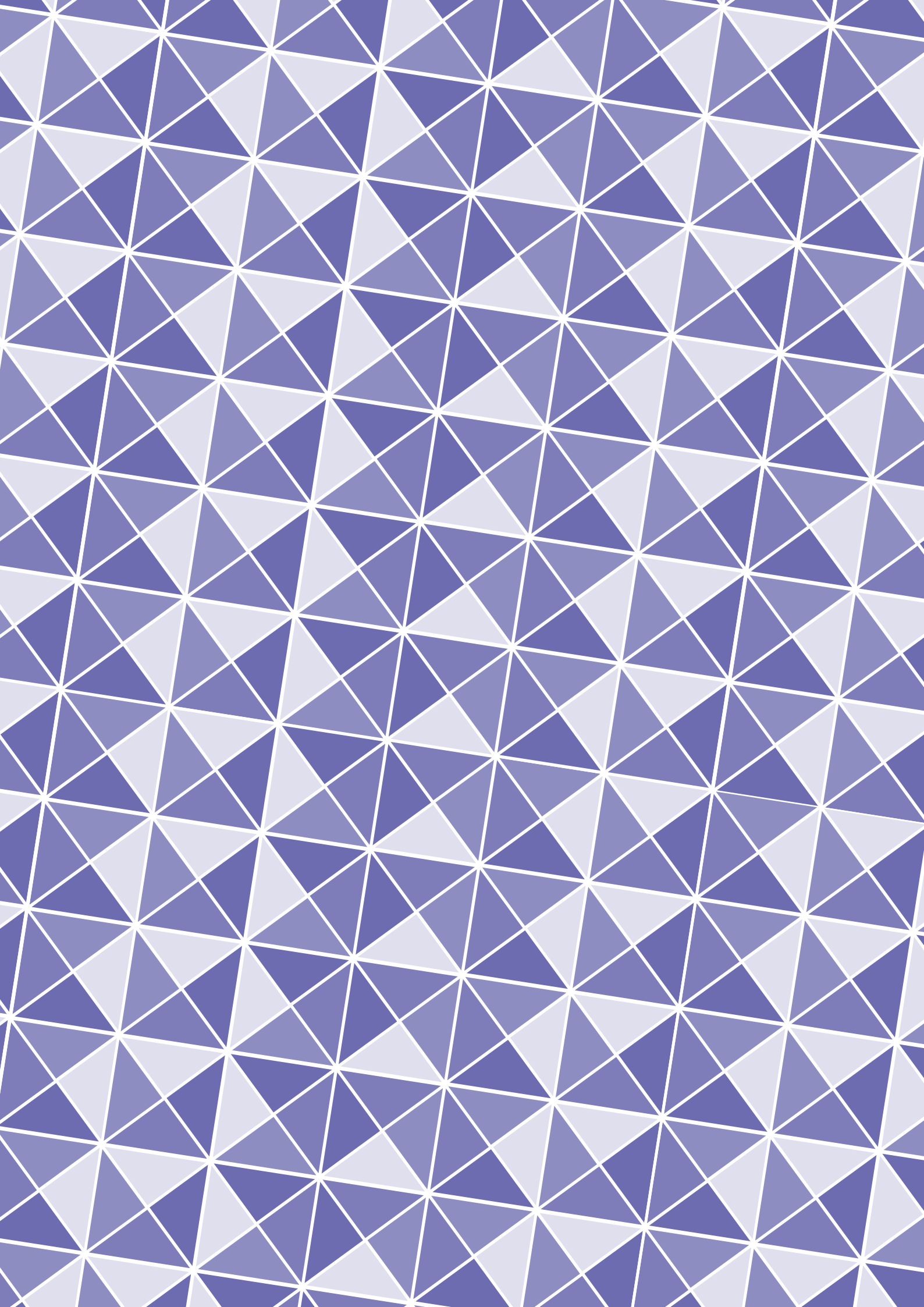Rachapoom Punsongserm, Pittaya Suvakunta

Print quality optimization in screen printing by AM and FM screening using Taguchi's Grey Relational Analysis technique
Soumen Basak, Saritha P.C, Kanai Chandra Paul

Revolution-bump mapping with texture function adjustment according to the geometry of the revolved object
Anouar Ragragui, Adnane Ouazzani Chahdi, Amina Arbah, Hicham El Moubtahij, Akram Halli, Khalid Satori

JGED

JOURNAL OF GRAPHIC
ENGINEERING AND DESIGN

1/2025

Volume 16, Number 1, March 2025.

Contents

Cultural authenticity and purchase intention of Chinese luxury brand logo

ABSTRACT

Chinese domestic luxury brands (CDLBs) increase in both sales and attention in academic research, due to rise of inconspicuousness consumption. However, there is little research on how cultural authenticity in logo influences on purchase intention of CDLBs. Based on signaling theory and power distance belief, this paper investigates this research gap by taking the cultural authenticity as signalling, inconspicuousness and brand trust as evaluation, and purchase intention as outcome. The study also examines the mediating effect of power distance belief between the inconspicuousness and purchase intention. Across three experiments, the researchers collected survey data from 210 individuals who lived in Beijing, Shanghai, Guangzhou, Shenzhen and Hangzhou, which are the cities which are ranked as highest luxury consumption cities in China. According to the findings of the study, the impact of cultural authenticity in logo on purchase intention is significant, and this impact is observed both directly and indirectly through the effects of inconspicuousness and brand trust. This study's results offer valuable information on methods to enhance customers' perception of cultural authenticity and increase their intention to purchase for CDLBs.

Wang Zheng (ID)
Louis Ringah Kanyan (ID)
Musdi Bin Shanat (ID)

University Malaysia Sarawak, Faculty of Applied and Creative Arts, Malaysia

Corresponding author:
Wang Zheng
e-mail:
thomas.wang.design@gmail.com

————————

Introduction

In recent years, a confluence of global events has indelibly shaped the contours of foreign capital investment within China. Notable among these transformative events are the far-reaching repercussions of the COVID-19 pandemic and the intricacies of trade regulations, particularly those stemming from the administration of former U.S. President Trump. These multifaceted dynamics have precipitated a discernible decline in foreign capital infusion, ushering in a period marked by a perceptible deceleration of the once-dominant paradigm of "globalization" (Liu et al., 2021).

This evolving global landscape has not only exerted profound effects on economic dimensions but has also wrought consequential shifts in consumer behavior and preferences, notably within the Asian market, with China

standing as a focal point. Within this narrative, the erstwhile juggernauts of the global luxury market—Gucci, Burberry, Chanel, and the like—have grappled with the challenge of maintaining their market share, while local brands in the Asian context have experienced a pronounced ascendance, an observation documented by Gupta & Wright (2019).

This transformative landscape extends its influence into the realm of China's luxury market, renowned for its voracious appetite for opulent consumption, particularly in the domain of Western luxury brands.

However, a noteworthy transformation is underway as of late, where Chinese domestic luxury brands (CDLBs) such as Shanghai Tang, Shang Xia, and MaoGeping have emerged as notable contenders. These brands have captured the discerning gaze of Chinese consumers,

embarking on a trajectory marked by surging sales and the burnished glow of an enhanced brand reputation (Wu et al., 2017).

The ascent of CDLBs has aroused considerable academic curiosity, resulting in numerous inquiries into the motivations behind the shifting purchasing behaviors of Chinese consumers. Central to this transformation is the concept of cultural authenticity, a defining factor influencing consumer choices between local and Western luxury brands. Cultural authenticity embodies distinctive cultural elements that bear the imprints of integrity and aesthetic grace, emanating from a specific culture. It demands exclusive cultural elements from a particular origin, aligning with the cultural values and aesthetic sensibilities of discerning consumers. In the hands of brand custodians, this concept assumes the role of a venerated vessel, encapsulating brand authenticity (Beverland, 2005; Napoli, Dickinson-Delaporte & Beverland, 2016).

While a multitude of studies have scrutinized the impact of various factors, such as size, shape, color, and typeface, on brand logos (Zheng, Shanat & Kanyan, 2022; Jiang, Gao & Shi, 2016), the intricate relationship between cultural authenticity and brand logos has remained a relatively underexplored terrain. Examination of Chinese cultural elements into logo design and its intricate dance with purchase intention unveiled a compelling narrative of positivity, illustrating the symbiotic relationship between the incorporation of Chinese traditional elements in brand logos and the fertile ground of purchase intention.

Nonetheless, it is essential to acknowledge that this prior scholarly exploration primarily centered on global luxury brands, leaving a research gap concerning the nexus between cultural authenticity and purchase intention in the distinctive context of CDLBs.

In this study, the researcher invokes the signaling theory by Spence (2002) as our theoretical underpinning, a construct that invites us to delve into the intricate realm of signals that shape consumer perceptions. While the original theory predominantly probes the realm of perception, a more expansive perspective, as illuminated by Mavlanova, Benbunan-Fich & Koufaris (2012), recognizes that brands profoundly influence the entirety of the consumer experience. This expanded view posits that individuals cultivate perceptions of brand authenticity based on cultural elements or heritage (Morhart et al., 2015), with consumption intention being guided by the perceived authenticity of the brand and the evocation of nostalgic experiences (Song & Kim, 2022).

Thus, this study extends this theory, scrutinizing the complex interplay between cultural authenticity, inconspicuousness, brand trust, and power distance belief, all of which significantly influence purchase intention.

Inconspicuousness, a hallmark of CDLBs, conveys luxury with subtlety, eschewing ostentation in favor of nuanced design elements (Kapferer, 2015). Yet, within academic circles, a gap persists—a paucity of understanding concerning the impact of CDLBs' brand logos on inconspicuousness and purchase intention.

To navigate this academic terrain, the researcher harness the prism of power distance belief (PDB), a facet of personal values stemming from the broader construct of power distance (Hofstede, 2001). PDB encapsulates individual expectations and acceptance of the asymmetries that underpin social interactions (Oyserman, 2006). It is a concept that has played a pivotal role in shaping beliefs and values, particularly within the domain of luxury consumption. Previous investigations have unveiled the notion that consumers characterized by low PDB exhibit a greater inclination toward embracing inconspicuous luxury items, as evidenced in the research of Jiang, Gao & Shi (2021). In this study, the researcher position PDB as a mediating factor, a bridge that connects the realms of inconspicuous consumption and purchase intention.

Furthermore, our study scrutinizes the role of brand trust in relation to the cultural authenticity embedded within CDLBs' logos. Trust, akin to an intangible thread, weaves the bonds of consumer-brand relationships, a concept that has gained prominence in branding literature since the late 1980s, particularly in the context of relationship marketing (Lantieri & Chiagouris, 2009). While prior research has illuminated the positive correlation between brand trust and purchase intention (Delgado-Ballester, 2004), there remains a dearth of studies explicitly examining the interplay of cultural authenticity within the ambit of CDLBs.

In light of the preceding literature and the research revelations hitherto expounded, our study embarks on a mission to unearth the intricate relationship between cultural authenticity and purchase intention within the realm of CDLBs. In the pursuit of this noble objective, the researcher meticulously dissect the profound impact of cultural authenticity on the domains of inconspicuousness and brand trust, weaving an academic tapestry of enlightenment. The researcher offers twofold contributions to the academic arena.

Firstly, it refines its focus, zeroing in on the intricate domain of cultural authenticity within CDLBs' logos, thereby extending the applicability of the signaling theory and shedding light on its relevance to purchase intention. In doing so, it seeks to empower brand custodians and future scholars with insights into the intricate dance between cultural authenticity and consumer intent. Secondly, it endeavors to infuse new vitality into the exploration of cultural elements' sway over consumer behavior. By untangling the enigmatic relationships between cultural authenticity,

inconspicuousness, brand trust, and power distance belief, our study aspires to mend the fragmented quilt of research and create new vistas of inquiry.

Literature Review and Hypothesis Development

CDLBs, and Cultural Authenticity (CA)

The idea of luxury originated from the Latin word "luxuria", meaning "extras of life" (Danziger, 2005). These extra or non-essential goods or services contribute to a luxurious lifestyle by offering excessive comfort or convenience beyond basic necessities. Brand researchers often identify "luxury" as the highest echelon of prestigious brand categories (Vigneron & Johnson, 2004). The definition of "Chinese Domestic Luxury Brands" or CDLBs is the it must originate in China, and its headquarter is also located in China, as well as the major managerial members should be Chinese (i.e., CEO, Chief Designer, the founder).

A brand must first be successful and recognized in its home market before it can expand internationally. If it fails to appeal to domestic consumers, it will have difficulty gaining traction abroad. The two successful examples of CDLBs are Shanghai Tang and Shang Xia, which there are extensive researches upon the two brands already (Guu & Huang, 2014; Heine & Gutsatz, 2015; Heine & Phan, 2013; Zhiyan, Borgerson & Schroeder, 2013). One factor that contributes to their success is fusing Chinese traditional culture into their brand and product design, showing their cultural authenticity (Heine & Gutsatz, 2015; Schroeder, Borgerson & Wu, 2015). The concept of authenticity is a complex one that encompasses multiple dimensions such as philosophical, psychological, and spiritual. Authenticity involves determining what is real and what is fake and can be defined as the genuineness, reality, or truth of something, as stated by Kennick (1985). Ram, Björk & Weidenfeld (2016) further explored the idea of authenticity, acknowledging its multi-faceted nature. For instance, Shanghai Tang incorporates Chinese elements in a refined manner. The brand has successfully captured the essence of China's sophistication, charm, cultural history, and liveliness (Shanghai Tang, 2010).

Culture plays a significant role in global marketing, and it's widely acknowledged that cultural background influences consumer behavior. (Steenkamp, 2019). There's general agreement that culture and cultural meanings serve as resources for branding processes and practices, and these cultural resources can be leveraged for effective brand development (Balmer, 2013; Allen, Fournier & Miller, 2008). Cultural authenticity, unlike brand authenticity, it is referring to how true to its culture (Beverland & Farrelly, 2010).

In this research, cultural authenticity of a brand is defined as the customer's perspective on the genuineness and veracity of the brand's cultural heritage, as it pertains to its origin. Given the fact that different consumers might perceive the message differently, it is necessary for the brand to determine the right audience in the right place. Using traditional cultural elements in branding can evoke a sense of shared identity and authenticity among members of a particular cultural group. This can be both convincing and credible on a cultural level (Ko & Lee, 2011). Using Shanghai Tang as an example, the value proposition of Chinese cultural heritage is integrated into its entire brand management process, including brand identity (logo and name), product development, and brand communications (Ko & Lee, 2011). As for Shang Xia, the notion of reviving Chinese traditional craftsmanship as core idea of the brand, as well as shown on entire brand visual, product and the stores (Schroeder, Borgerson & Wu, 2014). Therefore, incorporating of Chinese traditional elements and cultural heritage can be used as a tool that forms cultural authenticity and strengthen the competitiveness (Urde, Greyser & Balmer, 2007).

CDLBs' logo and CA

Due to the impact of brand logos on brand communication, researchers have placed a great emphasis on the visual design aspects of logo marks, particularly when it comes to the success of imply western culture in the logo (Henderson et al., 2003). The brand logo not only conveys the brand's core values, mission, and messages, but also reflects its cultural heritage. This makes the logo a significant factor in shaping consumers' perceptions of the brand (Salciuviene et al., 2010; Yorkston & Menon, 2004). For instance, the brand name "Shanghai Tang" is composed of two words which hold specific significance. By incorporating part of the founder's name, the brand name suggests an air of authenticity (Paulicelli & Clark, 2008). Therefore, logos often time utilized to establish desired brand associations (van Riel & van den Ban, 2001). Brand logo design can be comprised with logotype and mark (Southworth, 2019). The definition of logotype described as the name written in a unique typeface without any additional decorative elements (Doyle & Bottomley, 2006).

Pervious researches states that the use of language in the brand logotype is suggested as a way to communicate the brand's cultural authenticity (Larsen et al., 2002; Marian & Neisser, 2000). Thus, some CDLBs might have both English and Chinese characters in their logotype (i.e., Shanghai Tang), whereas other might only include English characters (i.e., Shang Xia) or Chinese characters (i.e., Maotai). The study conduct by Southworth (2019) suggests that the English characters alone might be a better choice for the brands that indicates western culture, however, the combination

of using both English and Chinese in the logotype has more positive impact on the cultural authenticity.

The brand mark, like the brand logo, is a powerful tool for communicating a brand's cultural authenticity. By incorporating visual elements that are specific to a brand's cultural heritage, the brand mark can create a strong sense of identity and establish credibility with customers (Safeer et al., 2022; Southworth, 2019). Committing to a specific visual or design style plays a crucial role in establishing cultural authenticity, Southworth (2019) in his study further proves that the cultural design elements in brand mark can have the positive influence on brand cultural authenticity, especially for Asian (i.e., Chinese) brands. The use of symbols and communication that embodies Chinese cultural elements has the potential to not only reflect the essence of China's cultural heritage but also evoke strong cultural associations and emotions in consumers, as stated by Huang, Huang & Wu (2019). The results of Southworth (2019) also indicates that a logo, particularly a logo symbol (mark), can possess a remarkable ability to transmit the cultural authenticity of a brand.

Inconspicuousness in CDLBs

Podoshen, Li & Zhang (2011) explored the phenomenon of Chinese consumers purchasing Western-style luxury goods as a means of showcasing prestige and social status, a behavior that is more prevalent in China and often referred to as conspicuous consumption. However, the once exclusive realm of luxury goods has become increasingly diluted due to the mass market penetration of luxury brands, the rise of nouveaux riche consumers engaging in conspicuous consumption, and the abundance of high-quality counterfeit products. This shift has caused a reorientation in the preferences of the elite, upper class consumers, who tend to shy away from overt status symbols and opt for more understated brands that rely on subtle design cues to communicate their prestige (Han, Nunes & Dreze, 2010). This means that inconspicuous luxury brands are characterized by having a low level of visual visibility, using subtle or discreet design elements, and avoiding any overt display of the wealth or social status of the consumers (Wu et al., 2017).

Over recent years, many researches start to pay attention of the rise of inconspicuousness in luxury purchasing (Wu et al., 2017). Based on the literal meaning, the "Inconspicuous consumption" has referred to the routine consumption of 'ordinary' goods and service.

Nevertheless, Berger & Ward (2010) found that some consumers avoid products with clear brand markings and instead use subtle signals only noticeable to those with the right knowledge. Inconspicuous consumption explained as not publicly display the social status and big logo (Berger & Ward, 2010).

These inconspicuous consumers try to stand out from the crowd by using these secret markers and reject flashy status symbols.

Chinese luxury brands that incorporate traditional and historical Chinese culture are becoming popular and gaining market share. These locally grown brands are attracting attention and interest (Heine & Gutsatz, 2015; Schroeder, Borgerson & Wu, 2015). Moreover, some studies also suggest that traditional cultural elements have potential positive correlation with inconspicuousness (Eckhardt, Belk & Wilson, 2015; Wu et al., 2017).

Cultural authenticity, as nonfinancial social assets, also possessed by the consumer in the particular cultural domain (Thornton, 1996). The consumption of historical and traditional elements in products and branding campaigns has the ability to evoke nostalgia and a feeling of being connected to an authentic past, which can lead to a sacred and mythic response (Zhou et al., 2013). Furthermore, in some collectivist societies, like China, nostalgia is the importance of relationships with others compare to the individualistic societies like the US. The study conducted by Wu et al. (2017) also suggests the positive correlation between Chinese cultural authenticity in brand design can induce inconspicuousness among Chinese consumers.

Wu (2022) also explored the process of building an inconspicuous Chinese luxury brand, which one of his suggestions is to exhibit authentic culture. In line with above discussion, the researcher develops the following hypothesis:

H1: The cultural authenticity has positive impact on inconspicuousness in CDLBs

Inconspicuousness and purchase intention in CDLBs

Previous studies mainly focused on the conspicuous luxury purchase intention. Based on the signaling theory, people purchase luxury to show their taste, wealth as well as their social status (Hennigs et al., 2012; Janssen, Vanhamme & Leblanc, 2017; Ko, 2020; Schroeder, Borgerson & Wu, 2015).

However, the trend towards inconspicuous luxury consumption can be attributed to the decline of traditional luxury goods as an indicator of wealth, a growing preference for subtlety over ostentation, and a heightened desire for sophistication and recognition from members of one's social group (Eckhardt, Belk & Wilson, 2015). Generally speaking, many young, wealthy consumer tend to hide their social status, and facilitating social equality by conducting inconspicuous luxury items (Jiang, Gao & Shi, 2021).

According to Berger & Ward (2010), individuals who possess a significant amount of cultural capital, tend to gravitate towards luxury brands that are subtle and have low visibility. The reason being that these types of luxury brands use discreet signals in their design and are only noticeable to those within the same group who have the necessary knowledge and understanding to recognize them. In line with above discussion, the researcher develops the following hypothesis:

H2a: Inconspicuousness has positive impact on purchase intention in CDLBs

PDB used as a common theory to predict and explain the consumption behaviour in luxury world (Jiang, Gao & Shi, 2021), as well as the general consumption. It reflects an individual's perspective on status differences, making it a significant factor in determining luxury consumption. Researches have shown that consumers with differing levels of PDB have distinct views towards consumption. The concept of PDB highlights the attitude towards status differences, making it a crucial factor in determining luxury consumption patterns. Studies have started to distinguish between inconspicuous and conspicuous luxury consumption, and are now exploring the reasons behind inconspicuous luxury consumption (Berger & Ward, 2010; Han, Nunes & Dreze, 2010).

Furthermore, the previous study suggests that the consumer hold with high power distance belief will more likely buying conspicuous luxury products. On the contrary, the individual holds low power distance belief will have more interest in inconspicuous luxury items (Brun & Castelli, 2013; Gil et al., 2012; Kim et al., 2012; Schade et al., 2016). The mechanism behind it might because the wealthy, low PD individuals tend

to feel uncomfortable to showing their status publicly, and willing to promote social equality by purchasing inconspicuous items (Eckhardt, Belk & Wilson, 2015).

Based on the discussion, the researcher makes the following hypothesis:

H2b: The influence of inconspicuousness on purchase intention is mediated by PDB

CA and Brand Trust (BT) of CDLBs

Cultural authenticity has been repeatedly linked to brand trust (Eggers et al., 2013). Kumar & Steenkamp (2013) recently argued that Asian brands may need to highlight their cultural authenticity to improve consumers' trust. Trust is another important factor for Chinese luxury brands expend domestically as well as globally (Southworth, 2019). Brand trust refers to the confidence a customer has in the brand to deliver what they expect from it. The concept of brand trust plays a crucial role in the success of small-to-medium sized businesses. Eggers et al. (2013) discovered that the authenticity of a brand can lead to an increase in trust, thereby promoting growth across industries.

Napoli et al. (2014) found that consumers who view a brand as culturally authentic also tend to view it as credible, and credibility is the critical factor that construct brand trust (Southworth, 2019).

Based on these findings, the researcher makes the following hypothesis:

H3: Cultural authenticity has positive impact on CDLBs' brand trust
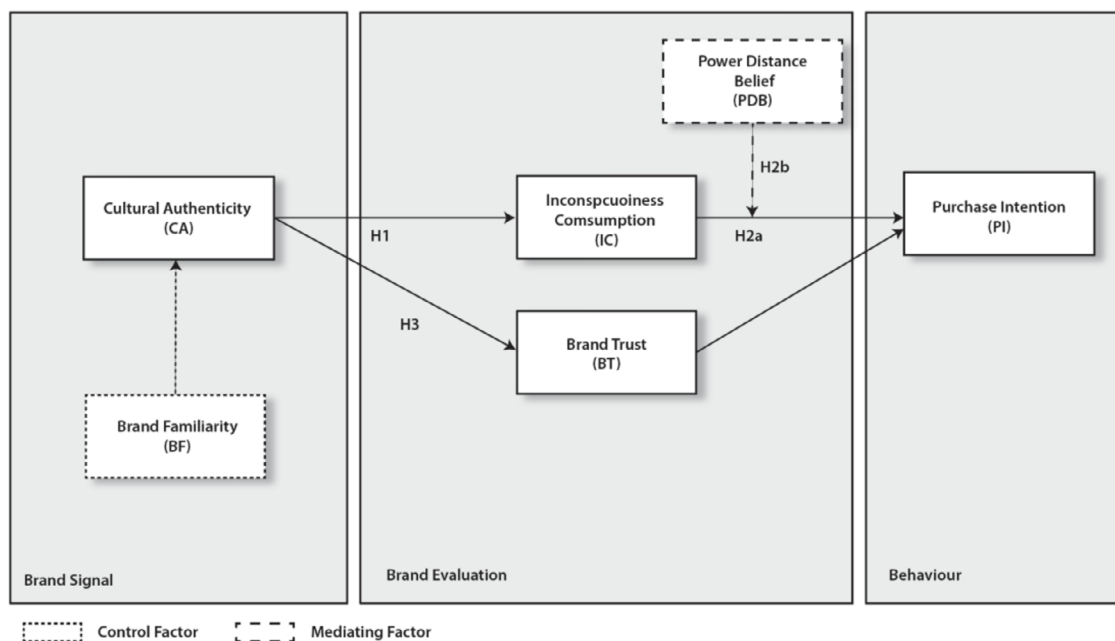
» **Figure 1:** *Theoretical Framework*

Brand familiarity (BF) as a controlling factor

BF is the knowledge that consumers acquire from brands and then retain in their memory through brand association. As a control variable, prior research has recognized that BF can affect purchase intention and brand attitude. Thus, we expect that BF will have an effect on purchase intention and brand trust in cultural authenticity as a controlling factor In CDLBs.

Methodology

Stimulates

To ensure that the results of the study accurately reflect the individuals' perceptions and not be influenced by the product categories, it is important to choose luxury products from a single product category (Lim & Ang, 2008). To ensure accurate results, three studies were conducted using fictitious products and brands to avoid any preconceived notions of the participants. Furthermore, the participants acknowledged that.

To manipulate the cultural authenticity level of the CDLBs' logo, the researcher conducted pre-study interviews with seven professors (3 Males and 4 Females, Average age: 41.6) and 20 graduate students (7 Males and 13 Females, Average age: 19.53) in business administration, who mostly had a research focus on cultural marketing. In order to determine suitable aspects of Chinese culture, the researcher adds the elements that repeatedly been recognized as representation of traditional Chinese cultural elements such as Chinese knot, bamboo as well as calligraphy and Song Ti (Chinese serif typeface). Furthermore, various literature review, semiotics, design, and history literatures also suggest that these elements are typical Chinese elements, therefore, further verify the effectiveness of selected cultural elements.

Realistic representation was achieved by using the logos on T-shirts, handbags, and store signs (Zheng, Shanat & Kanyan, 2022). Additionally, research has shown that brand familiarity has a positive impact on consumer perception of brand logos. To assess this, the researcher conducted surveys on brand familiarity before each study. The studies all applied with the fictional brand name and run the familiarity check, the result shows ("familiar", 1 = very unfamiliar, 7 = very familiar) ($M_{familiarity-Low CA}$ = 3.11, $M_{familiarity-High CA}$ =3.69, t (225) = 0.412, p > 0.1) the fictional brand familiarity does not significant in both low AC and High AC brand logo, therefore, the fictional brand name is valid for the studies. The level of cultural authenticity (CA) of the two logos is also been evaluated by the participants based on the scales 1 to 7 (1 = "not authentic at all", 7 = "very authentic", α = 0.72),

the result shows the significant difference in cultural authenticity ($M_{CA-Low CA}$ = 3.18, $M_{CA-High CA}$ =6.22, F (2, 220) = 0.412, p = 0.025), therefore, the two logos are valid for this study.

Participants

The study used Questionnaire Star, the largest online questionnaire website in China, to distribute and collect questionnaires from September to December 2022 in order to ensure effective and complete data collection from participants. 225 questionnaires were collected, but after removing those with conflicting or repeating answers to 8 consecutive questions, only 210 were deemed valid. The respondents are from cities: Shanghai, Hangzhou, Beijing, Guangzhou, Shenzhen. These five cities have been ranked as top 5 cities in luxury consumptions, and having tremendous fan, as well as aesthetic taste of luxury fashion. The gender distribution of participants was fairly balanced, with similar numbers of men and women taking part. The majority of participants were aged between 18 and 35, with an average of 22.79 years old, indicating that they have well-developed aesthetic tastes and values. 69.3% of which are female. The education level of the participants was largely high, with the majority being well-educated. Only 8.1% of participants had overseas experience, which suggests that they have a strong connection to Chinese cultural elements. 70.4% of participants had luxury shopping experience, and 46.2% of the participants heard or shopped CDLB before, therefore, the participants have sufficient knowledge and experience about luxury, as well as Chinese luxury brands. The participants in the study are from families with an annual household income greater than 500,000 CNY, which is considered the Chinese middle class.

Experiment 1

Procedure

In this experiment, the researcher tested whether the cultural authenticity has correlation with inconspicuousness, and the purchase intention as well as mediating effect of power distance. The participants been randomly divided into two groups to view the two logo that displayed on the T-shirt and bag.

Initially, participants were asked to respond to questions related to their belief in power distance, using a Likert scale consisting of five items, ranging from 1 ("strongly disagree") to 5 ("strongly agree"). The questions included statements such as "People in higher positions should make most decisions without consulting people in lower positions," "People in higher positions should not ask the opinions of people in lower positions too frequently," "People in higher positions should avoid social interaction with people in lower positions," "People in lower

positions should not disagree with decisions by people in higher positions," and "People in higher positions should not delegate important tasks to people in lower positions."

Subsequently, the participants been asking about the following questions and rate the 5 points scale Likert chart. Participants were instructed to read an imaginary scenario in which they were shopping for a T-shirt in a luxury store. The scenario was adapted from (Pino et al., 2019). The questions include "How visible is the T-shirt's logo?", anchored at the extreme by "Not visible at all" and "Extremely visible"; "Do you think this logo attracts attention?", anchored at the extreme by "Not at all" and "attract a lot attention"; "The logo on the shirt is perceived with privilege?" anchored at the extreme by "Not at all" and "a lot of privilege"; "The logo on the shirt is perceived with social status?", anchored at the extreme by "Not at all" and "a lot of social status"; finally, the direct question been ask "How conspicuous the logo is?", anchored at the extreme by "Not conspicuous" and "really conspicuous".

Result and discussion

An ANOVA test reveals the main effect of cultural authenticity in CDLB's logo and its correlation with conspicuousness. The result ($M_{Conspicuousness-low\ CA}$ =2.32, $M_{Conspicuousness-high\ CA}$ = 3.44, $F_{(1,192)}$ = 7.33, $p < 0.014$, see Figure 2) shows the significant difference in high and low cultural authenticity, means the positive correlation with conspicuousness. The result supports the H1, the higher cultural authenticity in CDLBs' logo, the less conspicuousness.

Level of Conspicuousness by Cultural Authenticity of CDLB's Logo

ANOVA results: F(1, 192) = 7.33, p < .014

» **Figure 2:** *Experiment 1 result*

Experiment 2

Procedure

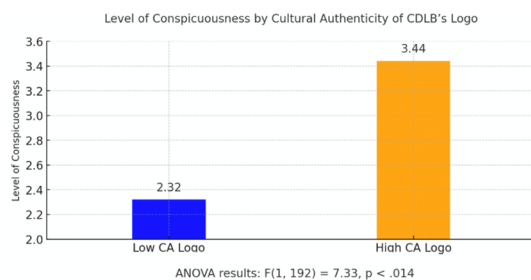Based on the experiment 1, the experiment 2 examines the conspicuousness and purchase intention, meanwhile, examining the mediating effect of power distance belief. Initially, participants were asked to respond to questions related to their belief in power distance, using a five-item Likert scale that ranged from 1 ("strongly disagree") to 5 ("strongly agree"). The questions used to measure belief in power distance consisted of five items, which were presented using a Likert scale ranging from 1 ("strongly

disagree") to 5 ("strongly agree"). These items included statements such as "People in higher positions should make most decisions without consulting people in lower positions," "People in higher positions should not ask the opinions of people in lower positions too frequently," "People in higher positions should avoid social interaction with people in lower positions," "People in lower positions should not disagree with decisions made by people in higher positions," and "People in higher positions should not delegate important tasks to people in lower positions."

Additionally, participants' purchase intention was measured using three items, including "I would purchase one of the wallets in the store," "I would consider buying a T-shirt from this store," and "The probability that I would consider buying a T-shirt from this store is high." All items were measured on a five-point Likert scale that ranged from 1 ("strongly disagree") to 5 ("strongly agree") (Deng & Wang, 2020).

Result and discussion

One way ANOVA test reveal the result that inconspicuousness is positively correlated to purchase intention (PI) of CDLBs ($M_{PI-High\ Conspicuousness}$=3.17, $M_{PI-Low\ Conspicuousness}$ = 4.03, $F_{(1,187)}$ = 5.81, $p < 0.03$, see Figure 3). Therefore, the hypothesis H2a is supported.

A mediation analysis was conducted to examine whether power distance mediates the relationship between inconspicuousness and purchase intention of Chinese luxury brands. The results of the regression analyses indicate that there was a significant negative direct effect of inconspicuousness on purchase intention for high power distance consumers (β =-.40, $p < .05$), and a significant positive direct effect for low power distance consumers (β = .60, $p < .001$).

This suggests that high power distance consumers have lower purchase intention when the brand logo is inconspicuous, whereas low power distance consumers have higher purchase intention under the same condition. A bootstrap analysis revealed that the indirect effect of inconspicuousness on purchase intention through power distance was also significant (ab =-.07, 95% CI [-.12,-.03]).

Furthermore, the total effect of inconspicuousness on purchase intention was also significant (c = .20, $p < .05$). However, when power distance was included as a mediator in the model, the direct effect of inconspicuousness on purchase intention for high power distance consumers was further reduced (c' =-.10, $p > .05$), suggesting partial mediation by power distance. Based on the result, H2b hypothesis is also supported.

As per the study results, power distance belief plays a partial mediating role in the association between incon-

spicuousness and purchase intention of Chinese luxury brands. The findings suggest that high power distance consumers show lower purchase intention when the brand logo is inconspicuous, while low power distance consumers exhibit higher purchase intention under the same circumstances.
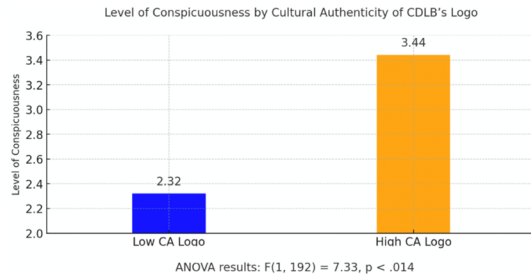
» **Figure 3:** *Experiment 2 main effect*

Experiment 3

Procedure

The experiment 3 examined the cultural authenticity relation brand trust. The experiment 3 also applied with 5 scale Likert questionnaire that ranged from 1 ("strongly disagree") to 5 ("strongly agree").

The questions included "How likely would you be to recommend the brand to your peers and colleagues?" "How likely would you be to discuss about the brand with your peers and colleagues?" and "Do you believe that the brand would be trustworthy?".

Result and discussion

The results indicated a significant positive correlation between cultural authenticity and brand trust, $F(1, 194) = 33.56$, $p < .001$, $\eta^2 = .148$. Post-hoc analyses showed that there were significant differences in the mean scores for brand trust between the low cultural authenticity group ($M = 3.08$, $SD = 0.83$) and the high cultural authenticity group ($M = 4.06$, $SD = 0.71$), $t (194) = 6.73$, $p < .001$, $d = 0.95$.

Participants in the high cultural authenticity group were significantly more likely to recommend the brand ($M = 4.21$, $SD = 0.68$) and discuss it with their peers and colleagues ($M = 3.95$, $SD = 0.78$) compared to those in the low cultural authenticity group (recommend: $M = 3.31$, $SD = 0.76$, $t (194) = 8.15$, $p < .001$, $d = 1.15$; discuss: $M = 2.86$, $SD = 0.89$, $t(194) = 9.17$, $p < .001$, $d = 1.29$).

In summary, the results of this study indicate that Chinese domestic luxury brands that score high on cultural authenticity are viewed as more trustworthy by consumers. These brands are also more likely to be recommended and discussed among peers and colleagues, compared to those with low cultural authenticity scores.

Discussion

The aim of research was to find how the cultural authenticity of CDLB's logo will influence of the purchase intention. And the three experiments were conducted and shown the positive impact of cultural authenticity on purchase intention.

Conclusion

The results of the three experiments confirm the significance of including cultural authenticity in CDLBs' logo design, as evidenced by its positive impact on both purchase intention and brand trust. The findings suggest a direct and positive correlation between cultural authenticity and inconspicuous branding, as well as brand trust. Moreover, the results validate the mediating effect of power distance belief on the relationship between inconspicuous branding and purchase intention. As such, this study offers both practical and theoretical contributions to the field.

Theoretical contribution

This study makes several important theoretical contributions. Firstly, it is the first research to examine the impact of cultural authenticity in visual elements on the purchase intention of Chinese domestic luxury brands. While previous research has focused on the effect of different languages on foreign branding, decision-making, and brand trust (Portal, Abratt & Bendixen, 2019; Southworth, 2019), little attention has been paid to the role of cultural authenticity in consumer behavior research. This study addresses this gap and provides insights into why Chinese consumers, particularly those with low power distance, are more drawn to logos with high cultural authenticity.

Secondly, the study contributes to the existing signaling theory, particularly in the context of marketing and logo design. While previous studies have confirmed the positive impact of cultural authenticity on purchase intention in Chinese time-honored brands like restaurants (Song & Kim, 2022), this study demonstrates that cultural authenticity also influences inconspicuousness and brand trust. The study shows that the signaling theory can effectively explain how consumers perceive cultural authenticity in Chinese domestic luxury fashion brands.

Thirdly, the study sheds light on the mediating effect of power distance belief. The results suggest that power distance belief acts as a mediator and has an indirect effect on purchase intention. Therefore, the study highlights the importance of aligning signals with the characteristics of signalers, such as power distance beliefs. Additionally, the study analyzes conspicuousness in emerging markets and emphasizes that conspicuous brand marking as a marketing tactic remains relevant in such markets.

However, the study also suggests that CDLBs can apply inconspicuous strategies even in emerging markets like China. Thus, the study provides a contextual contribution to the field.

Practical contribution

The study's findings have significant marketing implications for Chinese luxury brand marketers, as they need to tailor their brand marketing communication strategies based on their target market. While previous research has indicated that Chinese domestic luxury brand marketers should incorporate Chinese traditional elements in their clothing and product designs, this study highlights the importance of incorporating these elements into logo design as well. By doing so, brands can enhance brand trust and inconspicuousness, which are critical factors that influence purchase intention.

Moreover, luxury brand marketers need to consider their brand strategy and align it with consumers' power distance beliefs, as suggested by Kim & Zhang (2014). Marketers can use segmentation and profiling techniques to identify and engage with high power distance belief consumers effectively. However, marketers also need to be cautious about applying cultural authenticity in their logos as consumers' power distance beliefs may affect their purchase intention. Higher power distance individuals may have lower purchase intention for inconspicuous luxury brands that incorporate cultural authenticity in their logos.

Therefore, this study highlights the importance of understanding the target market and using a nuanced approach to brand marketing communication strategies to achieve desirable outcomes for Chinese domestic luxury brands. By doing so, marketers can effectively engage with their target market and improve brand image, trust, and purchase intention.

Limitation and future research direction

The study has made progress in advancing the understanding of the concept of cultural authenticity and its impact on purchase intention of CDLBs. The first limitation is the research only consider the Chinese market, but exclude the participants from different countries, i.e., United States, since these counties have different purchasing behaviour. Furthermore, the individuals from the different cultural environment be considered as different signal receivers, therefore, the future study can extend this research, as well as signaling theory by investigating the different cultural background. Secondly, the future study can also examine the visual complexity and how it impacts CDLBs' logo, since various studies suggest that Chinese traditional elements usually come with more complex visual appearance, therefore, visual complexity

might be one of the factors that influence how individual perceives the brand as well as the purchase intention of CDLBs. This research and pervious literature also state the rise of inconspicuous consumption in China, however, the future study can also investigate into specific segment of CDLBs, for example, jewelry, cosmetic or furniture. Moreover, the future study can also examine what segment of CDLBs is having better response when applying cultural authenticity in their brand logo.

Certainly, addressing these pressing queries would be a valuable contribution to the study of luxury goods consumption, cultural authenticity and purchase intention. By investigating these questions, researchers and marketers could gain a deeper understanding of how cultural authenticity affects consumer behavior and purchasing decisions, which could lead to more effective marketing strategies and better outcomes for Chinese domestic luxury brands. The methodology employed in this study is not without limitations. For instance, the experiments conducted did not incorporate diverse Chinese traditional elements in the logotypes.

Therefore, future research endeavors should be designed with a broader range of features to address this aspect. Furthermore, future studies can expand the application of the logo to various scenarios, such as handbags, watches, and store signage. This is particularly relevant as these scenarios have been examined in previous research endeavors. By exploring the logo's effectiveness and impact in diverse contexts, a more comprehensive understanding can be gained as well (Zheng, Shanat & Kanyan, 2022).

Furthermore, future studies could benefit from incorporating a greater diversity of survey locations. Rather than solely focusing on the top five cities, it would be advantageous to include cities that possess significant potential for luxury consumption, such as Chengdu. Additionally, expanding the inclusion criteria to encompass a wider range of age groups would enhance the comprehensiveness of the research.

Funding

References

Allen, C. T., Fournier, S. & Miller, M. (2008) Brands and their meaning makers. In: Haugtvedt, C. P., Herr, P. M. & Kardes, F. R. (eds.) *Handbook of Consumer Psychology*. New Jersey, Lawrence Erlbaum Associates, pp. 781–822.

Balmer, J. M. T. (2013) Corporate heritage, corporate heritage marketing, and total corporate heritage communications: What are they? What of them? *Corporate Communications: An International Journal.* 18 (3), 290–326. Available from: doi: 10.1108/CCIJ-05-2013-0031

Berger, J. & Ward, M. (2010) Subtle signals of inconspicuous consumption. *Journal of Consumer Research*. 37 (4), 555–569. Available from: doi: 10.1086/655445

Beverland, M. B. & Farrelly, F. J. (2010) The quest for authenticity in consumption: Consumers' purposive choice of authentic cues to shape experienced outcomes. *Journal of Consumer Research.* 36 (5), 838-856. Available from: doi: 10.1086/615047

Beverland, M. B. (2005) Crafting brand authenticity: The case of luxury wine. *Journal of Management Studies*. 42 (5), 1003–1029. Available from: doi: 10.1111/j.1467-6486.2005.00530.x

Brun, A. & Castelli, C. (2013) The nature of luxury: A consumer perspective. *International Journal of Retail & Distribution Management*. 41 (11–12), 823–847. Available from: doi: 10.1108/IJRDM-01-2013-0006

Danziger, P. N. (2005) *Let Them Eat the Cake: Marketing Luxury to the Masses As well as the Classes*. Chicago, Dearborn Trade Publishing.

Delgado-Ballester, E. (2004) Applicability of a brand trust scale across product categories: A multigroup invariance analysis. *European Journal of Marketing*. 38 (5/6), 573–592. Available from: doi: 10.1108/03090560410529222

Deng, X. & Wang, L. (2020) The impact of semantic fluency on consumers' aesthetic evaluation in graphic designs with text. *Journal of Contemporary Marketing Science*. 3 (3), 433–446. Available from: doi: 10.1108/jcmars-08-2020-0034

Doyle, J. R. & Bottomley, P. A. (2006) Dressed for the occasion: Font-product congruity in the perception of logotype. *Journal of Consumer Psychology*. 16 (2), 112-123. Available from: doi: 10.1207/s15327663jcp1602_2

Eckhardt, G. M., Belk, R. W. & Wilson, J. A. J. (2015) The Rise of Inconspicuous Consumption. *Journal of Marketing Management.* 31 (7-8), 807-826. Available from: doi: 10.1080/0267257X.2014.989890

Eggers, F., O'Dwyer, M., Kraus, S., Vallaster, C. & Güldenberg, S. (2013) The impact of Brand authenticity on Brand trust and SME growth: A CEO perspective. *Journal of World Business*. 48 (3), 340-348. Available from: doi: 10.1016/j.jwb.2012.07.018

Gil, L. A., Kwon, K. N., Good, L. K. & Johnson, L. W. (2012) Impact of self on attitudes toward luxury brands among teens. *Journal of Business Research.* 65 (10), 1425–1433. Available from: doi: 10.1016/j.jbusres.2011.10.008

Gupta, S. & Wright, O. (7 February 2019) How global brands can respond to local competitors. *Harvard Business Review*. Available from: https://hbr.org/2019/02/how-global-brands-can-respond-to-local-competitors [Accessed 20th August 2024].

Guu, A. & Huang, M. (2014) *A study of consumer perception of a Chinese luxury fashion apparel brand in Sweden*. MSc thesis – partial fulfillment. University of Borås.

Han, J., Nunes, J. & Dreze, X. (2010) Signaling status with luxury goods: The role of brand prominence. *Journal of Marketing*. 74 (4), 15–30. Available from: doi: 10.1509/jmkg.74.4.015

Heine, K. & Gutsatz, M. (2015) Luxury Brand Building in China: Eight Case Studies and Eight Lessons Learned. *Journal of Brand Management*. 22 (3), 229-245. Available from: doi: 10.1057/bm.2014.25

Heine, K. & Phan, M. (2013) A Case Study of Shanghai Tang. *Asia Marketing Journal*. 15 (1). Available from: doi: 10.53728/2765-6500.1507

Henderson, P. W., Cote, J. A., Leong, S. M. & Schmitt, B. (2003) Building strong brands in Asia: Selecting the visual components of image to maximize Brand strength. *International Journal of Research in Marketing*. 20 (4), 297-313. Available from: doi: 10.1016/j.ijresmar.2003.03.001

Hennigs, N., Wiedmann, K. P., Klarmann, C., Strehlau, S., Godey, B., Pederzoli, D., Neulinger, A., Dave, K., Aiello, G., Donvito, R., Taro, K., Táborecká-Petrovičová, J., Santos, C. R., Jung, J. & Oh, H. (2012) What is the Value of Luxury? A Cross-Cultural Consumer Perspective. *Psychology and Marketing*. 29 (12), 1018-1034. Available from: doi: 10.1002/mar.20583

Hofstede, G. (2001) *Culture's consequences: Comparing values, behaviors, institutions and organizations across nations*. Thousand Oaks, Sage Publications.

Huang, W., Huang, Y. F. & Wu, J. F. (2019) Influence and enlightenment of cultural identity on consumption intention of Chinese elements. *Packaging Engineering*. 40 (6), 179-183.

Janssen, C., Vanhamme, J. & Leblanc, S. (2017) Should luxury brands say it out loud? Brand conspicuousness and consumer perceptions of responsible luxury. *Journal of Business Research*. 77, 167–174. Available from: doi: 10.1016/j.jbusres.2016.12.009

Jiang, L., Gao, H. & Shi, L. H. (2021) The effect of power distance beliefs on the inconspicuous versus conspicuous consumption of luxury accessories in China and the USA. *Journal of Marketing Management*. 37 (15-16), 1459–1489. Available from: doi: 10.1080/0267257X.2021.1913214

Kapferer, J.-N. (2015) The future of luxury: Challenges and opportunities. *Journal of Brand Management*. 21, 716-726. Avaiable from: doi: 10.1057/bm.2014.32

Kennick, W. E. (1985) Art and Inauthenticity. *The Journal of Aesthetics and Art Criticism*. 44 (1), 3-12. Available from: doi: 10.2307/430535

Kim, K. H., Ko, E., Xu, B. & Han, Y. (2012) Increasing customer equity of luxury fashion brands through nurturing consumer attitude. *Journal of Business Research*. 65 (10), 1495-1499. Available from: doi: 10.1016/j.jbusres.2011.10.016

Kim, Y. & Zhang, Y. (2014) The Impact of Power-Distance Belief on Consumers' Preference for Status Brands. *Journal of Global Marketing*. 27 (1), 13–29. Available from: doi: 10.1080/08911762.2013.844290

Ko, E. & Lee, S. (2011) Cultural heritage fashion branding in Asia. *Advances in Culture, Tourism and Hospitality Research*. 5, 89-109. Available from: doi: 10.1108/S1871-3173(2011)0000005008

Ko, E. (2020) Luxury brand advertising: theory and practice. *International Journal of Advertising*. 39 (6), 757–760. Available from: doi: 10.1080/02650487.2020.1786916

Kumar, N. & Steenkamp, J.-B. E. M. (2013) *Brand Breakout: How Emerging Market Brands Will Go Global*. New York, Palgrave MacMillan. Available from: doi: 10.1057/9781137276629

Lantieri, T. & Chiagouris, L. (2009) Brand trust in an age without trust: expert opinions. *Journal of Consumer Marketing*. 26 (2), 78–86. Available from: doi: 10.1108/07363760910940447

Larsen, S. F., Schrauf, R. W., Fromholt, P. & Rubin, D. C. (2002) Inner speech and bilingual autobiographical memory: a Polish-Danish cross-cultural study. *Memory*. 10 (1), 45-54. Available from: doi: 10.1080/09658210143000218

Lim, E. A. C. & Ang, S. H. (2008) Hedonic vs utilitarian consumption: a cross-cultural perspective based on cultural conditioning. *Journal of Business Research*. 61 (3), 225-232. Available from: doi: 10.1016/j.jbusres.2007.06.004

Liu, H., Schoefer, K., Fastoso, F. & Tzemou, E. (2021) Perceived brand globalness/localness: a systematic review of the literature and directions for further research. *Journal of International Marketing*. 29 (1), 77-94. Available from: doi: 10.1177/1069031X20973184

Marian, V. & Neisser, U. (2000) Language-dependent recall of auto biographical memories. *Journal of Experimental Psychology: General*. 129 (3), 361-368. Available from: doi: 10.1037//0096-3445.129.3.361

Mavlanova, T., Benbunan-Fich, R. & Koufaris, M. (2012) Signaling theory and information asymmetry in online commerce. *Information & Management*. 49 (5), 240–247. Available from: doi: 10.1016/j.im.2012.05.004

Morhart, F., Malär, L., Guèvremont, A., Girardin, F. & Grohmann, B. (2015) Brand authenticity: An integrative frame work and measurement scale. *Journal of Consumer Psychology*. 25 (2), 200–218. Available from: doi: 10.1016/j.jcps.2014.11.006

Napoli, J., Dickinson, S. J., Beverland, M. B. & Farrelly, F. (2014) Measuring consumer-based Brand authenticity. *Journal of Business Research*. 67 (6), 1090–1098. Available from: doi: 10.1016/j.jbusres.2013.06.001

Napoli, J., Dickinson-Delaporte, S. & Beverland, M. B. (2016) The brand authenticity continuum: strategic approaches for building value. *Journal of Marketing Management*. 32 (13–14), 1201-1229. Available from: doi: 10.1080/0267257X.2016.1145722

Oyserman, D. (2006) High power, low power, and equality: Culture beyond individualism and collectivism. *Journal of Consumer Psychology*. 16 (4), 352–356. Available from: doi: 10.1207/s15327663jcp1604_6

Paulicelli, E. & Clark, H. (2008) *The fabric of cultures-fashion, identity, and globalization*. London, Routledge.

Pino, G., Amatulli, C., Peluso, A., Nataraa, R. & Guido, G. (2019) Brand prominence and social status in luxury consumption: A comparison of emerging and mature markets. *Journal of Retailing and Consumer Services*. 46, 163–172. Available from: doi: 10.1016/j.jretconser.2017.11.006

Podoshen, J. S., Li, L. & Zhang, J. (2011) Materialism and Conspicuous Consumption in China: A Cross-cultural Examination. *International Journal of Consumer Studies*. 35 (1), 17–25. Available from: doi: 10.1111/j.1470-6431.2010.00930.x

Portal, S., Abratt, R. & Bendixen, M. (2019) The role of brand authenticity in developing brand trust. *Journal of Strategic Marketing*. 27 (8), 714–729. Available from: doi: 10.1080/0965254X.2018.1466828

Ram, Y., Björk, P. & Weidenfeld, A. (2016) Authenticity and place attachment of major visitor Attractions. *Tourism Management*. 52, 110-122. Available from: doi: 10.1016/j.tourman.2015.06.010

Safeer, A. A., Chen, Y., Abrar, M., Kumar, N. & Razzaq, A. (2022) Impact of perceived brand localness and globalness on brand authenticity to predict brand attitude: a cross-cultural Asian perspective. *Asia Pacific Journal of Marketing and Logistics*. 34 (7), 1524–1543. Available from: doi: 10.1108/APJML-05-2021-0297

Salciuviene, L., Ghauri, P. N., Streder, R. S. & Mattos, C. (2010) Do Brand names in a foreign language lead to different Brand perceptions?. *Journal of Marketing Management*. 26 (11–12), 1037-1056. Available from: doi: 10.1080/0267257X.2010.508976

Schade, M., Hegner, S., Horstmann, F. & Brinkmann, N. (2016) The impact of attitude functions on luxury brand consumption: An age-based group comparison. *Journal of Business Research*. 69 (1), 314–322. Available from: doi: 10.1016/j.jbusres.2015.08.003

Schroeder, J. E., Borgerson, J. L. & Wu, Z. (2014) A Brand Culture Approach to Brand Literacy: Consumer Co-Creation and Emerging Chinese Luxury Brands. *Advances in Consumer Research*. 42. Available from: doi: 10.2139/ssrn.2511638

Schroeder, J., Borgerson, J. L. & Wu, Z. (2015) A brand culture approach to Chinese cultural heritage brands. *Journal of Brand Management*. 22 (3), 261-279. Available from: doi: 10.1057/bm.2015.12

Shanghai Tang. (2010) *Our History*. Available from: https://www.shanghaitang.com/our-story [Accessed 20th August 2024].

Song, H., & Kim, J. H. (2022) Developing a brand heritage model for time-honoured brands: extending signalling theory. *Current Issues in Tourism*. 25 (10), 1570-1587. Available from: doi: 10.1080/13683500.2021.1926441

Southworth, S. S. (2019) U.S. Consumers' Perception of Asian Brands' Cultural Authenticity and Its Impact on Perceived Quality, Trust, and Patronage Intention. *Journal of International Consumer Marketing*. 31 (4), 287–301. Available from: doi: 10.1080/08961530.2018.1544528

Spence, M. (2002) Signaling in retrospect and the informational structure of markets. *American Economic Review.* 92 (3), 434-459. Available from: doi: 10.1257/00028280260136200

Steenkamp, J. B. (2019) Global versus local consumer culture: theory, measurement, and future research directions. *Journal of International Marketing*. 27 (1), 1-19. Available from: doi: 10.1177/1069031X18811289

Thornton, S. (1996) *Club Cultures: Music, Media, and Subcultural Capital.* Middletown, Wesleyan University Press.

Urde, M., Greyser, S. A. & Balmer, J. M. T. (2007) Corporate brands with a heritage. *Journal of Brand Management*. 15 (1), 4–19. Available from: doi: 10.1057/palgrave.bm.2550106

van Riel, C. B. & van den Ban, A. (2001) The added value of corporate logos- An empirical study. *European Journal of Marketing*. 35 (3/4), 428-440. Available from: doi: 10.1108/03090560110382093

Vigneron, F. & Johnson, L. W. (2004) Measuring perceptions of brand luxury. *Journal of Brand Management*. 11, 484-506. Available from: doi: 10.1057/palgrave.bm.2540194

Wu, Z. (2022) Crafting Inconspicuous Luxury Brands Through Brand Authenticity in China. *Frontiers in Psychology*. 13. Available from: doi: 10.3389/fpsyg.2022.826890

Wu, Z., Luo, J., Schroeder, J. E. & Borgerson, J. L. (2017) Forms of inconspicuous consumption: What drives inconspicuous luxury consumption in China?. *Marketing Theory*. 17 (4), 491–516. Available from: doi: 10.1177/1470593117710983

Yorkston, E. & Menon, G. (2004) A sound idea: Phonetic effects of Brand names on consumer judgments. *Journal of Consumer Research*. 31 (1), 43–51. Available from: doi: 10.1086/383422

Zheng, W., Shanat, M. B. & Kanyan, L. R. (2022) The Effect of Serif and San Serif Typeface of Luxury Fashion Logotype on Chinese Consumers' Brand Perception. *Journal of Business Administration Research*. 11 (2), 9-18. Available from: doi: 10.5430/jbar.v11n2p9

Zhiyan, W., Borgerson, J. & Schroeder, J. (2013) *From Chinese Brand Culture to Global Brands*. London, Palgrave Macmillan, pp. 151–166. Available from: doi: 10.1057/9781137276353_6

Zhou, L, Wang, T., Zhang, Q. & Mou, Y. (2013) Consumer Insecurity and Preference for Nostalgic Products: Evidence from China. *Journal of Business Research*. 66 (12), 2406-2411. Available from: doi: 10.1016/j.jbusres.2013.05.027

Enhancing accessibility of Thai government mobile applications through effective use of typefaces, type sizes, and colour contrast: A technical review

ABSTRACT

This study reviewed the legibility of Thai typefaces, type sizes, and co-lour contrast in mobile applications provided by Thai government offices. Although the Electronic Government Agency (Public Organization) (EGA) has introduced the Government Website Standards and Government Mobile Application Standards, these standards need to cover the design of Thai typographical concerns such as legibility and visibility in great detail. This study aimed to identify typographical issues that may arise in these mobile applications and gain a deeper understanding of the subject matter. The findings of this study could lead to future investigations that provide a better understanding of the topic and contribute to the development of appropriate standards and legislation. We conducted an in-depth analysis of Thai Govern-ment mobile applications on Android focusing on public service areas. Using a smartphone to take screenshots and a vector graphics design program to measure physical type sizes based on the Bo Baimai height measurement, we measured the use of typefaces, type sizes, and colour contrast to ensure accessibility to all users. Additionally, we used a colour contrast analyser application to measure colour contrast and ensure accessibility to all users. Our study provides insights to improve user experiences with these applica-tions and highlights that Thai web and mobile standards lack suitable fonts and sizes. We identified two main categories of Thai typefaces: conventional text fonts and Roman-like Thai fonts. Most Thai mobile applications used letter sizes bigger than 1.2 mm in Bo Baimai height, but some used smaller sizes, which could be worse for reading. The smallest type sizes for body text ranged from 1 to 1.7 mm. Regarding contrast ratios, we found that regular text in selected mobile applications did not meet the Web Content Accessibili-ty Guidelines (WCAG) 2.1 enhanced contrast requirement of a 7:1 ratio. How-ever, some contrast ratios for large text met the 4.5:1 requirement. Some regular text with a 4.5:1 contrast ratio requirement passed the WCAG 2.1 minimum contrast test, whereas some large text with a 3:1 contrast ratio re-quirement also met the criteria. Our study suggests the need for developing better standards and regulations for Thai fonts, sizes, and colour contrasts in mobile applications to ensure accessibility for all users.

Rachapoom Punsongserm [1,3] (iD)
Pittaya Suvakunta [2,3] (iD)

[1] Thammasat University, Faculty of Fine and Applied Arts, Pathum Thani, Thailand
[2] Thammasat University, Bangkok, College of Interdisciplinary Studies, Thailand
[3] Thammasat University, Thammasat University Research Unit in Social Design, Pathum Thani, Thailand

Corresponding author:
Rachapoom Punsongserm
e-mail: pruchapo@tu.ac.th

————————

KEY WORDS

Background

Mobile applications have become indispensable to our lives, offering unprecedented convenience and efficiency. From communication to entertainment, shopping to banking, mobile applications have transformed how we access information and services. These applications have revolutionised the way we communicate, enabling us to stay connected with our loved ones through messaging applications, irrespective of our location. Moreover, mobile applications have significantly impacted education, providing students with interactive and engaging learning experiences that enhance their skills and knowledge.

Mobile applications have also expanded to the public sector, including government services, providing citizens with fast and efficient access to government services and information. Mobile government applications have transformed how citizens interact with their government, empowering them to participate in civic engagement and decision-making processes. These applications have enabled citizens to pay taxes, renew licenses, report issues, access public records, and receive alerts and notifications from their government.

Furthermore, mobile government applications have enhanced the quality of government services, enabling government agencies to respond promptly to citizens' needs and efficiently manage public resources. They have also increased transparency and accountability, allowing citizens to monitor government activities and hold public officials accountable. Mobile government applications have contributed significantly to the digital transformation of government services, making them more efficient, accessible, and citizen-centric.

Although the Thai government has taken steps to encourage universal design policies (Office of the National Economic and Social Development Council, 2016, p.148), more focus still needs to be on inclusive typography principles. Although universal design is a multi-disciplinary approach, architectural and environmental design have been given more attention than other design disciplines. After reviewing guidelines from Thai government departments and organisations and research from experts, including the Department of Packaging and Materials Technology, Faculty of Agro-Industry, Kasetsart University (n.d.), National Office for Empowerment of Persons with Disabilities (n.d.), Office of the Higher Education Commission (2013), Office of Transport and Traffic Policy and Planning (2015), The Association of Siamese Architects Under Royal Patronage (2014) and research by Sawangjaroen, Emphandhu & Kulachol (2017), it was found that there should be more specific principles for inclusive design regarding Thai typography because the current guidelines are outdated and based on old general principles or foreign research.

There is a need to pay more attention to the importance of inclusive design and self-knowledge expansion in this area.

Regarding typography, legibility and readability are crucial factors to consider. After all, only some have perfect eyesight, whether they wear glasses or not. This is why typographers must consider reading efficacy when choosing letterforms or typefaces. The legibility of a font can significantly affect how easy it is to read (Noel, 2015; Slattery & Rayners, 2009), which is why it is so important to invest time and resources into the development of typography in every language.

Unfortunately, the legibility of fonts has not been extensively researched in Thailand, which poses a challenge for visually impaired individuals and the ageing population. More data is needed to recommend optimal Thai letterforms suitable for low-vision or general readers. Although some scientific studies have examined Thai letterforms (Rattanakasamsuk, 2013; Teeravarunyou & Laosirihongthong, 2003; Waleetorncheepsawat et al., 2012), they have yet to discuss or suggest design practices for improving legibility. These studies have evaluated which typeface or type size was more legible but have yet to provide in-depth explanations of aspects of letterforms that influence recognition under tested conditions.

When it comes to design, the focus should always be on the people interacting with the product. It is about creating something that looks good and ensuring that it meets the user's needs and elicits a positive response (Frascara, 2015). One crucial aspect of communication design is inclusive typography, which can help visually impaired individuals continue reading even when their visual acuity is low (Ompteda, 2009). By incorporating principles of inclusive typography, designers can create accessible products for a broader range of people.

Awan et al. (2021) have identified several barriers to smartphone application usage, categorised into five distinct categories: sensory function, cognition, motor skills/impairment, mental model, and financial limitation. According to their research, sensory function-related issues, such as small font size, screen size, font type, buttons, and colour contrast, were found to be the most commonly reported barriers to the usability of web and smartphone applications. Awan et al. (2021) also discovered that these sensory function-related issues had the highest critical value among the identified barriers.

Typefaces are an essential aspect of mobile application design. It is an important decision because it guarantees users can easily read the text on their devices. Furthermore, the type sizes are uniform and well-suited throughout the applications, making them simple to navigate. Colour contrast is also a crucial factor to consider when designing mobile applications.

Using contrasting colours guarantees that vital components such as buttons, headings, and text are noticeable on the screen. This enhances usability and ensures that users can rapidly and effortlessly locate the required information.

According to Serra et al. (2015), it is of utmost importance to evaluate the accessibility of mobile applications in e-government and m-government to identify accessibility issues that require immediate attention. Established methods of evaluations in the field of Human-Computer Interaction, such as tests with target users or accessibility audits conducted by experts using heuristics or guidelines, can be employed for performing accessibility evaluations (Serra et al., 2015).

Despite the fact that accessibility audits with guidelines can only address some of the challenges that disabled users may face (Power et al., 2012), they remain valuable in identifying common issues that can be avoided (Serra et al., 2015). The insights gained from these evaluations can help to improve the accessibility of mobile applications, which is crucial for creating inclusive technology.

According to WCAG 2.1 Understanding Docs, in minimum contrast (AA), text (including image of text) has a contrast ratio of at least 4.5:1 for regular-size text and at least 3:1 for large-scale text (at least 18 points/24 pixels or bold and at least 14 points/18.5 pixels) unless the text is purely decorative (World Wide Web Consortium: W3C, 2016a; World Wide Web Consortium: W3C, 2022a; World Wide Web Consortium: W3C, 2023a). For enhanced contrast (AAA), text (including image of text) has a contrast ratio of at least 7:1 for regular-sized text and at least 4.5:1 for large-scale text (at least 18 points/24 pixels or bold and at least 14 points/18.5 pixels) unless the text is purely decorative (World Wide Web Consortium: W3C, 2016b; World Wide Web Consortium: W3C, 2022b; World Wide Web Consortium: W3C, 2023b).

Despite the efforts made by the Electronic Government Agency (Public Organization) (EGA), Thailand has introduced the Government Website Standards (EGA, 2012; EGA, n.d.) and Government Mobile Application Standards (EGA, 2015).

However, these standards need to cover the design of Thai typographical concerns such as legibility and visibility in great detail. Further attention should be given to this aspect to ensure an optimal user experience for Thai readers.

For this reason, the current study aimed to reveal and review issues with Thai typefaces, focusing on typeface classifications, type sizes, and colour contrast used in Thai government mobile applications. This study will contribute to an awareness of the problems that may inspire future studies of the development of Thai government mobile applications based on positive typographic design.

Method

When evaluating the accessibility of mobile applications, two primary methods are generally accepted.

The first method involves assessing the application against a checklist of accessibility guidelines through either manual inspection by accessibility experts (Nielsen, 1993; Nugroho, Santosa & Hartanto, 2022; Serra et al., 2015) or by using automated tools (Ross et al., 2020; Silva, Eler & Fraser, 2018). This method can be complemented by using disability simulation software (Choo, Balan & Lee, 2019). However, it should be noted that such simulations may produce only partially accurate results (Tigwell, 2021).

The second method involves user-centred evaluation, where end-users test the software (Grellmann et al., 2018; Nugroho, Santosa & Hartanto, 2022).

Arias et al. (2022) have proposed an approach that involves examining user reviews to determine the accessibility status of applications. User reviews can be valuable in revealing how accessible the application is perceived to be by end-users.

Eler et al. (2018) identified two approaches to performing mobile accessibility testing: manual testing and automated tools. Manual testing involves meticulously exploring and inspecting the application, as well as checking every user interface component. Google offers two practical tools for this purpose- the UI Automator (Google for Developers, 2024a) and the Accessibility Scanner (Google, 2024; Google Play, 2023). However, the manual approach may need to be more efficient for larger applications or frequent testing. In such cases, developers may rely on tools like Lint (Google for Developers, 2024b), Espresso (Google for Developers, 2024c), and Robolectric (Robolectric, 2023) to partially automate accessibility testing tasks. While Lint can only scrutinise static properties that stem from the source code, testing frameworks such as Espresso and Robolectric can dynamically examine accessibility properties during test execution. Notably, comparable tools exist for iOS, such as Earl-Grey (GitHub, 2024a) and KIF (GitHub, 2024b).

The current study focused on identifying and examining issues regarding Thai typefaces, specifically typeface classifications, type sizes, and colour contrast used in Thai government mobile applications. The study aimed to raise awareness about the problems that might need a more in-depth investigation in future research. To achieve this, simple technical methods were employed to determine type sizes and colour contrast in the Thai government mobile applications. While this approach may require more time and attention to detail than automated tools, it could provide valuable insights that will be useful in addressing the identified issues.

Survey for Thai Government Mobile Applications

The present study focused on the Thai government mobile applications available on Android. We carefully selected a range of applications covering public service areas such as health care, taxes, essential utilities, and more. Our sample of applications was compiled from the offices of the Thai government, and we have provided a detailed overview in Figure 1 and Table 1.

These applications are readily accessible to the public, and we believe they can offer valuable and convenient resources to Thai citizens.

Measurement of Type Sizes on Thai Government Mobile Applications

We took screenshots of each selected mobile application's user interface (UI) using a smartphone (Infinix Zero 5G 2023) to measure the physical type sizes used on Thai government mobile applications.

This smartphone has a resolution of 1080 x 2460 pixels and is displayed on a screen diagonal of 6.78 inches, with a screen width of 2.7300 inches and a screen height of 6.2158 inches. This screen size of 6.78 inches is considered to have a large screen (Samsung, 2024).

We set the font size on the screen display to the largest option. After taking the screenshots, we imported them into Adobe Illustrator 2021. We resized them from 1080 x 2460 pixels to 196.560 x 447.538 pixels so that the sizes of the resized images would conform to the physical screen size of 2.7300 x 6.2158 inches.

Various studies included in this review provided recommendations for font size, with inconsistent use of metric systems. However, the most common metric used was "points." For instance, in their studies, Chatrangsan & Petrie (2019), Darroch et al. (2005), Hou et al. (2020), Kong et al. (2011), Lege et al. (2013), Wang et al. (2009), Yeh (2015), Yeh (2020), and Ziefle (2010) all employed points as their unit of measurement for font size.

Other studies used pixels (Hou et al., 2020; Wang et al., 2009), millimetres (Fujikake et al., 2007; Hasegawa et al., 2009; Hou et al., 2020; Punsongserm, 2019; Punsongserm, 2020; Punsongserm, Sunaga & Ihara, 2017a; Punsongserm, Sunaga & Ihara, 2017b; Punsongserm, Sunaga & Ihara, 2018a; Punsongserm, Sunaga & Ihara, 2018b), or arcminutes of visual angle (Hasegawa et al., 2009; Punsongerm, 2023; Punsongserm & Suvakunta, 2022a; Punsongserm & Suvakunta, 2022b) to indicate font size.

To ensure inclusive communication with a diverse range of readers across various fields, we recommend utilising all metric systems with conversions for font size.

» **Figure 1:** *Examples of selected Thai government mobile applications*

The point size measurement is typically used to determine the font size unit of a typographic design.

However, it is essential to note that different typefaces composed in the same point size can affect the size of the x-height. According to Legge & Bigelow (2011, p.19), measures of x-height provide a convenient metric that is familiar to both typographers and vision researchers.

Similarly, Punsongserm, Sunaga & Ihara (2017a) used Bo Baimai height measurements to define Thai-type sizes in their study. This method provides normalisation by the character's height /บ/ (Bo Baimai) and accurately regulates the equalisation of character heights within any font.

As a result, we have also adopted the Bo Baimai height measurement (Punsongserm, 2019; Punsongserm, 2020; Punsongserm, Sunaga & Ihara, 2017a; Punsongserm, Sunaga & Ihara, 2017b; Punsongserm, Sunaga & Ihara, 2018a; Punsongserm, Sunaga & Ihara, 2018b; Punsongserm & Suvakunta, 2022a; Punsongserm & Suvakunta, 2022b) in millimetres and pixels to measure the physical type sizes used on Thai government mobile applications.

Table 1

List of selected Thai government mobile applications

No.	Application Name	Category	Provider
1	ทางรัฐ (Thang rath) Version 2.5.0	Government Services	Digital Government Development Agency, Thailand (https://play.google.com/store/apps/details?id=th.or.dga.citizenportal)
2	ThaID Version 2.4.0	Government Services	The Bureau of Registration Administration (https://play.google.com/store/apps/details?id=th.go.dopa.bora.dims.ddopa)
3	RDU รู้เรื่องยา Version 1.5.9	Medicine	Digital Government Development Agency, Thailand (https://play.google.com/store/apps/details?id=com.uhosnet)
4	Clicknic Version 3.4.14	Medical Services	Clicknic Institute of Disease Prevention and Control (SorBor-Mor.), Office of Health Promotion Fund (SorSor.) Thammasat University Chalermprakiet Hospital (https://play.google.com/store/apps/details?id=co.clicknic.clicknicandroid)
5	หมอพร้อม (Mor Prom) Version 1.2.1	Medical Services	Ministry of Public Health (https://play.google.com/store/apps/details?id=com.mor.promplus)
6	สมุดสุขภาพผู้สูงอายุ (Bluebook) Version 2.8.2	Health Care	Department of Health (Thailand) (https://play.google.com/store/apps/details?id=com.moph.anamai.bluebook)
7	สมุดสุขภาพ (Smud Sukhaphap) Version 2.0.0	Health Care	Department of Health (Thailand) (https://play.google.com/store/apps/details?id=th.go.moph.anamai.healthbook)
8	MyMo by GSB Version 2.15.0	Finance & Bank	Government Savings Bank (https://play.google.com/store/apps/details?id=com.mobilife.gsb.mymo)
9	เป๋าตัง (Paotang) Version 12.4.1	Finance & Utility	Krungthai Bank PCL. (https://play.google.com/store/apps/details?id=com.ktb.customer.qr)
10	RD Smart Tax Version 3.3.0	Revenue	The Revenue Department (https://play.google.com/store/apps/details?id=com.revenuedepartment.app)
11	ภาษีไปไหน (Phasi Pai Nai) Version 2.3.2	Government Spending	Digital Government Development Agency, Thailand (https://play.google.com/store/apps/details?id=th.or.ega.spending)
12	PDMO Version 2.7.6	Public Debt	Public Debt Management Office (https://play.google.com/store/apps/details?id=com.zealtech.pdmo)
13	PEA Smart Plus Version 3.2.11	Public Utility: Electricity Authority	Provincial Electricity Authority (https://play.google.com/store/apps/details?id=com.esrith.pea_mobile)
14	PWA Plus Life Version 3.5.2	Public Utility: Water Supply	Provincial Waterworks Authority (https://play.google.com/store/apps/details?id=th.co.pwa.pwamobile)

In the field of vision science, Swearer (2018) postulated that visual angle is an essential metric that plays a significant role in indicating the size of visual stimuli without explicitly stating their distance or size. Additionally, the visual angle can be used to express intraocular dimensions, predict the space an image will subtend on the retina, and describe the relative location of separate retinal images. Moreover, the visual angle is employed to specify the size of spatial frequency gratings. The visual angle, as Swearer (2018) explains, originates from incoming light rays at the nodal point of the eye and is dependent on multiple factors, such as the size of the stimulus, its distance from the observer, and whether or not it is viewed in the frontal plane. In a simplified model, the visual angle is formed from the light rays from two points of a viewed object, in height, width, or depth, as they enter the eye and is proportional to the angle projected onto the retina. Consequently, the subtended image's size is determined by the visual angle. When an object is viewed at different distances, it will have different retinal sizes, as similarly sized objects viewed at different distances.

De Valois & De Valois (1988) and O'Shea (1991) discovered that objects of varying sizes can appear to have the same visual angle if they are situated at appropriate distances from the observer. This phenomenon has significant implications for visual perception and must be taken into account when designing and conducting experiments in the field of visual cognition.

According to Swearer (2018), the expression of visual angle subunits is measured in minutes and seconds of arc. A degree is equivalent to 60 arcmin, and an arcmin is equivalent to 60 arcsec. In calculating visual angle (θ), the geometrical formulas are crucial in relating visual angle, size, and distance. These formulas are based on the size of the stimulus object (S0) at a specified viewing distance (D0), among other factors. Additionally, the retinal image size (Si) is dependent on an average image distance (Di) of 17 mm from the lens of the eye to the retina. As stated by Swearer (2018), the calculation for visual angle is expressed as $\theta = 2 \arctan(S0/2D0)$. However, for visual angles smaller than 10°, the calculation can be simplified to $\theta = \arctan(S0/D0)$.

As part of the present study, we have not only conducted measurements of physical sizes (Bo Baimai height) of type sizes across various Thai government mobile applications but have also calculated the visual angles that would be perceived based on these measurements. To maintain consistency and accuracy, we defined the viewing distance as 40 cm, which aligns with the traditional near point for optometric examinations and is a typical reading distance for paper media (Boccardo, 2021).

Figure 2 presents the formula for calculating the visual angle of Thai letterforms, accompanied by a practical example. Assuming that we have to compute the visual angle for Bo Baimai with a height of 1.5 mm and a viewing distance of 40 cm (400 mm), we can apply the specified values in the formula (Step 1). This would lead us to the computation of 2 · arctan(0.001875) (Step 2). The arctan of 0.001875 is equivalent to 0.10742946069325° (Step 3). Consequently, we can discern that the visual angle of Bo Baimai's height of 1.5 mm, viewed from a distance of 40 cm, is 0.2149° (Step 4).

$$\text{Visual Angle} = 2 \cdot \arctan\left(\frac{\frac{\text{Bo Baimai height}}{2}}{\text{Viewing Distance}}\right)$$

$$(1) \qquad 2 \cdot \arctan\left(\frac{\frac{1.5}{2}}{400}\right)$$

$$(2) \qquad 2 \cdot \arctan\left(0.001875\right)$$

$$(3) \qquad 2 \times 0.10742946069325$$

$$(4) \qquad 0.2149$$

» **Figure 2:** *Formula and examples for Thai letterforms' visual angle calculation*

Measurement of Colour Contrast on Thai Government Mobile Applications

Numerous tools are available that can assist in checking colour contrast on digital screens. These applications are readily accessible via web browsers. Prominent examples include the Color Contrast Checker developed by the Institute for Disability Research, Policy, and Practice (WebAIM, 2024), the Contrast Checker by Adobe (Adobe, 2024), and the APCA Contrast Calculator by Myndex Research (Myndex, 2024).

Alternatively, individual contrast checker tools can be installed on Windows and Mac operating systems, such as the Colour Contrast Analyzer (CCA) provided by TPGi (TPGi, 2023). Additionally, mobile contrast checker tools are also accessible. The A11Y: Audit + Color Contrast app by Accessible Resources Ltd (Accessible Resources, 2024) and the Accessibility Scanner app by Google (Google Play, 2023) can be employed for this purpose. These applications mentioned above are designed to comply with the feature compliance indicators for WCAG.

In our current study, we utilised the CCA version 3.2.1 developed by TPGi (TPGi, 2023) to measure the colour contrast of screenshots of selected Thai government mobile applications (as seen in Figure 3). This application is designed to meet the feature compliance indicators for WCAG 2.1 (World Wide Web Consortium: W3C, 2018), which is crucial for ensuring accessibility to all users. As a part of our analysis, we used this application to assess the colour contrast of foregrounds (texts) and backgrounds on selected Thai government mobile applications that were imported into Adobe Illustrator 2021 after the procedure of type size measurement was completed (see the previous topic).

To provide a brief and precise summary of the research conducted, we have incorporated a diagram in Figure 4. This diagram encapsulates an array of activities that were carried out during the study

Results and Discussion

According to Table 1, some Thai government mobile applications are equipped with a feature that prevents users from taking screenshots. After examining the data, we have identified four such applications that offer this protection: ThaID, หมอพร้อม (Mor Prom), MyMo by GSB, and เป๋าตัง (Paotang).

This is an essential feature for those concerned about privacy and security while using these applications. It is reassuring that these applications are taking steps to protect their users this way; however, we could not measure these mobile applications' type sizes and colour contrasts.
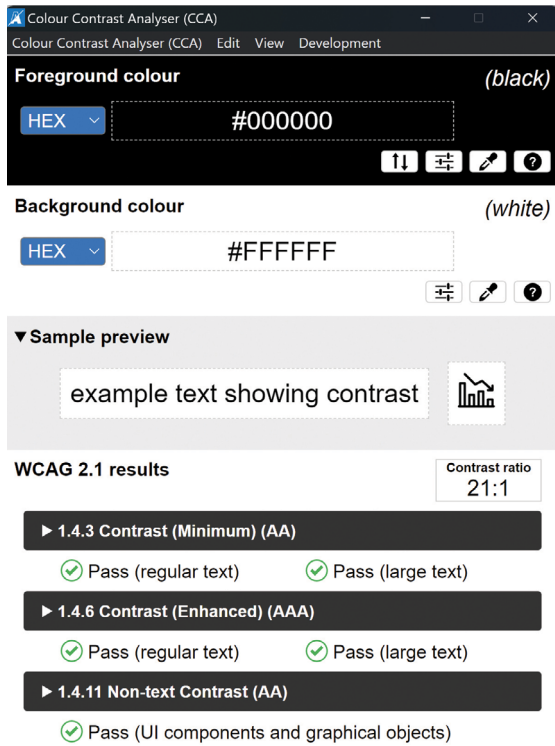
» **Figure 3:** *User interface of CCA version 3.2.1*

Regulations and Standards

In accordance with Strategy 6, Stratagem 6.5 of the Information and Communication Technology Policy Framework 2011–2020, fostering online learning communities and promoting solid social integration is imperative. The EGA has established the Government Mobile Application Standard Version 1.0 to comply with the government's framework.

This standard ensures that mobile application development meets technical standards and requirements, including personal data protection and security protocols (EGA, 2015). However, it is important to note that the Thai Government Mobile Application Standard does not recommend appropriate Thai typefaces and sizes for application users.

Use of Typefaces, Type Sizes, and Colour Contrast on Thai Government Mobile Applications

Typefaces

After conducting our initial survey of Thai government mobile applications, we delved deeper into the fonts used in these applications. Our analysis revealed two main categories of Thai typefaces: Thai conventional text fonts and Roman-like Thai fonts, as depicted in Figure 5. To illustrate our findings further, we compiled a table (Table 2) that showcases the typefaces used in each selected Thai government mobile application.

Table 2 shows that the ทางรัฐ (Thang Rath) application is the only one to have used a Thai conventional text typeface exclusively for words and texts. In contrast, the สมุดสุขภาพผู้สูงอายุ (Bluebook), สมุดสุขภาพ (Smud Sukhaphap), RD Smart Tax, and PEA Smart Plus applications have used Roman-like Thai typefaces. Some other applications have mixed two typeface categories for their words and texts. It is important to note that no regulations or standards in Thailand dictate the proper typeface for screens or mobile devices. However, Thai conventional text fonts are crafted with expert precision, featuring distinct letter elements that make them easily identifiable to readers. These elements, such as the line,
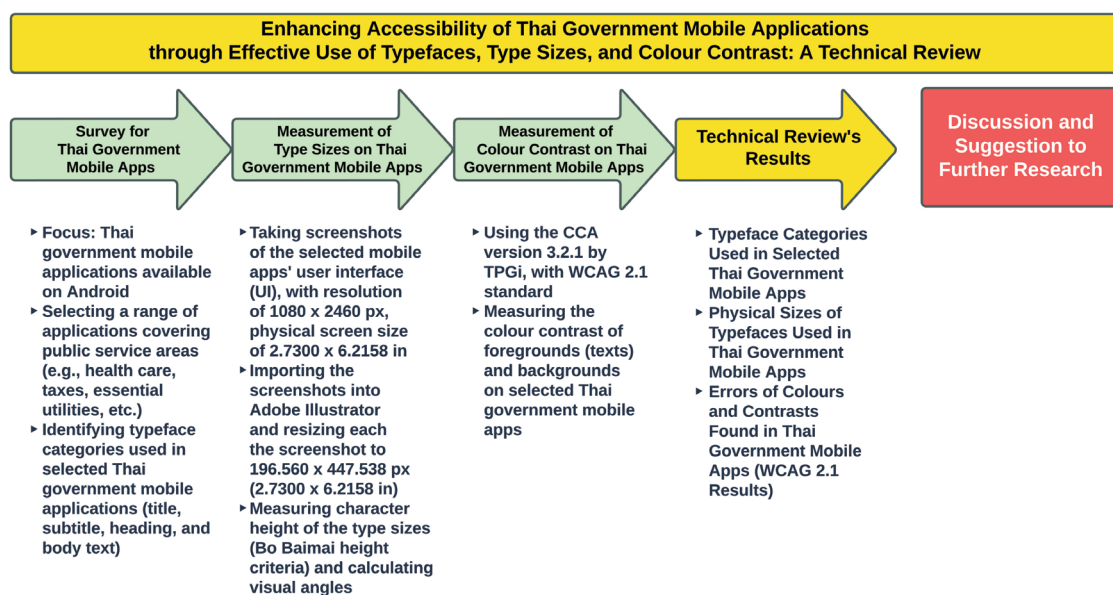
» **Figure 4:** *Activities conducted in the present study*

first loop, tail, second loop, foot, beak, limb, and core, are meticulously designed, as Punsongserm, Sunaga & Ihara (2017a) pointed out. In contrast, Thai fonts that resemble Roman or Latin letterforms often overlook or ignore these unique features, according to Punsongserm, Sunaga & Ihara (2018c). This contrast underscores the importance of selecting the right font for effective communication in the Thai language, ensuring that all readers can easily understand and comprehend the content.

» **Figure 5:** *Examples of typefaces used in selected Thai government mobile applications*

In a study on Thai fonts conducted by Kamollimsakul, Petrie & Power (2014a), using a conservative font, a Thai conventional text font, is more efficient and leads to quicker reading on web pages than a modern font, a Roman-like Thai font. Interestingly, both younger and older adults preferred conservative fonts over modern ones. Later, Punsongserm, Sunaga & Ihara (2018c) analysed the legibility and visibility of general words using two methodologies. The study included ten fonts commonly used in Thailand, including five conventional and five Roman-like Thai fonts. The findings showed that Thai conventional fonts were more readable than Roman-like Thai fonts, and readers had fewer errors in identifying single words and word strings, especially in low-illumination environments. In particular, using Roman-like Thai fonts resulted in significantly more misread words than Thai conventional fonts. These results suggest that when it comes to legibility and visibility, Thai conventional fonts are a better choice than Roman-like Thai fonts.

Furthermore, a recent study by Punsongserm & Suvakunta (2022a) found that using Thai conventional text fonts enhanced the readers reading Thai conventional fonts in less time than Roman-like fonts. The study revealed that readers of all ages had an easier time reading drug labels with Thai conventional text fonts, especially Thai UD font.

Table 2
Checklist of typefaces used in selected Thai government mobile applications

No.	Application Name	Used Typeface			
		Conventional Text Typeface		Roman-Like Thai Typeface	
		Title, Subtitle, Heading	Body	Title, Subtitle, Heading	Body
1	ทางรัฐ (Thang Rath) Version 2.5.0	●	●	-	-
2	RDU รู้เรื่องยา Version 1.5.9	●	●	●	●
3	Clicknic Version 3.4.14	●	●	●	●
4	สมุดสุขภาพผู้สูงอายุ (Bluebook) Version 2.8.2	-	-	●	●
5	สมุดสุขภาพ (Smud Sukhaphap) Version 2.0.0	-	-	●	●
6	RD Smart Tax Version 3.3.0	-	-	●	●
7	ภาษีไปไหน (Phasi Pai Nai) Version 2.3.2	●	●	●	●
8	PDMO Version 2.7.6	●	●	●	●
9	PEA Smart Plus Version 3.2.11	-	-	●	●
10	PWA Plus Life Version 3.5.2	●	●	●	●

Interestingly, the study also showed significant differences in reading times between younger and older participants, with younger participants having faster reading times and older participants having slower reading times.

These findings underline the importance of using easily readable fonts, especially for crucial information such as drug labels. Moreover, a further study by Punsongserm & Suvakunta (2022b) indicated that conventional text typefaces with distinctive key letter features have a lower misreading in word accuracy compared to Roman-like Thai fonts when reading drug label contents.

Type Sizes

After conducting an in-depth study on the mobile applications developed by the Thai government, we analysed the size of the letters displayed. Our research used millimetre and pixel units to measure the characters' sizes. We discovered that the smallest text size used in the selected Thai government mobile applications was approximately 0.6420 mm (1.8198 px) in Bo Baimai height (PWA Plus Life application).

Table 3 presents the physical sizes and visual angles of typefaces used in the selected mobile applications.

Based on the study conducted on mobile applications such as ทางรัฐ (Thang Rath), RDU รู้เรื่องยา, Clicknic, ภาษีไปไหน (Phasi Pai Nai), PDMO, and RD Smart Tax, the current study found that most of these applications tend to use letter sizes bigger than 1.2 mm in Bo Baimai height for words, phrases, and short sentences (Tables 3).

However, some applications like สมุดสุขภาพผู้สูงอายุ (Bluebook), สมุดสุขภาพ (Smud Sukhaphap), PEA Smart Plus, and PWA Plus Life used smaller font sizes of 1 mm or less, as shown in Tables 3. It is important to note that font size can affect the user experience, so choosing a type size that is easy to read for all users is necessary. Furthermore, for body text, the smallest type sizes used ranged from 1 to 1.7 mm in applications like RDU รู้เรื่องยา, Clicknic, RD Smart Tax, and ภาษีไปไหน (Phasi Pai Nai).

The objects we see depend on distance. Several studies have looked into the viewing distances of young adults while reading a smartphone.

Table 3

Physical sizes and visual angles of typefaces used in Thai government mobile applications

No.	Application Name	Type Size (Bo Baimai Height)							
		Title, Subtitle, Heading				Body			
			Milli-meter	Pixel	Degree (°) (Viewing Distance = 400 mm)		Milli-meter	Pixel	Degree (°) (Viewing Distance = 400 mm)
1	ทางรัฐ (Thang Rath) Version 2.5.0	Min	1.2860	3.6454	0.1842				
		Max	2.4350	6.9024	0.3488				
2	RDU รู้เรื่องยา Version 1.5.9	Min	1.2870	3.6479	0.1843	Min	1.0280	2.9128	0.1473
		Max	2.2320	6.3265	0.3197	Max	2.2430	6.3593	0.3213
3	Clicknic Version 3.4.14	Min	1.2220	3.4636	0.1750	Min	1.6670	4.7254	0.2388
		Max	3.0170	8.5519	0.4322	Max	1.9260	5.4595	0.2759°
4	สมุดสุขภาพผู้สูงอายุ (Bluebook) Version 2.8.2	Min	8.3500	2.3659	0.1196				
		Max	2.4260	6.8761	0.3475				
5	สมุดสุขภาพ (Smud Sukhaphap) Version 2.0.0	Min	1.0250	2.9061	0.1468				
		Max	4.6280	131.188	0.6629				
6	RD Smart Tax Version 3.3.0	Min	1.4130	4.1952	0.2024	Min	1.3480	3.8211	0.1931
		Max	2.3100	6.5480	0.3309	Max	1.6050	4.5496	0.2299
7	ภาษีไปไหน (Phasi Pai Nai) Version 2.3.2	Min	1.2850	3.6435	0.1841		1.6690	4.7310	0.2391
		Max	2.5020	7.0923	0.3584				
8	PDMO Version 2.7.6	Min	1.2860	3.6454	0.1842				
		Max	3.9150	11.0984	0.5608				
9	PEA Smart Plus Version 3.2.11	Min	1.0330	2.9268	0.1480				
		Max	3.5300	10.005	0.5056				
10	PWA Plus Life Version 3.5.2	Min	6.4200	1.8198	0.0920				
		Max	2.9500	8.3631	0.4226				

Long et al. (2017) found that the mean viewing distance over 60 minutes was 29.2 ± 7.3 cm, with the viewing distance being significantly more significant during the first, second, and fifth 10-minute periods than during the final 10-minute period. Yoshimura et al. (2017) reported that the viewing distance of smartphones in a sitting position ranged from 13.3 to 32.9 cm among participants, whereas in the lying position, it ranged from 9.9 to 21.3 cm.

In addition, Panke et al. (2019) found that the viewing distance for digital active tasks was found to be shorter (29.3 ± 4.7 cm) compared to passive tasks (32.3 ± 6.0 cm). Additionally, the study found that the viewing distance for digital passive tasks was shorter (32.3 ± 6.0 cm) compared to hardcopy passive tasks (34.4 ± 5.9 cm). Finally, Boccardo (2021) examined viewing distance in presbyopic and nonpresbyopic age groups and found that the average viewing distance was 36.1 ± 7.2 cm while sitting and 37.4 ± 6.8 cm while standing. It is important to note that the average viewing distance differed among genders and age groups.

It is essential to consider the appropriate type size when designing materials to be viewed by both young and older adults. According to Santayayon, Pipitpukdee & Phantachat (2011), the minimum Thai type size recommended for a viewing distance of 50 cm is 2 mm, corresponding to a visual angle of 0.2292°. However, if the viewing distance were to decrease to 45 cm, 40 cm, 35 cm, 30 cm, 25 cm, 20 cm, 15 cm, or 10 cm, the corresponding visual angles would be 0.2546°, 0.2865°, 0.3274°, 0.3820°, 0.4584°, 0.5730°, 0.7639°, and 1.1459°, respectively. It is important to remember these conversions when designing materials to ensure they are easily viewable for all intended audiences.

A drug label study conducted by Punsongserm & Suvakunta (2022a) suggested that the optimal range of type sizes for easy readability among readers of diverse backgrounds may be between 1.3 and 2 mm in Bo Baimai height for reading body text. The study further recommended using larger sizes for headlines, subheads, and text typed with Roman-like Thai typefaces.

From this, it can be safely assumed that using letter sizes larger than 1.3 mm in Bo Baimai height can be highly effective for screen-based reading for readers. However, it is crucial to remember that the effectiveness of reading also relies on the category of typefaces, thickness stroke, letter spacing, and other factors. To improve mobile application standards or guidelines, it is essential to conduct further research to validate our assumptions.

At type size of 1.3 mm in Bo Baimai height, the viewing distance of 50 cm, 45 cm, 40 cm, 35 cm, 30 cm, 25 cm, 20 cm, 15 cm, or 10 cm, the corresponding visual angles would be 0.1490°, 0.1655°, 0.1862°, 0.2128°, 0.2483°, 0.2979°, 0.3724°, 0.4966°, and 0.7448°, respectively.

Regarding optometric examinations, the traditional near point is typically 40 cm (Boccardo, 2021). This distance is commonly used for reading paper media. It corresponds to a visual angle of 0.1862° at a minimum type size of 1.3 mm in Bo Baimai height. However, recent smartphone viewing distance studies suggested that the mean viewing distance over 60 minutes is 29.2 cm (Long et al., 2017), with a corresponding visual angle of 0.2551°. Additionally, when using smartphones in a sitting or lying position, the farthest viewing distance is typically 32.9 cm or 21.3 cm (Yoshimura et al., 2017), with corresponding visual angles of 0.2264° and 0.3497°, respectively. It is also worth noting that the average viewing distance for presbyopic and nonpresbyopic age groups is around 36–37 cm when sitting or standing (Boccardo, 2021), with corresponding visual angles of 0.2063° and 0.1992°, respectively. These visual angles are similar to those described in Santayayon, Pipitpukdee & Phantachat (2011) (i.e., a visual angle of 0.2292°).

Lastly, Punsongserm & Suvakunta (2022b) recommended a minimum Thai type size of 1.3–2 mm Bo Baimai height for reading body text at viewing distances that provide visual angles exceeding 0.200° to assure legibility for readers.

Following the WCAG 2.1 Understanding Docs guidelines (World Wide Web Consortium: W3C, 2022a; World Wide Web Consortium: W3C, 2022b) is essential for text and image contrast. This means that regular-sized text should have a contrast ratio of at least 4.5:1. In contrast, the larger text should have a ratio of at least 3:1 (at least 18 points/24 pixels or bold and at least 14 points/18.5 pixels). To better understand what this means in terms of typeface, we can look at the cap height and x-height of typefaces like Times New Roman, Arial, Helvetica, and Univers. For example, at 14-point size, the cap height of these typefaces ranges from 3.270 to 3.566 mm, whereas the x-height ranges from 2.209 to 2.583 mm (Punsongserm & Suvakunta, 2022b).

Furthermore, we measured and found that at an 18-point size, the cap height ranges from 4.204 to 4.585 mm, whereas the x-height ranges from 2.841 to 3.321 mm. By keeping these measurements in mind, we can ensure that our text is easily readable and accessible to all users.

A study conducted by Kamollimsakul, Petrie & Power (2014a) found that both younger and older adults showed a preference for the conservative font type (Thai conventional text font) over the modern font type (Roman-like Thai font) when presented with web pages. However, font size preferences varied depending on the age group. Younger adults preferred font sizes of 14 and 16 points over 12 points, while older adults preferred 16 points over 12 and 14 points. Based on the study's findings, it is recommended to use the conservative font type for both younger and older adults.

The appropriate font size depends on the font type used. For the conservative type, font sizes 12 points or larger are recommended for younger adults, while 14 points or larger are recommended for older adults. For the modern font type, 14 points or larger font sizes are suitable for younger adults, while 16 points or larger are acceptable for older adults. The study by Kamollimsakul, Petrie & Power (2014a) involved a viewing distance of approximately 57 cm between the eyes of 42 participants and the monitor. However, the calculation of visual angles should be based on the Bo Baimai height.

It is important to note that determining the visual angles for each point size of the conservative and modern fonts tested in the experiment is not feasible, as the names of the fonts were not provided in the study, and their Bo Baimai height is unknown. Moreover, the formula proposed by Legge & Bigelow (2011) for calculating visual angles from point unit to degree is not applicable in this case, as the given formula was formulated under the condition of the viewing distance of 40 cm, whereas the viewing distance in the study by Kamollimsakul, Petrie & Power (2014a) was 57 cm.

Although Legge & Bigelow (2011) have proposed a formula to calculate visual angles from point unit to degree, based on Bo Baimai height criteria, this formula may not be suitable for Thai fonts due to the structural dissimilarities between Thai and Roman fonts. The Thai writing system consists of horizontally composed consonants, vowels, signs, and marks, whereas some vowels, tone marks, and signs are placed in the vertical space. This contrasts with other languages, such as English, which arranges all characters horizontally.

Furthermore, Figure 6 shows a comparison of the lines and areas of a Thai font (Upper) and a Roman font (Lower) (Rojarayanont, 2001). It is evident that the two font types differ in structure. Figure 7 further highlights that the consonants of Thai letterforms are smaller in lowercase compared to Roman fonts, which is influenced by the number of vertical lines and arranging areas being more than in Thai fonts. Therefore, it is essential to consider these structural differences in Thai fonts before applying the formula proposed by Legge & Bigelow (2011) to calculate visual angles.

Regarding text in books and newspapers in Thailand, keeping the text font size within 12 to 16 points is essential. However, it should be at most 7 points for packaging, as Punsongserm, Sunaga & Ihara (2017a) recommended. This is crucial for readability and accessibility for all readers. We measured the Bo Baimai height of Cordia New and TH Sarabun New typefaces at point sizes 12, 14, and 16. For Cordia New, the Bo Baimai heights at these point sizes were 1.693 mm, 1.97 mm, and 2.252 mm, respectively. For TH Sarabun New, the Bo Baimai heights at these point sizes were 1.66 mm, 1.931 mm,

and 2.208 mm, respectively. At 7 points, the Bo Baimai heights for Cordia New and TH Sarabun New were 0.983 mm and 0.963 mm, respectively. We observed that the Bo Baimai heights of Cordia New and TH Sarabun New at point size 16 are 2.252 mm and 2.208 mm, respectively. This is similar to the x-height of Times New Roman at 14-point size, which is 2.209 mm. However, because the Thai and Roman letterforms differ, they cannot be directly compared. Thai conventional text fonts have certain letter features that make them more complex and require a larger size to be legible.

Conversely, using the typical point sizes 12, 14, and 16 would result in a Bo Baimai height ranging from 1.66 to 2.252 mm.
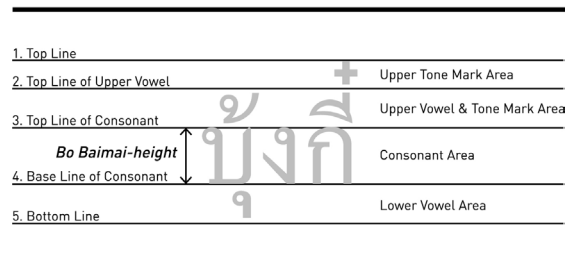
» **Figure 6:** *Upper: Lines and areas of a Thai font. Lower: Lines and areas of a Roman font (Rojarayanont, 2001)*

» **Figure 7:** *Comparing Thai and Roman fonts of the same point size with different typefaces (Cordia New and Arial)*

At a viewing distance of 40 cm, these physical sizes would convert to visual angles of 0.2378° and 0.3226°, respectively, which are well above the minimum legibility threshold of 0.2000° for most readers. However, in some cases where smaller point sizes are used, such as 10, the Bo Baimai height would be 1.411 mm (for Cordia New) or 1.383 mm (for TH Sarabun New). In these cases, the corresponding visual angles would be 0.2021° and 0.1981°, respectively, which are still acceptable to most readers.

Therefore, when defining text size with point measurement on Thai mobile applications, it is essential to consider the readability for general readers. A minimum size of 10 points for standard Thai text fonts is acceptable, whereas a size of at least 12 points is recommended for all readers. This ensures that the text is easily legible and accessible for all users, regardless of their visual abilities.

A recent study by Punsongserm (2023) examined the legibility of different text fonts, namely FT Manifest UD, Cordia New, and TH Sarabun New, with 36 Thai consonants at varying viewing distances. A sample of 31 Thai volunteers, comprising 12 males and 19 females aged between 18 and 60 and categorised into three groups- adolescent-young adults, older adults, and individuals working in graphic design and related fields- participated in the study. The study's findings revealed that perceiving Thai text letterforms at visual angles greater than 0.2000° can significantly improve their legibility compared to lower visual angles. Specifically, at a visual angle of 0.2387°, the average percentage of correct responses ranged from 92.29 to 93.19, while at a visual angle of 0.1790°, the average percentage of correct responses was between 80.92 and 86.8. However, at a visual angle of 0.1432°, the average percentage of correct responses ranged from 70.79 to 77.06, and at 0.1432°, it was between 62.90 and 72.31. These findings could be informative in selecting the appropriate font and visual angle to enhance the legibility of Thai text.

Colour Contrast

In Thailand, the Thai Web Content Accessibility Guidelines 2010: Document Number 1 Version 2.0 (Ministry of Digital Economy and Society, 2010) and the Government Website Standard Version 1.0 (EGA, 2012) have defined the contrast ratios of text and background colour based on WCAG 2.0, 2.1, and 2.2. These guidelines focus on minimum contrast (Level AA) and enhanced contrast (Level AAA) (Worldwide Web Consortium: W3C, 2016a; Worldwide Web Consortium: W3C, 2016b; Worldwide Web Consortium: W3C, 2022a; Worldwide Web Consortium: W3C, 2022b; Worldwide Web Consortium: W3C, 2023a; Worldwide Web Consortium: W3C, 2023b). The visual presentation of text and images of text must have a contrast ratio of at least 4.5:1 for minimum contrast (Level AA), except for large-scale text and its images, which must have a contrast ratio of at least 3:1.

Additionally, for enhanced contrast (Level AAA), the visual presentation of text and images of text must have a contrast ratio of at least 7:1, except for large-scale text and its images, which must have a contrast ratio of at least 4.5:1. These guidelines ensure that web content in Thailand is accessible to all, regardless of visual ability.

Furthermore, as per the Government Website Standard and Government Website Standard Version 2.0 (EGA, n.d.), Thai websites must adhere to the guidelines set by the Worldwide Web Consortium: W3C, following the Web Content Accessibility Guidelines 2.0: WCAG 2.0 on the A-Level Success Criterion (A). In addition, the Government Mobile Application Standard Version 1.0 (EGA, 2015) has recommended considering readability and visibility when choosing colours and avoiding combinations that hinder these aspects. However, it is worth noting that this standard does not delve into the specifics of contrast ratio or reference the WCAG.

We considered using the CCA version 3.2.1 application to measure the standard contrast ratios that conform to the WCAG 2.0, 2.1, and 2.2 in the selected Thai mobile applications. In this way, we can ensure that the mobile application is accessible to all individuals, including those with visual impairments. After carefully reviewing each mobile application, we focused solely on the WCAG 2.1 results that the CCA identified as having one or more errors that did not pass.

Based on the data presented in Tables 4 and 5, the CCA application has revealed that the contrast ratios for the selected mobile application for regular text did not meet (did not pass) the WCAG 2.1 enhanced contrast (Level AAA) requirement of a 7:1 ratio. Nevertheless, some contrast ratios met the WACG 2.1 requirement for large text with a 4.5:1 contrast, and 29.92% of them passed the test.

When we consider WCAG 2.1 results of minimum contrast (Level AA) in Tables 4 and 5, it is worth noting that some regular text with a 4.5:1 contrast ratio requirement passed the test with a 29.92% pass rate. In comparison, some large texts with a 3:1 contrast ratio requirement also met the criteria and had a higher pass rate of 55.12%.

Some mobile applications had trouble meeting the minimum contrast ratios WCAG 2.1 (Level AA) required. Specifically, RDU รู้เรื่องยา and สมุดสุขภาพผู้สูงอายุ (Bluebook) had many errors in meeting these standards, as shown in Table 4. In contrast, some mobile applications are quite accessible when displaying large text with a contrast ratio of at least 3:1. Examples of such applications include ทาง รัฐ (Thang Rath; Table 4), สมุดสุขภาพ (Smud Sukhaphap; Table 4), and ภาษีไปไหน (Phasi Pai Nai; Table 5).

The role of colour contrast in enhancing the readability of text on digital screens is significant.

Numerous studies have investigated the impact of colour contrast on reading performance and preferences. For instance, Kamollimsakul, Petrie & Power (2014b) revealed that the choice of colours used on webpages could significantly impact the performance and preferences of both young and older adults using Thai language websites. Interestingly, the study found that commonly used colour combinations such as black on white, white on black, and sepia on off-white had no apparent effect on task completion rate or reading time for both age groups. However, there were noticeable differences in colour preferences between the two groups. Younger adults preferred black text on a white background or sepia text on an off-white background, while older adults favoured black text on white backgrounds. Based on these findings, the study recommended using black text on a white background for both age groups and sepia text on an off-white background, particularly for younger users. The study also advised all web users to avoid white text on black backgrounds. These insights provide a valuable foundation for evidence-based design guidelines for Thai websites and mobile applications that cater to younger and older users.

Similarly, Zorko et al. (2017) explored the impact of foreground and background colours on readability on digital screens. The research findings were consistent with those obtained for readability on printed materials, with black text on a white background being the most readable combination. Interestingly, the group reading this sample took the longest average time but made the fewest mistakes. The study also revealed that the black foreground-white background combination is the least stressful for the eyes. However, black text on a yellow foreground is the least readable colour combination, with the highest number of mistakes. Surprisingly, the study found that green text on an orange background and red text on a green background produced unexpected results. Even though these combinations are proven to be the least readable on printed materials, this research shows that they are suitable for reading on a digital screen.

Furthermore, Ojanpää & Näsänen (2003) examined the effects of luminance and colour contrast on the search for information on display devices. The study found that visual search times, the number of eye fixations, and mean fixation durations increased strongly with decreasing luminance contrast despite the presence of colour contrast. Thus, moderate or even high colour contrast does not guarantee quick visual perception if the luminance contrast between characters and background is small. Therefore, good visibility of alphanumeric information in user interfaces requires clear luminance (brightness) difference between foreground and background.

The colour contrast used in digital design can significantly affect user experience. These studies provide valuable insights into choosing appropriate colour combinations for digital screens. Further research is needed to explore the impact of contrast ratios and colours in web and mobile application design.

Table 4 (part 1)
Errors of colours and contrasts found in Thai government mobile applications (1)

| Application Name | Colour and Contrast | | | WCAG 2.1 Results | | | |
| | Foreground (Hex colour code) | Background (Hex colour code) | Contrast Ratio | AA | | AAA | |
				Regular Text	Large Text	Regular Text	Large Text
ทางรัฐ (Thang Rath) Version 2.5.0	#797979	#FFFFFF	4.4:1	✗	✓	✗	✗
	#2F6447	#FBFFFB	6.9:1	✓	✓	✗	✓
	#FFFFFF	#3D855C	4.461:1	✗	✓	✗	✗
	#FEFEFE	#78C07C	2.2:1	✗	✗	✗	✗
	#3E865C	#FFFFFF	4.4:1	✗	✓	✗	✗
RDU รู้เรื่องยา Version 1.5.9	#FCFFFF	#F5C144	1.7:1	✗	✗	✗	✗
	#FFFFFF	#52A8DD	2.6:1	✗	✗	✗	✗
	#FFFFFB	#A0B965	2.2:1	✗	✗	✗	✗
	#666666	#FFFFFF	5.7:1	✓	✓	✗	✓
	#FFFFFF	#E78E48	2.5:1	✗	✗	✗	✗
	#9D9D9D	#FFFFFF	2.7:1	✗	✗	✗	✗
	#E68E49	#FFFFFE	2.5:1	✗	✗	✗	✗
	#CBCBCB	#FFFFFF	1.6:1	✗	✗	✗	✗
	#FFFFFF	#EAA05D	2.2:1	✗	✗	✗	✗
	#F9E2CC	#EAA05D	1.7:1	✗	✗	✗	✗
	#666666	#FFFFFF	5.7:1	✓	✓	✗	✓
	#FFFFFF	#A267A4	4.2:1	✗	✓	✗	✗

Table 4 (part 2)

Errors of colours and contrasts found in Thai government mobile applications (1)

Application Name	Colour and Contrast						
	Foreground (Hex colour code)	Background (Hex colour code)	Contrast Ratio	WCAG 2.1 Results			
				AA		AAA	
				Regular Text	Large Text	Regular Text	Large Text
RDU รู้เรื่องยา Version 1.5.9	#FCFDFB	#B080AF	3.1:1	✖	✓	✖	✖
	#A267A4	#FFFFFF	4.2:1	✖	✓	✖	✖
	#B0B0B0	#FFFFFF	2.2:1	✖	✖	✖	✖
	#FFFFFF	#F4BF57	1.7:1	✖	✖	✖	✖
	#F4BF58	#FFFFFF	1.7:1	✖	✖	✖	✖
	#F9FFF7	#9BC556	2:1	✖	✖	✖	✖
Clicknic Version 3.4.14	#5F605F	#EBEEF0	5.4:1	✓	✓	✖	✓
	#9D9D9D	#DFDFDF	2:1	✖	✖	✖	✖
	#68C0D4	#F6F5F5	1.9:1	✖	✖	✖	✖
	#427F8E	#F5F5F7	4.1:1	✖	✓	✖	✖
	#6A6A6A	#F5F5F5	5:1	✓	✓	✖	✓
	#5E5E5E	#EAEAEA	5.4:1	✓	✓	✖	✓
	#ADADAD	#EAEAEA	1.9:1	✖	✖	✖	✖
	#FFFFFF	#81CBDD	1.8:1	✖	✖	✖	✖
	#747474	#FFFFFF	4.7:1	✓	✓	✖	✓
	#9D9D9D	#FFFFFF	2.7:1	✖	✖	✖	✖
	#666666	#FFFFFF	5.7:1	✓	✓	✖	✓
	#68C0D4	#FFFFFF	2.1:1	✖	✖	✖	✖
สมุดสุขภาพผู้สูงอายุ (Bluebook) Version 2.8.2	#FFFFFF	#4BA2D7	2.8:1	✖	✖	✖	✖
	#4CA3D6	#FFFFFF	2.8:1	✖	✖	✖	✖
	#E8AC43	#FFFFFF	2:1	✖	✖	✖	✖
	#4A78ED	#FFFFFF	4:1	✖	✓	✖	✖
	#D83289	#FFFFFF	4.4:1	✖	✓	✖	✖
	#7F7F7F	#FFFFFF	4:1	✖	✓	✖	✖
	#4CA5D7	#EAEAEA	2.3:1	✖	✖	✖	✖
	#57A45A	#EAEAEA	2.5:1	✖	✖	✖	✖
	#E7AC43	#EAEAEA	1.7:1	✖	✖	✖	✖
	#C92F23	#EAEAEA	4.459:1	✖	✓	✖	✖
	#55AC57	#FFFFFF	2.8:1	✖	✖	✖	✖
	#C82F22	#FFFFFF	5.4:1	✓	✓	✖	✓
	#FFFFFF	#64C13D	2.3:1	✖	✖	✖	✖
	#4697DE	#EFFCFE	3:1	✖	✖	✖	✖
	#5B5B5B	#FFFFFF	6.8:1	✓	✓	✖	✓
สมุดสุขภาพ (Smud Sukhaphap) Version 2.0.0	#E05244	#FAFAFA	3.7:1	✖	✓	✖	✖
	#FFFFFF	#468E60	4:1	✖	✓	✖	✖
	#AE4745	#FFFFFF	5.5:1	✓	✓	✖	✓
	#747474	#FFFFFF	4.7:1	✓	✓	✖	✓
	#4E4E4E	#EBEBEB	7:1	✓	✓	✖	✓
	#9D9D9D	#FAFAFA	2.6:1	✖	✖	✖	✖
	#9D9D9D	#FFFFFF	2.7:1	✖	✖	✖	✖
	#FFFFFF	#428459	4.491:1	✖	✓	✖	✖
	#6D737C	#FFFFFF	4.8:1	✓	✓	✖	✓
	#30663F	#FFFFFF	6.8:1	✓	✓	✖	✓
	#231E1D	#CD8270	5.5:1	✓	✓	✖	✓
	#231E1D	#BE533D	3.5:1	✖	✓	✖	✖

Table 5 (part 1)

Errors of colours and contrasts found in Thai government mobile applications (2)

| Application Name | Colour and Contrast | | | WCAG 2.1 Results | | | |
| | Foreground (Hex colour code) | Background (Hex colour code) | Contrast Ratio | AA | | AAA | |
				Regular Text	Large Text	Regular Text	Large Text
RD Smart Tax Version 3.3.0	#5DA943	#FFFFFF	2.9:1	✗	✗	✗	✗
	#747474	#FFFFFF	4.7:1	✓	✓	✗	✓
	#FFFFFF	#5DA943	2.9:1	✗	✗	✗	✗
	#6E6E6E	#F3F3F3	4.6:1	✓	✓	✗	✓
	#5A5A5A	#FFFFFF	6.9:1	✓	✓	✗	✓
	#F09A3A	#FDFDFD	2.2:1	✗	✗	✗	✗
ภาษีไปไหน (Phasi Pai Nai) Version 2.3.2	#696969	#FFFFFF	5.5:1	✓	✓	✗	✓
	#4D91BC	#FFFFFF	3.4:1	✗	✓	✗	✗
	#4D92BD	#FAFAFA	3.3:1	✗	✓	✗	✗
	#FFFFFF	#4C93BE	3.4:1	✗	✓	✗	✗
	#FFFFFF	#435993	6.8:1	✓	✓	✗	✓
	#E0783C	#F7F7F7	2.8:1	✗	✗	✗	✗
	#FFFFFF	#E1783D	3:1	✗	✓	✗	✗
	#E83628	#F7F7F7	3.9:1	✗	✓	✗	✗
	#586270	#F7F7F7	5.8:1	✓	✓	✗	✓
	#666666	#FFFFFF	5.7:1	✓	✓	✗	✓
	#F2B144	#295285	4.2:1	✗	✓	✗	✗
	#F9DD4C	#58636F	4.5:1	✓	✓	✗	✓
	#54A6C9	#F7F7F7	2.6:1	✗	✗	✗	✗
PDMO Version 2.7.6	#FFFEFF	#5164C8	5.2:1	✓	✓	✗	✓
	#BFBFBF	#FFFFFF	1.8:1	✗	✗	✗	✗
	#FFFEFF	#5780CE	3.9:1	✗	✓	✗	✗
	#FFFEFF	#C89F4A	2.5:1	✗	✗	✗	✗
	#A3A3A3	#FAFAFA	2.4:1	✗	✗	✗	✗
	#FFFFFF	#4D62C5	5.4:1	✓	✓	✗	✓
	#FFFFFF	#5D744B	5.2:1	✓	✓	✗	✓
	#FFFFFF	#71806B	4.2:1	✗	✓	✗	✗
	#4E2513	#CEA346	5.6:1	✓	✓	✗	✓
	#FFFFFB	#9C702E	4.4:1	✗	✓	✗	✗
	#CBCBCB	#FFFFFF	1.6:1	✗	✗	✗	✗
	#69C49C	#FFFFFF	2.1:1	✗	✗	✗	✗
	#EA6F7A	#FFFFFF	3:1	✗	✗	✗	✗
PEA Smart Plus Version 3.2.11	#6F6E75	#F3F0FD	4.49:1	✗	✓	✗	✗
	#B89C57	#7E3AA4	2.6:1	✗	✗	✗	✗
	#FFFEFF	#7E3AA4	6.9:1	✓	✓	✗	✓
	#C0B6C7	#7E3AA4	3.6:1	✗	✓	✗	✗
	#C9C9C9	#FFFFFF	1.7:1	✗	✗	✗	✗
	#6F6F70	#F3F0FE	4.471:1	✗	✓	✗	✗
	#EA766F	#FFFFFF	2.9:1	✗	✗	✗	✗
	#763D86	#F4F0FE	6.7:1	✓	✓	✗	✓
	#A5A3AA	#F4F0FE	2.2:1	✗	✗	✗	✗
	#B99C57	#F4F0FE	2.4:1	✗	✗	✗	✗
	#FFFFFF	#E05243	3.8:1	✗	✓	✗	✗
	#5F5F5F	#EDEDED	5.5:1	✓	✓	✗	✓

Table 5 (part 2)

Errors of colours and contrasts found in Thai government mobile applications (2)

Application Name	Colour and Contrast			WCAG 2.1 Results			
	Foreground (Hex colour code)	Background (Hex colour code)	Contrast Ratio	AA		AAA	
				Regular Text	Large Text	Regular Text	Large Text
PEA Smart Plus Version 3.2.11	#EA766F	#F3F0FE	2.6:1	✗	✗	✗	✗
	#FFFFFF	#D5D2DF	1.5:1	✗	✗	✗	✗
	#6F6F6F	#501D5E	2.5:1	✗	✗	✗	✗
PWA Plus Life Version 3.5.2	#3465B7	#FBFBFB	5.5:1	✓	✓	✗	✓
	#F8FBFF	#5153C0	6:1	✓	✓	✗	✓
	#9D9D9D	#F5F5F5	2.5:1	✗	✗	✗	✗
	#FFFFFE	#EDAA47	2:1	✗	✗	✗	✗
	#FFFFFE	#3363B8	5.8:1	✓	✓	✗	✓
	#F5F9FC	#4C81AC	3.9:1	✗	✓	✗	✗
	#4878B1	#FEFFFF	4.6:1	✓	✓	✗	✓
	#F5F9FB	#55A4C9	2.6:1	✗	✗	✗	✗
	#6D737C	#FFFFFF	4.8:1	✓	✓	✗	✓
	#3878F6	#FFFFFF	4:1	✗	✓	✗	✗
	#FFFFFF	#3878F6	4:1	✗	✓	✗	✗
	#FDFFFF	#74BCDA	2.1:1	✗	✗	✗	✗
	#FFFFFF	#72B467	2.5:1	✗	✗	✗	✗
	#FEFFFF	#4878B0	4.6:1	✓	✓	✗	✓
	#446F8D	#DCEDF5	4.476:1	✗	✓	✗	✗
	#565656	#EDEDED	6.3:1	✓	✓	✗	✓
	#FFFFFF	#6DA5F8	2.5:1	✗	✗	✗	✗
	#FFFEFE	#75D9BF	1.7:1	✗	✗	✗	✗

Conclusions

The proliferation of mobile applications has become an integral part of our daily lives, providing us with unparalleled convenience and efficiency for various purposes. The impact of mobile applications has also revolutionised how we interact with government services, offering citizens fast and efficient access to government-related information and services.

In line with this, Thai government mobile applications play a crucial role in the digital transformation of government services. A current technical review was conducted to evaluate the legibility of Thai typefaces, type sizes, and colour contrast in mobile applications provided by Thai government offices. One of the key findings of our study is that Thai web and mobile standards require more suitable fonts and sizes. We identified two main categories of Thai typefaces: conventional and Roman-like Thai fonts. We found that most Thai mobile applications use letter sizes of at least 1.2 mm in Bo Baimai height, but some use smaller sizes that may prove challenging to read. Choosing an easy-to-read font size is essential to improving user accessibility. The smallest type sizes for body text ranged from 1 to 1.7 mm.

We also found that contrast ratios for regular text in selected mobile applications did not meet the WCAG 2.1 enhanced contrast requirement of a 7:1 ratio. However, some contrast ratios for large text meet the 4.5:1 requirement. Some regular text with a 4.5:1 contrast ratio requirement passed the WCAG 2.1 minimum contrast test, whereas some large text with a 3:1 contrast ratio requirement also met the criteria. The study identified typographical issues that may arise in these mobile applications. It gained a deeper understanding of the subject matter.

However, the study has research gaps and limitations that future research must address.

The study focused solely on Android mobile applications, and future research should also investigate iOS applications. Since both Android and iOS mobile applications have a broad user base in Thailand, investigating both platforms would provide a better understanding of the typographical concerns in Thai government mobile applications. The study only focused on typographical concerns and did not cover the usability of mobile applications. Future research should investigate the usability of Thai government mobile applications to identify any issues that may affect user experiences.

Moreover, the study did not consider the impact of different lighting conditions on the legibility and visibility of Thai typefaces, type sizes, and colour contrast in mobile applications. Investigating the effect of different lighting conditions would provide insight into how typographical concerns affect user experiences in different environments.

The study only measured physical type sizes based on the Bo Baimai height measurement without considering other factors that could affect legibility, such as letter spacing, line spacing, and font style.

Future research should consider these factors to provide a more comprehensive understanding of the typographical concerns in Thai government mobile applications.

The study only used a colour contrast analyser application to measure colour contrast without considering the visual perception of users with different types of colour vision deficiencies. Investigating the impact of different kinds of colour vision deficiencies on the legibility of Thai typefaces and colour contrast would provide insight into how to design mobile applications accessible to all users.

Lastly, the study did not involve user testing to evaluate the legibility and visibility of Thai typefaces, type sizes, and colour contrast in mobile applications. Conducting user testing would provide a better understanding of the impact of typographical concerns on user experiences and identify any issues that may affect user satisfaction.

To conclude, future research should investigate the impact of different letter spacing, line spacing, and font styles on the legibility of Thai typefaces in mobile applications. Developing guidelines and standards for Thai typefaces, type sizes, and colour contrast in mobile applications that consider the needs of users with different types of colour vision deficiencies is also necessary.

Conducting user testing to evaluate the legibility and visibility of Thai typefaces, type sizes, and colour contrast in mobile applications is crucial. This may necessitate specialised blur simulation equipment such as blur glass filters and cataract simulation goggles. Collaboration with participants who have normal visual acuity, as well as those who are visually impaired and elderly, is equally important.

These efforts would provide insight into how to design mobile applications that are more user-friendly, accessible, and satisfying for all users.

Funding

References

Accessible Resources. (2024) *A11Y: Audit + Color Contrast*. Available from: https://www.accessibleresources.com/ [Accessed 25th January 2024]

Adobe. (2024) *Contrast Checker*. Available from: https://color.adobe.com/create/color-contrast-analyzer [Accessed 25th January 2024]

Arias, R. J., Kurtzhall, K., Pham, D., Mkaouer, W. M. & Elglaly, N. Y. (2022) Accessibility Feedback in Mobile Application Reviews: A Dataset of Reviews and Accessibility Guidelines. In: *CHI Conference on Human Factors in Computing Systems Extended Abstracts, CHI '22 Extended Abstracts, April 29-May 5, 2022, New Orleans, Louisiana*. New York, Association for Computing Machinery. pp. 1-7. Available from: doi: 10.1145/3491101.3519625

Awan, M., Ali, S., Ali, M., Abrar, M. F., Ullah, H. & Khan, D. (2021) Usability Barriers for Elderly Users in Smartphone App Usage: An Analytical Hierarchical Process-Based Prioritization. *Scientific Programming*. Available from: doi: 10.1155/2021/2780257

Boccardo, L. (2021) Viewing distance of smartphones in presbyopic and non-presbyopic age. *Journal of Optometry*. 14 (2), 120–126. Available from: doi: 10.1016/j.optom.2020.08.001

Chatrangsan, M. & Petrie, H. (2019) The effect of typeface and font size on reading text on a tablet computer for older and younger people. In: *Proceedings of the 16th Web For All 2019 Personalization - Personalizing the Web, W4A '19, 13-15 May 2019, San Francisco, California*. New York, Association for Computing Machinery. pp. 1-10. Available from: doi: 10.1145/3315002.3317568

Choo, W. T. K., Balan, K. R. & Lee, Y. (2019) Examining augmented virtuality impairment simulation for mobile app accessibility design. In: *Proceedings of the 2019 CHI Conference on Human Factors in Computing Systems, CHI '19, 4-9 May 2019, Glasgow, United Kingdom*. New York, Association for Computing Machinery. pp. 1-11. Available from: doi: 10.1145/3290605.3300605

Darroch, I., Goodman, J., Brewster, S. & Gray, P. (2005) The Effect of Age and Font Size on Reading Text on Handheld Computers. In: Costabile, M. F. and Paternò, F. (eds.) *IFIP TC 13 International Conference, Human-Computer Interaction - INTERACT 2005, 23-16 September 2005, Rome, Italy*. Berlin, Springer. pp. 253-266. Available from: doi: 10.1007/11555261_23

De Valois, R. L. & De Valois, K. K. (1988) *Spatial vision*. New York, Oxford University Press. Available from: doi: 10.1093/acprof:oso/9780195066579.001.0001

Department of Packaging and Materials Technology, Faculty of Agro-Industry, Kasetsart University. (n.d.) *The development of packaging for the aging society: An example that the industry needs change*. Retrieved January 6, 2023, Available from: https://packaging.oie.go.th/new/admin_control_new/html-demo/analysis_file/5812360794.pdf [Accessed 6th January 2023].

EGA (2012) *Government website standard*. Available from: https://moi.go.th/moi/wp-content/uploads/2019/11/20120823061245.pdf [Accessed 2nd March 2023].

EGA (2015) *Government mobile application standard version 1.0*. Available from: https://www.dga.or.th/wp-content/uploads/2021/02/Gov-Moblie-App-Std-1.pdf [Accessed 2nd March 2023].

EGA (n.d.) *Government website standard version 2.0.* Available from: https://standard.dga.or.th/wp-content/uploads/2021/05/มาตรฐานเว็บไซต์ภาครัฐ-เวอร์ชัน-2-1.pdf [Accessed 2nd March 2023].

Eler, M. M., Rojas, M. J., Ge, Y. & Fraser, G. (2018) Automated Accessibility Testing of Mobile Apps. In: *2018 IEEE 11th International Conference on Software Testing, Verification and Validation, ICST, 9-13 April 2018, Västerås, Sweden*. Piscataway, IEEE. pp. 116-126. Available from: doi: 10.1109/ICST.2018.00021

Frascara, J. (ed.) (2015). What is information design? In: *Information design as principled action: Making information accessible, relevant, understandable, and usable*. Illinois, Common Ground Publishing, pp. 5-55. Available from: 10.18848/978-1-61229-786-6/CGP

Fujikake, K., Hasegawa, S., Omori, M., Takada, H. & Miyao, M. (2007) Readability of character size for car navigation systems. In: *Symposium on Human Interface 2007, Human Interface and the Management of Information. Interacting in Information Environments, HCI2007, 22-27 July 2007, Beijing, China*. Berlin, Springer. pp. 503–509. Available from: doi: 10.1007/978-3-540-73354-6_55

GitHub. (2024a) *EarlGrey*. Available from: https://github.com/google/EarlGrey [Accessed 5th February 2024].

GitHub. (2024b) *KIF*. Available from: https://github.com/kif-framework/KIF [Accessed 5th February 2024].

Google. (2024) *Get started with Accessibility Scanner*. Available from: https://support.google.com/accessibility/android/answer/6376570?hl=en [Accessed 5th February 2024].

Google for Developers. (2024a) *Write automated tests with UI Automator*. Available from: https://developer.android.com/training/testing/other-components/ui-automator [Accessed 5th February 2024].

Google for Developers. (2024b) *Improve your code with lint checks*. Available from: https://developer.android.com/studio/write/lint [Accessed 5th February 2024].

Google for Developers. (2024c) *Espresso*. Available from: https://developer.android.com/training/testing/espresso [Accessed 5th February 2024].

Google Play. (2023) *Accessibility Scanner*. Available from: https://play.google.com/store/apps/details?id=com.google.android.apps.accessibility.auditor [Accessed 25th January 2024].

Grellmann, B., Neate, T., Roper, A., Wilson, S. & Marshall, J. (2018) Investigating mobile accessibility guidance for people with aphasia. In: *Proceedings of the 20th International ACM SIGACCESS Conference on Computers and Accessibility, ASSETS '18, 22-24 October 2018, Galway, Ireland*. New York, Association for Computing Machinery. pp. 410–413. Available from: doi: 10.1145/3234695.3241011

Hasegawa, S., Omori, M., Watanabe, T., Matsunuma, S. & Miyao, M. (2009) Legible Character Size on Mobile Terminal Screens: Estimation Using Pinch-in/Out on the iPod Touch Panel. In: Salvendy, G. and Smith, M. J. (eds.) *Symposium on Human Interface 2009, Human Interface and the Management of Information. Information and Interaction, HCI2009, 19-24 July 2009, San Diego, California*. Berlin. Springer. pp. 395-402. Available from: 10.1007/978-3-642-02559-4_43

Hou, G., Dong, H., Ning, W. & Han, L. (2020) Larger Chinese text spacing and size: effects on older users' experience. *Ageing and Society*. 40 (2), 389–411. Available from: doi: 10.1017/S0144686X18001022

Kamollimsakul, S., Petrie, H. & Power, C. (2014a) Web Accessibility for Older Readers: Effects of Font Type and Font Size on Skim Reading Webpages in Thai. In: Miesenberger, K., Fels, D., Archambault, D., Peňáz, P. and Zagler, W. (eds.) *14th International Conference, Computers Helping People with Special Needs, ICCHP 2014, 9-11 July, Paris, France*. Cham, Springer. pp. 332-339. Available from: 10.1007/978-3-319-08596-8_52

Kamollimsakul, S., Petrie, H. & Power, C. (2014b) The Effect of Text Color and Background Color on Skim Reading Webpages in Thai. In: Stephanidis, C. (ed.) *International Conference, HCI International 2014 - Posters' Extended Abstracts, HCI 2014, 22-27 June 2014, Heraklion, Crete*. Cham, Springer. pp. 615-620. Available from: doi: 10.1007/978-3-319-07854-0_106

Kong, Y. K., Lee, I., Jung, M. C. & Song, Y. W. (2011) The effects of age, viewing distance, display type, font type, colour contrast and number of syllables on the legibility of Korean characters. *Ergonomics*. 54 (5), 453–465. Available from: doi: 10.1080/00140139.2011.568635

Lege, R. P., Hasegawa, S., Hasegawa, A., Kojima, T., Miyao, M. (2013) Aging Effects on the Readability of Characters on E-Book Terminals. In: Stephanidis, C. and Antona, M. (eds.) *7th International Conference, Universal Access in Human-Computer Interaction: Applications and Services for Quality of Life, UAHCI 2013, 21-26 July 2013, Las Vegas, Nevada*. Berlin, Springer. pp. 356-363 Available from: doi: 10.1007/978-3-642-39194-1_42

Legge, G. E. & Bigelow, C. A. (2011) Does print size matter for reading? A review of findings from vision science and typography. *Journal of Vision*. 11 (5), 1-22. Available from: doi: 10.1167/11.5.8

Long, J., Cheung, R., Duong, S., Paynter, R. & Asper, L. (2017) Viewing distance and eyestrain symptoms with prolonged viewing of smartphones. *Clinical Experimental Optometry*. 100 (2), 133–137. Available from: doi: 10.1111/cxo.12453

Ministry of Digital Economy and Society. (2010) *TWCAG2010 (Thai web content accessibility guidelines 2010)*.

Available from: https://issuu.com/9rt9rt/docs/twcag2010 [Accessed 25th January 2024].

Myndex. (2024) *APCA Contrast Calculator*. Available from: https://www.myndex.com/APCA/ [Accessed 25th January 2024].

National Office for Empowerment of Persons with Disabilities, Ministry of Social Development and Human Security. (n.d.) *A guide to environment design for people with disabilities and people of all ages*. Available from: https://www.kkmuni.go.th/pdf-download/kkdisabled/civilization.pdf [Accessed 9th January 2023]

Nielsen, J. (1993) *Usability Engineering*. London, Academic Press.

Noel, G. (2015) Typography for people with aphasia: An exploratory study. In: *Information design as principled action: Making information accessible, relevant, understandable, and usable*. Illinois, Common Ground Publishing, pp. 236–248.

Nugroho, A., Santosa, I. P. & Hartanto, R. (2022) Usability Evaluation Methods of Mobile Applications: A Systematic Literature Review. In: *2022 International Symposium on Information Technology and Digital Innovation, ISITDI, 27-28 July 2022, Padang, Indonesia*. Piscataway, IEEE. pp. 92-95. Available from: doi: 10.1109/ISITDI55734.2022.9944401

O'Shea, R. P. (1991) Thumb's rule tested: Visual angle of the thumb's width is about 2 deg. *Perception*. 20 (3), 415-418. Available from: doi: 10.1068/p200415

Office of the Higher Education Commission. (2013) *Universal design for learning*. Bangkok, Ministry of Education (Thailand).

Office of the National Economic and Social Development Council. (2016) *National economic and social development plan (No. 12)*. Available from: https://www.nesdc.go.th/ewt_dl_link.php?nid=6422 [Accessed 25th July 2024].

Office of Transport and Traffic Policy and Planning. (2015) *Study on the development of facilities and services in the transport sector for the disabled and the elderly*. Available from: https://www.otp.go.th/uploads/tiny_uploads/ProjectOTP/2558/Project1-Older/FinalReport.pdf [Accessed 25th July 2024].

Ojanpää, H. & Näsänen, R. (2003) Effects of luminance and colour contrast on the search of information on display devices. *Displays*. 24 (4-5), 167–178. Available from: doi: 10.1016/j.displa.2004.01.003

Ompteda, V. K. (2009) Innovation in inclusive typography: A role for design research. In: *Proceedings of Include 2009 Conference, Include 2009, 5-8 April 2009, London, United Kingdom*. London, Royal College of Art. pp. 149-152.

Panke, K., Jakobsone, L., Svede, A. & Krumina, G. (2019) Smartphone viewing distance during active or passive tasks and relation to heterophoria. *Proceedings of the Fourth International Conference on Applications of Optics and Photonics – Volume 11207, AOP 2019, 31 May - 4 June 2019, Lisbon, Portugal*.

Bellingham, SPIE. Available from: doi: 10.1117/12.2527313

Power, C., Freire, A., Petrie, H. & Swallow, D. (2012) Guidelines are only half of the story: accessibility problems encountered by blind users on the web. In: *Proceedings of the SIGCHI Conference on Human Factors in Computing Systems, CHI '12, 5-10 May 2012, Austin, Texas*. New York, Association for Computing Machinery. pp. 433–442. Available from: doi: 10.1145/2207676.2207736

Punsongserm, R. (2019) Thai universal design font versus familiar Thai text fonts: The role of distinctive letterforms and suitable inter-letter space influence in blurred words. In: *Proceedings of Heritage & Vision: The 2019 International Conference on Design for Experience and Wellbeing, DEW 2019, 24-25 September 2019, Xi'an, China*. pp. 143–202.

Punsongserm, R. (2020) Comparative effectiveness of homologous Thai letterforms on visual word recognition: Thai universal design font versus familiar Thai text fonts. *Archives of Design Research*. 33 (3), 19–43. Available from: doi: 10.15187/adr.2020.08.33.3.19

Punsongserm, R. (2023) Effectiveness of Predominant Letterforms in Multi-Viewing Distances: Thai Universal Design Font Versus Familiar Thai Text Fonts. *Archives of Design Research*. 36 (4), 87–113. Available from: doi: 10.15187/adr.2023.11.36.4.87

Punsongserm, R., Sunaga, S. & Ihara, H. (2017a) Thai typefaces (Part 1): Assumption on visibility and legibility problems. *Archives of Design Research*. 30 (1), 5–23. Available from: doi: 10.15187/adr.2017.02.30.1.5

Punsongserm, R., Sunaga, S. & Ihara, H. (2017b) Thai typefaces (part 2): Criticism based on legibility test of some isolated characters. *Archives of Design Research*. 30 (2), 23–45. Available from: doi: 10.15187/adr.2017.05.30.2.23

Punsongserm, R., Sunaga, S. & Ihara, H. (2018a) Effectiveness of the homologous Thai letterforms on visibility under a simulated condition of low visual acuity. In: *Proceedings of Annual Conference of the 11th Typography Day, TYPODAY 2018, 2-3 March 2018, Mumbai, India*. Mumbai, Sir J. J. Institute of Applied Art. pp. 1-17.

Punsongserm, R., Sunaga, S. & Ihara, H. (2018b) Effectiveness of homologous Thai letterforms presented in parafoveal vision. *Information Design Journal*. 24 (2), 92–115. Available from: doi: 10.1075/idj.00002.pun

Punsongserm, R., Sunaga, S. & Ihara, H. (2018c) Roman-like Thai typefaces: Breakthrough or regression?. In: *Proceedings of Conference of ICDHS 10th+1: Back to the Future/The Future in the Past, 29-31 October 2018, Barcelona, Spain*. Barcelona, Edicions de la Universitat de Barcelona. pp. 580-585.

Punsongserm, R. & Suvakunta, P. (2022a) Do the small Thai font sizes on drug labels and documentation facilitate Thai readers? A practical review. *Archives of Design Research*. 35 (1), 51–73. Available from: doi: 10.15187/adr.2022.02.35.1.51

Punsongserm, R. & Suvakunta, P. (2022b) Optimal typeface and type size on Thai drug labeling and drug documentation: A recommendation for legal development. *Archives of Design Research*. 35 (4), 49–71. Available from: doi: 10.15187/adr.2022.11.35.4.49

Rattanakasamsuk, K. (2013) Elderly vision on legibility of Thai letters presented on LED panel. In: *Thanyaburi: Blooming color for life, ACA2013, 11-14 December 2013, Thanyaburi, Thailand*. Thanyaburi, Asia Color Association and Rajamangala University of Technology Thanyaburi. pp. 70-73.

Robolectric. (2023) *Robolectric: test drive your Android code*. Available from: https://robo-lectric.org/ [Accessed 5th February 2024].

Rojarayanont, P. (2001) The Attribute of a good Thai Font. In: *Thai Typeface*. Bangkok, National Electronics and Computer Technology Center, pp. 32-51.

Ross, S. A., Zhang, X., Fogarty, J. & Wobbrock, O. J. (2020) An Epidemiology-inspired Large-scale Analysis of Android App Accessibility. *Accessible Computing*. 13 (1), 1–36. Available from: doi: 10.1145/3348797

Samsung. (2024) *What size phone screen do I need?* Available from: https://www.samsung.com/uk/mobile-phone-buying-guide/what-screen-size/ [Accessed 29th January 2024].

Santayayon, M., Pipitpukdee, J. & Phantachat, W. (2011) A study of the legibility of Thai letters in Thai young adults aged 19–25 years old and older adults aged 60 years old and over. In: *Proceedings of the 5th International Conference on Rehabilitation Engineering & Assistive Technology, i-CREATe '11, 21-23 July 2011, Bangkok, Thailand*. Singapore, Singapore Therapeutic, Assistive & Rehabilitative Technologies (START) Centre. pp. 1-4.

Sawangjaroen, C., Emphandhu, D. & Kulachol, K. (2017) Guidelines of facilities design for all in national park. *Built Environment Inquiry Journal (BEI)*. 16 (2), 95–117.

Serra, C. L., Carvalho, P. L., Ferreira, P. L., Vaz, S. B. J. & Freire, P. A. (2015) Accessibility evaluation of e-government mobile applications in Brazil. *Procedia Computer Science*. 67, 348–357. Available from: doi: 10.1016/j.procs.2015.09.279

Silva, C., Eler, M. M. & Fraser, G. (2018) A survey on the tool support for the automatic evaluation of mobile accessibility. In: *Proceedings of the 8th International Conference on Software Development and Technologies for Enhancing Accessibility and Fighting Info-exclusion, DSAI'18, 20-22 June 2018, Thessaloniki, Greece*. New York, Association for Computing Machinery. pp. 286-293. Available from: doi: 10.1145/3218585.3218673

Slattery, T. J. & Rayners, K. (2009) The influence of text legibility on eye movements during reading. *Applied Cognitive Psychology*. 24 (8), 1129–1148. Available from: doi: 10.1002/acp.1623

Swearer, J. (2018) Visual Angle. In: Kreutzer, J. S., DeLuca, J. and Caplan, B. (eds.) *Encyclopedia of Clinical Neuropsychology*. Cham, Springer, pp. 3607-3608. Available from: doi: 10.1007/978-3-319-57111-9_1411

Teeravarunyou, S. & Laosirihongthong, T. (2003) Dynamic legibility of standard Thai fonts on traffic highway signs. In: *Proceedings of the 6th Asian Design International Conference, 14-17 October 2003, Tsukuba, Japan*. Tokyo, Science Council of Japan.

The Association of Siamese Architects Under Royal Patronage. (2014) *Building and environments design recommendation for all*. Available from: http://download.asa.or.th/03media/04law/ud/BAEDRFA.pdf [Accessed 25th July 2024].

Tigwell, W. G. (2021) Nuanced perspectives toward disability simulations from digital designers, blind, low vision, and color blind people. In: *Proceedings of the 2021 CHI Conference on Human Factors in Computing Systems, CHI '21, 8-13 May 2021, Yokohama, Japan*. New York, Association for Computing Machinery. pp. 1–15. Available from: doi: 10.1145/3411764.3445620

TPGi. (2023) *Colour Contrast Analyser (CCA)*. Available from: https://www.tpgi.com/color-contrast-checker/ [Accessed 2nd February 2023].

Waleetorncheepsawat, B., Pungrassamee, P., Obama, T. & Ikeda, M. (2012) Visual acuity of Thai letters with and without cataract experiencing goggles. *Journal of the Color Science Association of Japan*. 36, 216-217.

Wang, L., Sato, H., Rau, P. L. P., Fujimura, K., Gao, Q. & Asano, Y. (2009) Chinese text spacing on mobile phones for senior citizens. *Educational Gerontology*. 35 (1), 77–90. Available from: doi: 10.1080/03601270802491122

WebAIM. (2024) *Contrast Checker*. Available from: https://webaim.org/resources/contrast-checker/ [Accessed 25th January 2024].

World Wide Web Consortium: W3C. (2016a) *Understanding WCAG 2.0, contrast (minimum): Understanding SC 1.4.3*. Available from: https://www.w3.org/TR/UNDERSTANDING-WCAG20/visual-audio-contrast-contrast.html [Accessed 15th May 2023].

World Wide Web Consortium: W3C. (2016b) *Understanding WCAG 2.0, contrast (enhanced): Understanding SC 1.4.6*. Available from: https://www.w3.org/TR/UNDERSTANDING-WCAG20/visual-audio-contrast7.html [Accessed 15th May 2023].

World Wide Web Consortium: W3C. (2018) *Web content accessibility guidelines (WCAG) 2.1*. Available from: https://www.w3.org/TR/WCAG21/ [Accessed 15th May 2023].

World Wide Web Consortium: W3C. (2022a) *WCAG 2.2 understanding docs, understanding SC 1.4.3: Contrast (enhanced) (Level AA)*. Available from: https://www.w3.org/WAI/WCAG21/Understanding/contrast-minimum [Accessed 15th May 2023].

World Wide Web Consortium: W3C. (2022b) *WCAG 2.2 understanding docs, understanding SC 1.4.6: Contrast (enhanced) (Level AAA)*. Available from: https://www.w3.org/WAI/WCAG21/Understanding/contrast-enhanced [Accessed 15th May 2023].

World Wide Web Consortium: W3C. (2023a) *WCAG 2.2 understanding docs, understanding SC 1.4.3: Contrast (enhanced) (Level AA).* Available from: https://www.w3.org/WAI/WCAG22/Understanding/contrast-minimum [Accessed 15th May 2023].

World Wide Web Consortium: W3C. (2023b) *WCAG 2.2 understanding docs, understanding SC 1.4.6: Contrast (enhanced) (Level AAA).* Available from: https://www.w3.org/WAI/WCAG22/Understanding/contrast-enhanced [Accessed 15th May 2023].

Yeh, P. C. (2015) A Study on Visual Limitation of Age, Numerical Size, and Exposure Time While Users Operate Mobile Devices. *Perceptual and Motor Skills*. 121 (3), 823–831. Available from: doi: 10.2466/24.PMS.121c26x3

Yeh, P. C. (2020) Impact of button position and touchscreen font size on healthcare device operation by older adults. *Heliyon*. 6 (6). Available from: doi: 10.1016/j.heliyon.2020.e04147

Yoshimura, M., Kitazawa, M., Maeda, Y., Mimura, M., Tsubota, K. & Kishimoto, T. (2017) Smartphone viewing distance and sleep: An experimental study utilizing motion capture technology. *Nature and Science of Sleep*. 9, 59–65. Available from: doi: 10.2147/NSS.S123319

Ziefle, M. (2010) Information presentation in small screen devices: the trade-off between visual density and menu foresight. *Applied ergonomics*. 41 (6), 719–730. Available from: doi: 10.1016/j.apergo.2010.03.001

Zorko, A., Valenko, S. I., Tomiša, M., Keček, D. & Čerepinko, D. (2017) The impact of the text and background color on the screen reading experience. *Technical Journal*. 11 (3), 78–82.
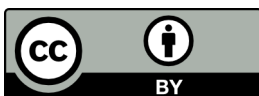
Print quality optimization in screen printing by AM and FM screening using Taguchi's Grey Relational Analysis technique

ABSTRACT

This is an experimental and statistical approach to assess the impact of AM and FM screen ruling in screen printing under the condition such as printing of a test target on both coated and uncoated paper with three different types of screen mesh count. The change in print quality according to the screen mesh count are focused here, because the screen mesh count is one of the key elements in screen printing that influences the ink flow through the mesh as well as the excellence of stencil image or halftone dots over the mesh. Under three different screen mesh count, the impact of AM and FM halftone in the print quality on both coated and uncoated paper grades are evaluated in the analysis part. The print quality assessment parameters taken as solid ink density, dot gain, hue error and print contrast at 30%, 50%, & 70% tonal areas of the print. Twelve different combinations of input variables such as coated and uncoated substrate, AM and FM halftone dots, 100 lpi, 120 lpi and 140 lpi screen mesh counts etc. are employed at different print trials. The print quality assessment and ranking of each experiment are done by Taguchi's Grey Relational Analysis, which is a best method to implement in the decision-making process of quality control.

KEY WORDS

Screen printing, AM and FM halftone dots, LPI, solid ink density, dot gain, hue error, print contrast, Taguchi's Grey Relational Analysis

Soumen Basak [1] (iD)
Saritha P.C [2] (iD)
Kanai Chandra Paul [1] (iD)

[1] Jadavpur University, Department of Printing Engineering, West Bengal, India
[2] Institute of Printing Technology and Government Polytechnic College, Department of Printing Technology, Kerala, India

Corresponding author:
Soumen Basak
e-mail:
soumen.basak@jadavpuruniversity.in

Introduction

The screen printing is one of the versatile printing technologies among the conventional printing method, that utilizes a stencil type image carrier for the printing function. The stencil is attachable over a screen mesh and the printing can be done by forcing ink through the stencil opening by a squeegee on to the substrate. Figure 1 shows the schematic diagram of a screen printing unit.

The printing technique is adaptable to deliver print on a wide range of substrate like paper, paperboard, glass, plastics, metals, ceramics etc. irrespective of their surface textures and shape (Kipphan, 2001). The characteristic of the screen mesh used is a major factor that influences the quality of printed elements in screen printing.
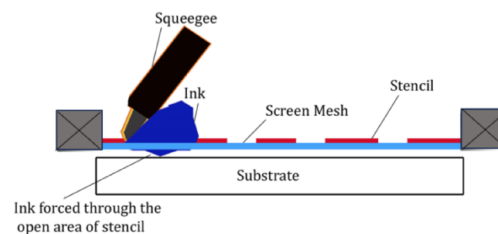
» **Figure 1:** *Schematic diagram of a screen-printing unit*

The commonly used screen mesh is nylon, polyester, stainless steel etc. in the industrial purposes. For screen mesh, the screen thread diameter and the open area of mesh is the two major critical parameters that describes the degree of reproducibility of halftone dots via screen printing method.

According to the studies, the fabric with more thread per linear distance is capable to deliver high print quality. At the same time, it should have enough open area to guide the passage of average pigment size of the ink through it to the substrate. Smaller thread diameter builds up finer screen mesh (Novaković et al., 2016). Figure 2 represents the woven structure of screen mesh used for transferring to the substrate.
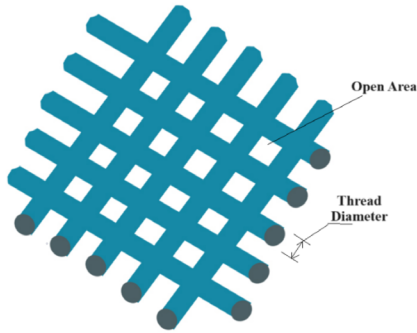
» **Figure 2:** *The woven structure of screen mesh*

In comparison to other printing methods, screen printing is relatively easy to print on any desired material. However, in order to get the right design with the correct print detail, print resolution, coverage and hand feel, etc., It is necessary to select the right mesh count and ink system for a particular design type. A higher mesh count resulted in high accuracy in design with less ink consumption, good hand feels and good background coverage. On the other hand, a lower mesh count resulted in poor background coverage, poor print detail, and poor print sharpness. There is no significant change in colour speed performance of the printed material with the change in mesh count (Dina, Uddin & Fatema, 2020).

In halftone reproduction, the size of halftone dot should be larger than that of the opening area of the screen mesh used otherwise dot loss or lack of image details in the final print will be the result. This is a common factor applicable to both AM and FM mode of halftone printing via screen printing process. Moreover, the halftone dot reproduction by screen printing is somewhat thoughtful in terms of screen mesh characteristics, accuracy of stencil preparation method, type of stencil used, characteristics of ink, squeegee pressure etc.

In graphic reproduction process, the FM dots are better in highlight and shadow areas and also gives better print results in those areas but fails in middle-tone, while the AM dots are better in middle-tone areas to give the better results (Poljacek Mahovic et al., 2005). The material that plans to print is equally important as the specifics of our screen print process. The composition, structure and characteristics of the printed items, along with the composition, viscosity and other properties of ink, all contribute to the quality of the screen printed matter (Cazac et al., 2018).

The Taguchi method is laid down by Genichi Taguchi, a Japanese engineer in 1950's and acts as a better concept for the improvement of quality of product and process involved in a manufacturing process. Taguchi's concept of robust design indicates the design which gives the production of goods with less sensitive responses towards the factors that causes variability in the manufacturing process (Kumar, 2020).

The Taguchi method is a better approach to apply in the industrial production activities that will entirely modify the outlook of production process on quality improvement and error free performance aspects (Roy, 2010).

The Grey Relational Analysis Concept is laid down by Deng Julong in 1982. This is a statistical approach that acts as a reliable decision-making tool in multiple criteria-based decision-making situations in various industrial based applications. Taguchi's GRA approach is useful methodology in the quality control process (Kumar & Baral, 2023).

The print quality assessment is probable with the quantitative analysis of dot gain, dot area, print contrast, hue error etc. The dot gain and dot area values that monitors the dot reproduction accuracy of the graphic reproduction at the final print. The print contrast value represents the accuracy of reproducing shadow details on the final print. The hue error that represents the percentage of change in actual hue in the final print (Dharavath, Bensel & Gaddam, 2005).

This research is an experimental study to find the influence of factors such as screen mesh ruling, AM and FM halftone dots, coated and uncoated paper grades etc. on the print quality of screen printing.

The attainment of best quality is assessed by Taguchi's Grey Relational Analysis method.

Methods

The research was conducted by printing an ideal grey scale image consisting of both AM and FM dots onto both coated and uncoated paper by screen printing method. Three different screen mesh ruling such as 100 lpi, 120 lpi and 140 lpi (lines per inch) were used to form the stencils.

The stencils consisting of halftone grey scale were fixed in flatbed semiautomatic screen printing machine:ATOM 1520, APL Machinery Pvt.Ltd. and prints were obtained on both coated and uncoated papers. The printed samples were subjected to the visual inspection by Digital Microscope (LEICA, S8APO) and the quantitative optical property measurement by Spectro-Densitometer (such as X-Rite Spectro Eye & TECHKON GmbH Spectro Dens).

The 30%, 50% and & 70% tonal areas (representing highlight area, middle tone area and shadow area respectively) were considered for quantitative assessment of the quality. The Solid Ink Density, Dot Gain, Hue Error and Print Contrast etc. of these tonal values were analysed with Taguchi's Grey Relational Analysis. The sequential flow of research work is shown in the illustration Figure 3.
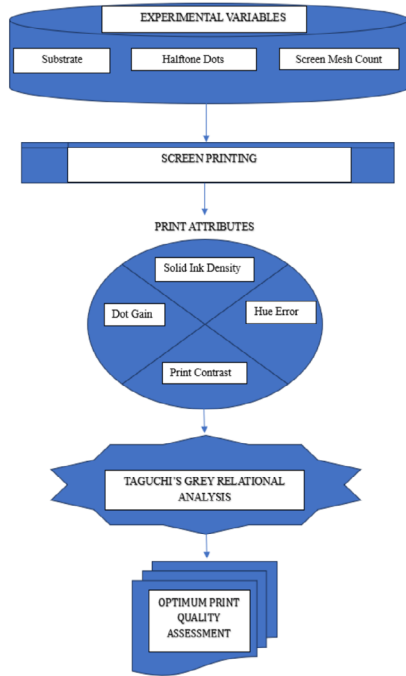
» **Figure 3:** *Work Flow*

The Table 1 represents the list of input variables taken for the process and the various parameters of the prints considered for assessing the print quality. These were taken as the key elements in the Taguchi's Grey Relational Analysis of this research work. Table 2 represents necessary equations used for assessment of print quality using Taguchi's Grey Relational Analysis technique.

Table 1

Elements taken for Taguchi's Grey Relational Analysis

No.	Input variables of experiment	Parameters
1	Coated Paper, 100 lpi Mesh, AM Dot	Solid Ink Density
2	Coated Paper, 120 lpi Mesh, AM Dot	
3	Coated Paper, 140 lpi Mesh, AM Dot	
4	Coated Paper, 100 lpi Mesh, FM Dot	
5	Coated Paper, 120 lpi Mesh, FM Dot	
6	Coated Paper, 140 lpi Mesh, FM Dot	Dot Gain
7	Uncoated Paper, 100 lpi Mesh, AM Dot	
8	Uncoated Paper, 120 lpi Mesh, AM Dot	Hue Error
9	Uncoated Paper, 140 lpi Mesh, AM Dot	Print Contrast
10	Uncoated Paper, 100 lpi Mesh, FM Dot	
11	Uncoated Paper, 120 lpi Mesh, FM Dot	
12	Uncoated Paper, 140 lpi Mesh, FM Dot	

Table 2

Equations used for assessment of print quality

Normalization of Performance Index Data,

For beneficial attributes (higher is better),

$$Xi^*(k) = \frac{Xi(k) - minXi(k)}{Xi(k) - Xi(k)} \tag{1}$$

For non-beneficial attributes (lower is better),

$$Xi^*(k) = \frac{max\ Xi(k) - Xi(k)}{Xi(k) - Xi(k)} \tag{2}$$

where,

$Xi^*(k)$ = Normalized value of ith data of 'k' responses.

$Xi(k)$ = Actual value of ith data of 'k' responses.

min $Xi(k)$ = Lowest value of $Xi(k)$ for 'k' responses.

max $Xi(k)$ = Highest value of $Xi(k)$ for 'k' responses.

Deviation Sequence,

$$\Delta i(k) = X_0^m(k) - Xi^*(k) \tag{3}$$

where,

$\Delta i(k)$ = Deviation sequence of ith data for 'k' responses.

$X_0^m(k)$ = Maximum value among the $Xi(k)$ elements of 'k' responses.

$Xi^*(k)$ = Normalized value of performance index of 'k' responses.

Grey Relational Co-efficient,

$$\xi i(k) = \frac{\Delta\ min\ +\ \xi\ \Delta\ max}{\Delta\ i(k) + \xi\ \Delta\ max} \tag{4}$$

where,

$\xi i(k)$ = Grey Relational Co-efficient of ith data for 'k' responses.

Δmin = Minimum value obtained from Deviation sequence.

Δmax = Maximum value obtained from Deviation sequence.

$\Delta i(k)$ = Deviation sequence of ith data for 'k' responses.

Dynamic Distinguished Coefficient (ξ) = 0-1(For multiple decision-making criteria, the value can take as 0.5).

Grey Relational Grade,

$$Yi = \frac{1}{n} \sum_{k=1}^{n} \xi i(k) \tag{5}$$

where,

Yi = Grey Relational Grade of ith data for 'k' responses.

n = Number of data responses

$\xi i(k)$ = Grey Relational Co-efficient of ith data for 'k' responses

Results

The Figure 4 to Figure 8 graphically represents the output responses such as: dot area, dot gain, hue error, print contrast and solid ink densities of reproduced image against the target dot percentage that ranging from 5% to 100% dot coverage with an incremental step of 5%. The Figure 4 and Figure 5 shows the Dot Area curve and followed by Dot Gain curve respectively. These curves show that, the dot area of printed sample is comparatively higher for FM dots on uncoated paper with 100 lpi mesh count. This represents the higher dot gain associated with uncoated paper with lower mesh count and FM dot combination in screen printing process.

Meanwhile, the AM dot print on coated paper with 140 lpi mesh count gives a better dot area reproduction when comparing to all other cases. This implies that, higher the mesh count lesser will be the dot gain and also the AM dots with smooth textured substrate also facilitates the attainment of optimum dot gain. Lower mesh count with FM dots is a poor choice in screen printing. Because the larger mesh openings of screen at lower mesh count will facilitate considerable loss of FM dot details on the stencil over the mesh and there will be high dot gain issues in the final reproduction due to larger openings.

Also, the uncoated paper facilitates the unpredictable dot gain due to the undesirable ink absorption on to its porous structure and unevenness of the surfaces. Also there is a chance of optical dot gain due to the light scattering effects from the paper surface. It has been observed that at highlight areas up to 15%, there is loss of dots with 140 lpi and 120 lpi mesh count in case of AM dots. This may be due to the inability of the screen mesh to carry the finer sized AM dots at those highlight areas.

Meanwhile the FM dots performed in a better way at the highlight and shadow areas only in the case of higher mesh count. The Figure 6 shows the graphical representation of Hue Error of print.

The overall Hue error is minimum for prints on coated paper with AM dots using 140 lpi screen mesh. The Hue Error remains constant till the 40% Dot Area. The higher Hue Error value is obtained for uncoated paper especially at the middle tone areas. However, the hue error is the indicator of purity of ink in the print and it is influenced by press conditions, and the spectral behaviour of the ink and substrate used.

The Figure 7 shows the Print Contrast curve, in which, the best print contrast is obtained for AM dot print on coated paper with 140 lpi mesh count and the lowest print contrast is found on the FM dot print on uncoated paper with 100 lpi mesh count. The print contrast represents the accuracy of tonal reproduction in contrast with the shadow details. The higher mesh count of screen with AM dot and smooth textured substrate improves the print contrast of screen printing. The Print Contrast is near about zero beyond 85% Dot Area in all the cases.

Figure 8 is a bar graph that shows the solid ink densities reproduced on the print, among which, the more vibrant colour of solid ink coverage is obtained for FM dots on coated paper with low mesh count. It was also observed that lower the screen mesh count, higher will be the ink deposit on the substrate.
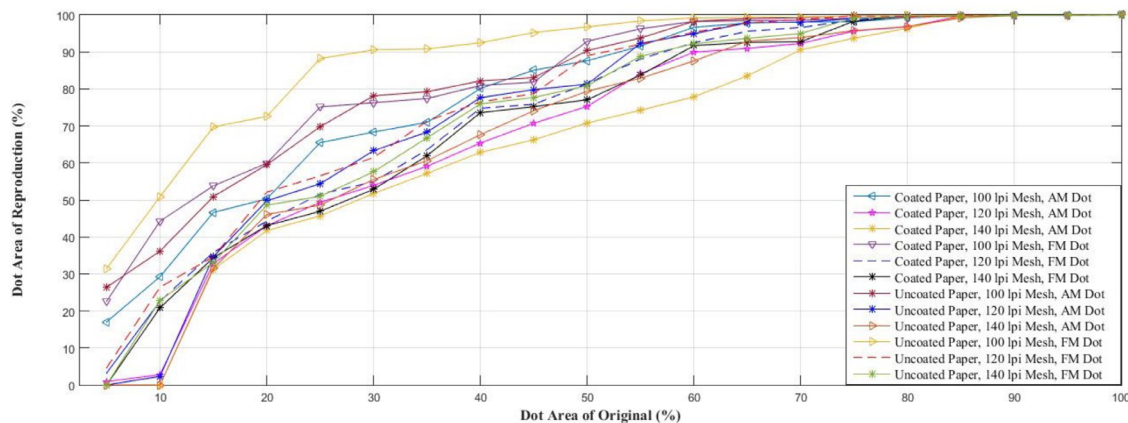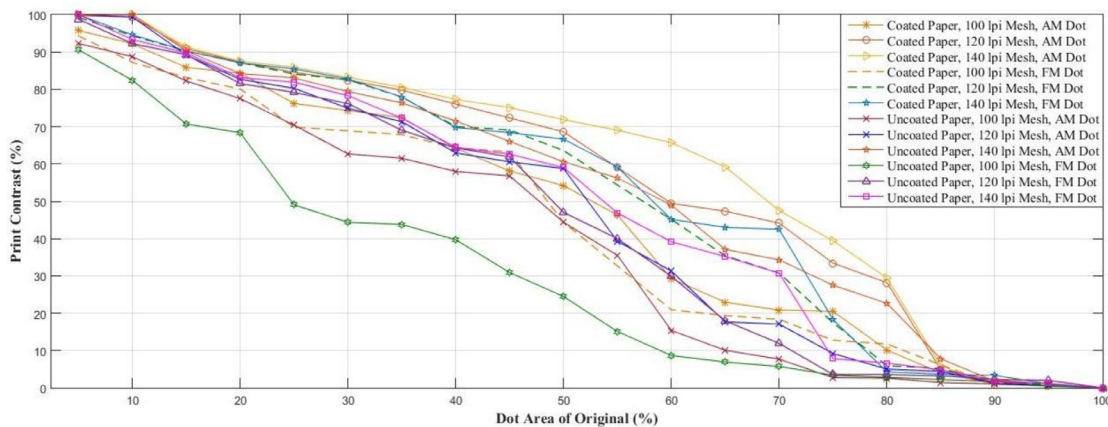

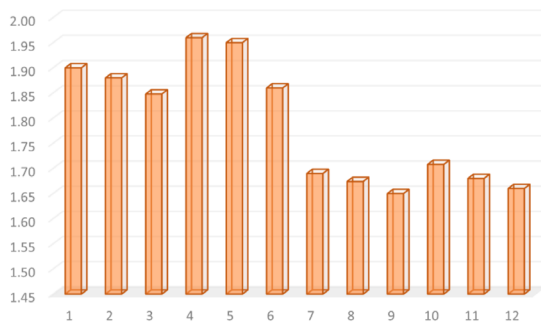» **Figure 4:** *Tonal Reproduction Curve for Dot area*
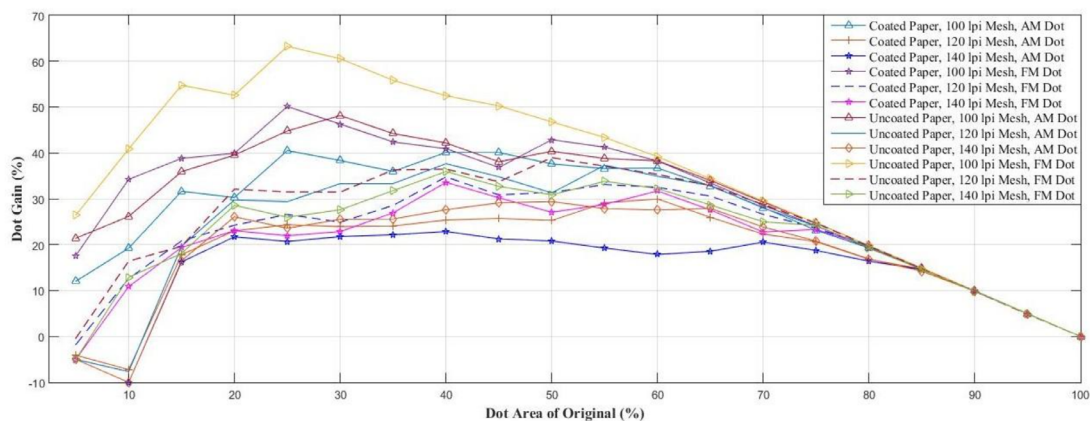
» **Figure 5:** *Variation in Dot Gain with respect to percentage Dot Area of the original*
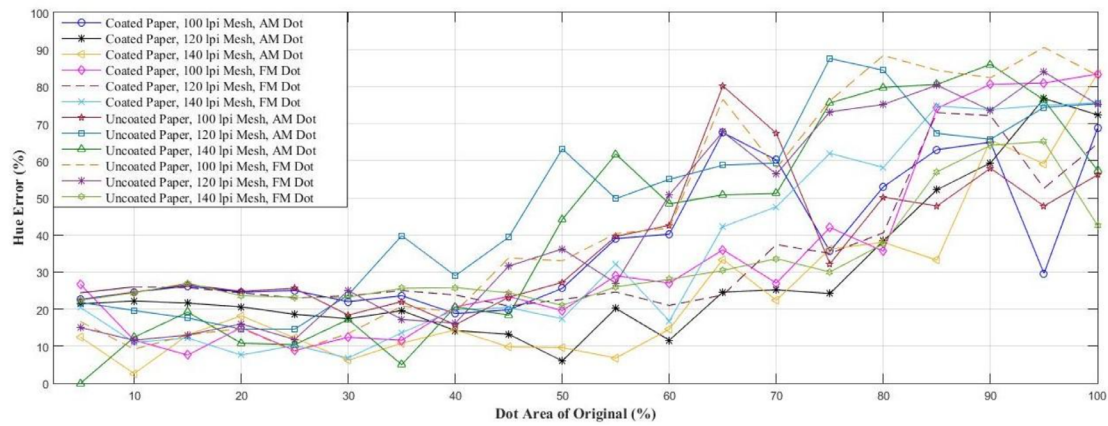
» **Figure 6:** *Variation in Hue Error with percentage Dot Area of the original*

» **Figure 7:** *Variation in Print Contrast with reference to percentage Dot Area of the original*

» **Figure 8:** *The solid ink density of various prints of different combination of Mesh and Substrate*

The Taguchi's Grey Relational Analysis is carried out in various stages such as Normalization of data (shown in Table 3), calculation of Deviation sequence (shown in Table 4), calculation of Grey Relational Coefficient (shown in Table 5).

Based on quality assessment parameters such as SID, Dot Gain, Hue Error and Print Contrast, each experimental approaches are ranked (vide shown in Table 6 to Table 15) and among which the high-est GRA score indicates the best print quality.

Discussions

The GRA index score for SID is shown in Table 6 indicates that the coated grade paper has the ability to reproduce better solid ink density by screen printing using different types of dots and mesh count than that of uncoated paper. The smooth surface texture of the coated paper enhances the excellent reproduction of solid ink density in all cases. But for uncoated paper, the irregular and matt surface texture diminishes such effects due to the uneven distribution of ink over the uncoated surface as well the undesirable light scattering effects from the paper.

At lower screen mesh count, the ink deposition on the substrate will be more in screen printing than that of higher screen mesh count. Here the 100 lpi screen mesh count can reproduce better solid ink densities than that of 140 lpi mesh count. The lower the screen meshes count more will be the mesh open areas, so the ink flow will be more and the heavier ink deposition will be the result. Also, at solid ink density deposition, the printed sample with FM dots offers higher optical densities than that of AM dots as shown in Table 6. The AM dot with low mesh count is also capable to deliver heavy ink deposition, but the FM dots are comparatively capable to give more vibrant colours than AM at solid densities.

Table 3

Normalised Data of Performance Index

Expe-riment No.	Solid Ink Density	Dot Gain at 30%	Dot Gain at 50%	Dot Gain at 70%	Hue Error at 30%	Hue Error at 50%	Hue Error at 70%	Print Contrast at 30%	Print Contrast at 50%	Print Contrast at 70%
1	0.81	0.57	0.35	0.16	0.16	0.66	0.16	0.77	0.63	0.36
2	0.74	0.94	0.83	0.81	0.40	1.00	0.94	0.98	0.93	0.92
3	0.64	1.00	1.00	1.00	1.00	0.94	1.00	1.00	1.00	1.00
4	1.00	0.37	0.15	0.10	0.67	0.76	0.90	0.63	0.42	0.30
5	0.97	0.92	0.59	0.32	0.07	0.71	0.67	0.98	0.83	0.60
6	0.68	0.97	0.76	0.75	0.97	0.80	0.44	0.99	0.89	0.88
7	0.13	0.32	0.25	0.02	0.35	0.63	0.00	0.47	0.42	0.05
8	0.08	0.70	0.60	0.17	0.06	0.00	0.18	0.79	0.72	0.27
9	0.00	0.90	0.67	0.63	0.41	0.33	0.36	0.90	0.76	0.68
10	0.19	0.00	0.00	0.00	0.62	0.53	0.21	0.00	0.00	0.00
11	0.10	0.75	0.30	0.08	0.00	0.47	0.24	0.82	0.48	0.15
12	0.03	0.85	0.61	0.50	0.10	0.74	0.75	0.87	0.73	0.60

Table 4

Deviation Sequence

Exper-iment No.	Solid Ink Density	Dot Gain at 30%	Dot Gain at 50%	Dot Gain at 70%	Hue Error at 30%	Hue Error at 50%	Hue Error at 70%	Print Contrast at 30%	Print Contrast at 50%	Print Contrast at 70%
1	0.19	0.43	0.65	0.84	0.84	0.34	0.84	0.23	0.37	0.64
2	0.26	0.06	0.17	0.19	0.60	0.00	0.06	0.02	0.07	0.08
3	0.36	0.00	0.00	0.00	0.00	0.06	0.00	0.00	0.00	0.00
4	0.00	0.63	0.85	0.90	0.33	0.24	0.10	0.37	0.58	0.70
5	0.03	0.08	0.41	0.68	0.93	0.29	0.33	0.02	0.17	0.40
6	0.32	0.03	0.24	0.25	0.03	0.20	0.56	0.01	0.11	0.12
7	0.87	0.68	0.75	0.98	0.65	0.37	1.00	0.53	0.58	0.95
8	0.92	0.30	0.40	0.83	0.94	1.00	0.82	0.21	0.28	0.73
9	1.00	0.10	0.33	0.37	0.59	0.67	0.64	0.10	0.24	0.32
10	0.81	1.00	1.00	1.00	0.38	0.47	0.79	1.00	1.00	1.00
11	0.90	0.25	0.70	0.92	1.00	0.53	0.76	0.18	0.52	0.85
12	0.97	0.15	0.39	0.50	0.90	0.26	0.25	0.13	0.27	0.40

Table 5 (part 1)

Grey Relational Coefficient

Exper-iment No.	Solid Ink Density	Dot Gain at 30%	Dot Gain at 50%	Dot Gain at 70%	Hue Error at 30%	Hue Error at 50%	Hue Error at 70%	Print Contrast at 30%	Print Contrast at 50%	Print Contrast at 70%
1	0.72	0.54	0.44	0.37	0.37	0.59	0.37	0.69	0.57	0.44
2	0.66	0.90	0.74	0.72	0.46	1.00	0.89	0.96	0.88	0.86
3	0.58	1.00	1.00	1.00	1.00	0.89	1.00	1.00	1.00	1.00
4	1.00	0.44	0.37	0.36	0.60	0.68	0.83	0.58	0.46	0.42
5	0.94	0.86	0.55	0.42	0.35	0.63	0.60	0.97	0.74	0.56
6	0.61	0.95	0.67	0.67	0.94	0.72	0.47	0.98	0.82	0.81
7	0.36	0.42	0.40	0.34	0.44	0.57	0.33	0.49	0.46	0.34
8	0.35	0.63	0.55	0.38	0.35	0.33	0.38	0.70	0.64	0.41
9	0.33	0.84	0.60	0.58	0.46	0.43	0.44	0.84	0.68	0.61

Table 5 (part 2)

Grey Relational Coefficient

Exper- iment No.	Solid Ink Density	Dot Gain at 30%	Dot Gain at 50%	Dot Gain at 70%	Hue Error at 30%	Hue Error at 50%	Hue Error at 70%	Print Contrast at 30%	Print Contrast at 50%	Print Contrast at 70%
10	0.38	0.33	0.33	0.33	0.57	0.51	0.39	0.33	0.33	0.33
11	0.36	0.67	0.42	0.35	0.33	0.49	0.40	0.73	0.49	0.37
12	0.34	0.77	0.56	0.50	0.36	0.66	0.67	0.80	0.65	0.55

Table 6

The Grey Relational Grade and Ranking for SID

Rank	Experimental variables	Grey Relational Grade	Experiment No.
1	Coated Paper, 100 lpi Mesh, FM Dot	1	4
2	Coated Paper, 120 lpi Mesh, FM Dot	0.939394	5
3	Coated Paper, 100 lpi Mesh, AM Dot	0.72093	1
4	Coated Paper, 120 lpi Mesh, AM Dot	0.659574	2
5	Coated Paper, 140 lpi Mesh, FM Dot	0.607843	6
6	Coated Paper, 140 lpi Mesh, AM Dot	0.580524	3
7	Uncoated Paper, 100 lpi Mesh, FM Dot	0.380835	10
8	Uncoated Paper, 100 lpi Mesh, AM Dot	0.364706	7
9	Uncoated Paper, 120 lpi Mesh, FM Dot	0.356322	11
10	Uncoated Paper, 120 lpi Mesh, AM Dot	0.351474	8
11	Uncoated Paper, 140 lpi Mesh, FM Dot	0.340659	12
12	Uncoated Paper, 140 lpi Mesh, AM Dot	0.333333	9

Table 8

The Grey Relational Grade and Ranking for 50% Dot Gain

Rank	Experimental variables	Grey Relational Grade	Experiment No.
1	Coated Paper, 140 lpi Mesh, AM Dot	1	3
2	Coated Paper, 120 lpi Mesh, AM Dot	0.743286	2
3	Coated Paper, 140 lpi Mesh, FM Dot	0.674287	6
4	Uncoated Paper, 140 lpi Mesh, AM Dot	0.60192	9
5	Uncoated Paper, 140 lpi Mesh, FM Dot	0.563111	12
6	Uncoated Paper, 120 lpi Mesh, AM Dot	0.552834	8
7	Coated Paper, 120 lpi Mesh, FM Dot	0.550254	5
8	Coated Paper, 100 lpi Mesh, AM Dot	0.43576	1
9	Uncoated Paper, 120 lpi Mesh, FM Dot	0.416692	11
10	Uncoated Paper, 100 lpi Mesh, AM Dot	0.398931	7
11	Coated Paper, 100 lpi Mesh, FM Dot	0.370185	4
12	Uncoated Paper, 100 lpi Mesh, FM Dot	0.333333	10

Table 7

The Grey Relational Grade and Ranking for 30% Dot Gain

Rank	Experimental variables	Grey Relational Grade	Experiment No.
1	Coated Paper, 140 lpi Mesh, AM Dot	1	3
2	Coated Paper, 140 lpi Mesh, FM Dot	0.945868	6
3	Coated Paper, 120 lpi Mesh, AM Dot	0.898934	2
4	Coated Paper, 120 lpi Mesh, FM Dot	0.860275	5
5	Uncoated Paper, 140 lpi Mesh, AM Dot	0.836995	9
6	Uncoated Paper, 140 lpi Mesh, FM Dot	0.768237	12
7	Uncoated Paper, 120 lpi Mesh, FM Dot	0.666259	11
8	Uncoated Paper, 120 lpi Mesh, AM Dot	0.626478	8
9	Coated Paper, 100 lpi Mesh, AM Dot	0.538942	1
10	Coated Paper, 100 lpi Mesh, FM Dot	0.441564	4
11	Uncoated Paper, 100 lpi Mesh, AM Dot	0.423592	7
12	Uncoated Paper, 100 lpi Mesh, FM Dot	0.333333	10

Table 9

The Grey Relational Grade and Ranking for 70% Dot Gain

Rank	Experimental variables	Grey Relational Grade	Experiment No.
1	Coated Paper, 140 lpi Mesh, AM Dot	1	3
2	Coated Paper, 120 lpi Mesh, AM Dot	0.720117	2
3	Coated Paper, 140 lpi Mesh, FM Dot	0.669859	6
4	Uncoated Paper, 140 lpi Mesh, AM Dot	0.575611	9
5	Uncoated Paper, 140 lpi Mesh, FM Dot	0.50187	12
6	Coated Paper, 120 lpi Mesh, FM Dot	0.424586	5
7	Uncoated Paper, 120 lpi Mesh, AM Dot	0.375753	8
8	Coated Paper, 100 lpi Mesh, AM Dot	0.372034	1
9	Coated Paper, 100 lpi Mesh, FM Dot	0.358086	4
10	Uncoated Paper, 120 lpi Mesh, FM Dot	0.352903	11
11	Uncoated Paper, 100 lpi Mesh, AM Dot	0.338944	7
12	Uncoated Paper, 100 lpi Mesh, FM Dot	0.333333	10

Table 10

The Grey Relational Grade and Ranking for 30% Hue Error

Rank	Experimental variables	Grey Relational Grade	Experiment No.
1	Coated Paper, 140 lpi Mesh, AM Dot	1	3
2	Coated Paper, 140 lpi Mesh, FM Dot	0.94	6
3	Coated Paper, 100 lpi Mesh, FM Dot	0.602564	4
4	Uncoated Paper, 100 lpi Mesh, FM Dot	0.566265	10
5	Uncoated Paper, 140 lpi Mesh, AM Dot	0.460784	9
6	Coated Paper, 120 lpi Mesh, AM Dot	0.456311	2
7	Uncoated Paper, 100 lpi Mesh, AM Dot	0.435185	7
8	Coated Paper, 100 lpi Mesh, AM Dot	0.373016	1
9	Uncoated Paper, 140 lpi Mesh, FM Dot	0.356061	12
10	Coated Paper, 120 lpi Mesh, FM Dot	0.350746	5
11	Uncoated Paper, 120 lpi Mesh, AM Dot	0.348148	8
12	Uncoated Paper, 120 lpi Mesh, FM Dot	0.333333	11

Table 11

The Grey Relational Grade and Ranking for 50% Hue Error

Rank	Experimental variables	Grey Relational Grade	Experiment No.
1	Coated Paper, 120 lpi Mesh, AM Dot	1	2
2	Coated Paper, 140 lpi Mesh, AM Dot	0.888199	3
3	Coated Paper, 140 lpi Mesh, FM Dot	0.715	6
4	Coated Paper, 100 lpi Mesh, FM Dot	0.677725	4
5	Uncoated Paper, 140 lpi Mesh, FM Dot	0.655963	12
6	Coated Paper, 120 lpi Mesh, FM Dot	0.632743	5
7	Coated Paper, 100 lpi Mesh, AM Dot	0.593361	1
8	Uncoated Paper, 100 lpi Mesh, AM Dot	0.574297	7
9	Uncoated Paper, 100 lpi Mesh, FM Dot	0.514388	10
10	Uncoated Paper, 120 lpi Mesh, FM Dot	0.486395	11
11	Uncoated Paper, 140 lpi Mesh, AM Dot	0.428144	9
12	Uncoated Paper, 120 lpi Mesh, AM Dot	0.333333	8

Table 12 (part 1)

The Grey Relational Grade and Ranking for 70% Hue Error

Rank	Experimental variables	Grey Relational Grade	Experiment No.
1	Coated Paper, 140 lpi Mesh, AM Dot	1	3
2	Coated Paper, 120 lpi Mesh, AM Dot	0.889328	2

Table 12 (part 2)

The Grey Relational Grade and Ranking for 70% Hue Error

Rank	Experimental variables	Grey Relational Grade	Experiment No.
3	Coated Paper, 100 lpi Mesh, FM Dot	0.830258	4
4	Uncoated Paper, 140 lpi Mesh, FM Dot	0.667656	12
5	Coated Paper, 120 lpi Mesh, FM Dot	0.6	5
6	Coated Paper, 140 lpi Mesh, FM Dot	0.471698	6
7	Uncoated Paper, 140 lpi Mesh, AM Dot	0.438596	9
8	Uncoated Paper, 120 lpi Mesh, FM Dot	0.39823	11
9	Uncoated Paper, 100 lpi Mesh, FM Dot	0.387263	10
10	Uncoated Paper, 120 lpi Mesh, AM Dot	0.378151	8
11	Coated Paper, 100 lpi Mesh, AM Dot	0.373134	1
12	Uncoated Paper, 100 lpi Mesh, AM Dot	0.333333	7

Table 13

The Grey Relational Grade and Ranking for 30% Print Contrast

Rank	Experimental variables	Grey Relational Grade	Experiment No.
1	Coated Paper, 140 lpi Mesh, AM Dot	1	3
2	Coated Paper, 140 lpi Mesh, FM Dot	0.97837	6
3	Coated Paper, 120 lpi Mesh, FM Dot	0.967088	5
4	Coated Paper, 120 lpi Mesh, AM Dot	0.961473	2
5	Uncoated Paper, 140 lpi Mesh, AM Dot	0.835247	9
6	Uncoated Paper, 140 lpi Mesh, FM Dot	0.798154	12
7	Uncoated Paper, 120 lpi Mesh, FM Dot	0.734116	11
8	Uncoated Paper, 120 lpi Mesh, AM Dot	0.700236	8
9	Coated Paper, 100 lpi Mesh, AM Dot	0.685541	1
10	Coated Paper, 100 lpi Mesh, FM Dot	0.575144	4
11	Uncoated Paper, 100 lpi Mesh, AM Dot	0.486471	7
12	Uncoated Paper, 100 lpi Mesh, FM Dot	0.333333	10

Table 14 (part 1)

The Grey Relational Grade and Ranking for 50% Print Contrast

Rank	Experimental variables	Grey Relational Grade	Experiment No.
1	Coated Paper, 140 lpi Mesh, AM Dot	1	3
2	Coated Paper, 120 lpi Mesh, AM Dot	0.879562	2
3	Coated Paper, 140 lpi Mesh, FM Dot	0.820181	6

Table 14 (part 2)

The Grey Relational Grade and Ranking for 50% Print Contrast

Rank	Experimental variables	Grey Relational Grade	Experiment No.
4	Coated Paper, 120 lpi Mesh, FM Dot	0.741233	5
5	Uncoated Paper, 140 lpi Mesh, AM Dot	0.677953	9
6	Uncoated Paper, 140 lpi Mesh, FM Dot	0.648809	12
7	Uncoated Paper, 120 lpi Mesh, AM Dot	0.644314	8
8	Coated Paper, 100 lpi Mesh, AM Dot	0.573083	1
9	Uncoated Paper, 120 lpi Mesh, FM Dot	0.488219	11
10	Coated Paper, 100 lpi Mesh, FM Dot	0.463068	4
11	Uncoated Paper, 100 lpi Mesh, AM Dot	0.462986	7
12	Uncoated Paper, 100 lpi Mesh, FM Dot	0.333333	10

Table 15

The Grey Relational Grade and Ranking for 70% Print Contrast

Rank	Experimental variables	Grey Relational Grade	Experiment No.
1	Coated Paper, 140 lpi Mesh, AM Dot	1	3
2	Coated Paper, 120 lpi Mesh, AM Dot	0.861357	2
3	Coated Paper, 140 lpi Mesh, FM Dot	0.805676	6
4	Uncoated Paper, 140 lpi Mesh, AM Dot	0.612611	9
5	Coated Paper, 120 lpi Mesh, FM Dot	0.555078	5
6	Uncoated Paper, 140 lpi Mesh, FM Dot	0.554395	12
7	Coated Paper, 100 lpi Mesh, AM Dot	0.439206	1
8	Coated Paper, 100 lpi Mesh, FM Dot	0.41748	4
9	Uncoated Paper, 120 lpi Mesh, AM Dot	0.407046	8
10	Uncoated Paper, 120 lpi Mesh, FM Dot	0.369722	11
11	Uncoated Paper, 100 lpi Mesh, AM Dot	0.344066	7
12	Uncoated Paper, 100 lpi Mesh, FM Dot	0.333333	10

Table 16 (part 1)

The Grey Relational Grade and Ranking for Overall Performance

Experiment No.	Experimental variables	Grey Relational Grade	Rank
3	Coated Paper, 140 lpi Mesh, AM Dot	0.946872	1
2	Coated Paper, 120 lpi Mesh, AM Dot	0.806994	2
6	Coated Paper, 140 lpi Mesh, FM Dot	0.762878	3
5	Coated Paper, 120 lpi Mesh, FM Dot	0.66214	4
12	Uncoated Paper, 140 lpi Mesh, FM Dot	0.585491	5

Table 16 (part 2)

The Grey Relational Grade and Ranking for Overall Performance

Experiment No.	Experimental variables	Grey Relational Grade	Rank
9	Uncoated Paper, 140 lpi Mesh, AM Dot	0.580119	6
4	Coated Paper, 100 lpi Mesh, FM Dot	0.573608	7
1	Coated Paper, 100 lpi Mesh, AM Dot	0.510501	8
8	Uncoated Paper, 120 lpi Mesh, AM Dot	0.471777	9
11	Uncoated Paper, 120 lpi Mesh, FM Dot	0.460219	10
7	Uncoated Paper, 100 lpi Mesh, AM Dot	0.416251	11
10	Uncoated Paper, 100 lpi Mesh, FM Dot	0.384875	12

The Table 7 shows the GRA index ranking for 30% dot gain, and it is noticed that the print quality of screen printing is highly dependable to the mesh count. Higher the screen mesh count, better will be the reproduction of finer details. The higher screen mesh count facilitates the better carrying of fine dot details of stencil over the mesh and also controls the ink flow through the mesh opening during printing.

At higher mesh count such as 140 lpi and 120 lpi, both coated paper and uncoated paper grades can reproduce the 30% tonal area better than that of 100 lpi mesh count. The 100 lpi screen mesh comparatively contains larger mesh opening and so fails to accurately carry the finer details of stencil on the mesh as well as to control the ink flow through the mesh during printing. The AM dots on coated paper with 140 lpi mesh count gives the best result. Even though, the FM dots at higher screen mesh count also works better at 30% dot area.

The GRA index ranking for 50% Dot gain shown are in Table 8 which indicates that the higher screen mesh count can control the dot gain at those middle tones than that of lower mesh count. Also, with higher screen mesh count the AM dots will perform better than FM dots especially in these middle tone areas. FM dots shows undesirable random shift of tonal values at this middle tone than AM dots. Also, the surface irregularities and porosity of uncoated paper always provides a tendency to undesirably absorb the ink and that will increase the chance of dot gain.

The GRA ranking of 70% Dot Gain as shown in Table 9 indicates that the higher mesh count of screen printing can reproduce better shadow details effectively. The AM dots printed on coated paper with 140 lpi mesh count gives the best result. Higher the screen mesh count better will be the ink flow through the mesh in printing and also better the halftone dot details on stencil over the mesh.

The Tables 10-12 are showing the GRA ranking of Hue Error at 30%, 50% and 70% tonal areas respectively. Higher the mesh count, lower will be the hue error irrespective of percentage dot area. It is observed that hue error is minimum in the case of AM dots in highlight, midtone and shadows. However, the hue error depends on the printing conditions, purity of ink, spectral behaviour of the substrate etc.

The Tables 13-15 shows the GRA index ranking for print contrast at 30%, 50% and 70% tonal areas respectively. All the cases indicate that, higher the mesh count better will be the print contrast. Lowering the mesh count will reduce the print contrast of reproduction.

The AM dot print with 140 lpi screen mesh count on coated grade paper shows the superior print contrast in all the cases. At higher screen mesh count the coated paper provides greater print contrast than uncoated grade. The print contrast indicates the accuracy of tonal area reproduction or shadow details in contrast with the solid area ink density.

The overall GRA index-based ranking given in Table 16 indicates that, at 140 lpi screen mesh count, the coated paper with AM dots is comparatively best in the print quality by considering the criteria like solid ink densities, dot gain, hue error and the print contrast. The result shows the importance of mesh count in screen printing in distinction with the type of substrate and the halftone mode of reproduction employed in the printing process.

As per the results, the screen mesh with higher thread counts such as 140 lpi is capable to deliver better print quality in screen printing than that of screen mesh with 120 lpi and 100 lpi mesh count. The screen mesh with high thread count indicates the less open area and its capability to hold more stencil details over the mesh than that of screen with lower mesh count.

Also, the lesser open area of 140 lpi screen mesh facilitates the better control over the ink flow through the mesh and thereby reduces the chance of dot gain under the circumstance of high squeegee pressure and low viscous screen printing ink.

Also, it is noticed that, the irregular surface textured substrate such as uncoated paper in such cases will accelerates the occurrence of undesirable dot gain at lower mesh count in screen printing.

It is also observed that the mode of halftone screening process such as AM and FM dots employed in the printing process influences the print quality.

Comparing AM with FM print quality in the result, it is found that the AM dot pattern gives the best print results at 30%, 50% and 70% tonal areas than FM dots.

This indicates that AM dots in middle-tone areas can produce better details in screen printing.

The FM dots are capable to reproduce vibrant colour than AM dots but shows an undesirable random shift of tonal values from highlight to shadow region. This leads to the loss of details at the middle-tones considerably. At the same time, the AM dots are better in reproducing middle tone gradations when comparing with FM dot reproduction.

The problem faced by FM dots in this kind may be due to its fine size and the randomly distributed feature that all made it less likely capable to the various features of screen printing process like: complications of stencil making process, mesh opening, stencil adhesion requirements with the screen, squeegee pressure, ink pigment particle size and its viscosity etc.

The microscopic view of the dot reproduction is shown vide in Figures 9-14 that gives a better understanding about the nature of dot reproduction of both AM and FM dots on coated and uncoated grade paper at different screen mesh count.

Figures 9a-9f represent the microscopic image (enlarged to 80x) of 30% dot area printed on both coated and uncoated paper substrates produced by different combinations of screen mesh. The image is made up of AM dots only. Figure 9c shows that 140 lpi screen mesh on coated paper provides the sharp image with uniform ink distribution which confirms the Taguchi's GRA ranking made in the analysis. Figure 9b represents image printed through 120 lpi on coated images are darker in appearance and hence it confirms the analysis made by Taguchi's GRA method which is the second best.

Figures 10a-10f show the microscopic images of 50% dot area of print made up of AM dots on both coated and uncoated papers by using stencils made on different screen meshes. Figure 10c shows 140 lpi mesh gives the best print quality as compared to others. This confirms the Taguchi's GRA analysis results as obtained.

Figures 11a-11f represent the microscopic images of 70% dot area of print of grey scale formed with AM dots taken on both coated and uncoated paper substrates through the stencils formed on different screen meshes. Figure 11c shows the minimum dot gain as compared to others. This confirms the Taguchi GRA analysis as given in Table 9 and Table 16.
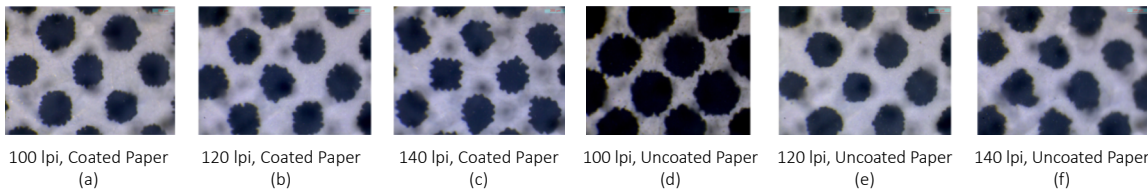
Figures 12a-12f are the microscopic images of the prints of 30% dot area obtained through stencils made on different lpi screen mesh adopting FM dots. The pictures show dot gain is minimum in print of 140 lpi mesh on coated paper but dots are irregular in shape in all the cases.

Figures 13a-13f represent the microscopic images of prints obtained through stencils made on different lpi screen mesh by using FM screening. These shows that dots are not at all clear and gain is more in all the cases.
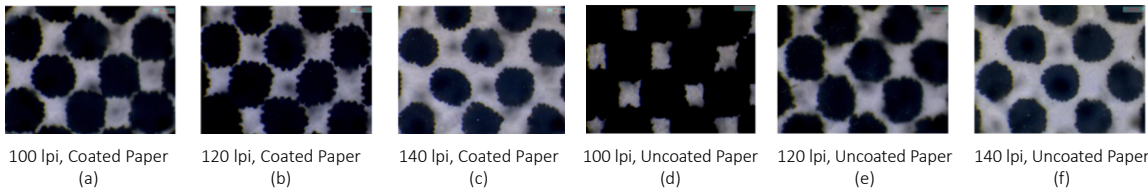
Figures 14a-14f are the microscopic images of 70% dot area of FM dots through the stencils made on different lpi screen meshes. This shows dot gain is minimum in case of 140 lpi mesh on coated paper vide Figure 12c which confirms the Taguchi's GRA analysis.
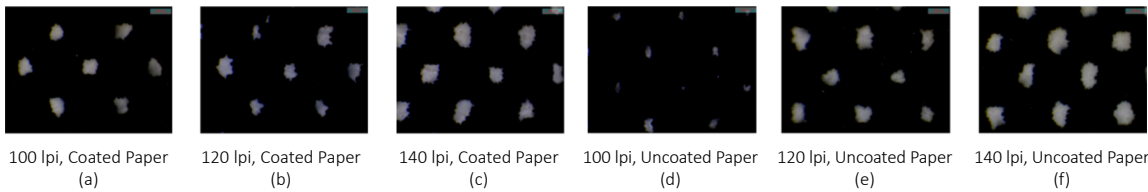
Conclusion

The experimental study conducted with this research work was designed in such a way to find the influence of AM and FM dots on coated and uncoated paper under three different screen mesh ruling in the screen printing process. The print quality assessment was done through the scientific approach of Taguchi's Grey Relational Analysis by considering the major factors influencing the print quality such as solid ink density, dot gain, hue error

| 100 lpi, Coated Paper (a) | 120 lpi, Coated Paper (b) | 140 lpi, Coated Paper (c) | 100 lpi, Uncoated Paper (d) | 120 lpi, Uncoated Paper (e) | 140 lpi, Uncoated Paper (f) |

» **Figure 9:** *The microscopic view of AM dot at 30% dot area*

| 100 lpi, Coated Paper (a) | 120 lpi, Coated Paper (b) | 140 lpi, Coated Paper (c) | 100 lpi, Uncoated Paper (d) | 120 lpi, Uncoated Paper (e) | 140 lpi, Uncoated Paper (f) |

» **Figure 10:** *The microscopic view of AM dot at 50% dot area*

| 100 lpi, Coated Paper (a) | 120 lpi, Coated Paper (b) | 140 lpi, Coated Paper (c) | 100 lpi, Uncoated Paper (d) | 120 lpi, Uncoated Paper (e) | 140 lpi, Uncoated Paper (f) |

» **Figure 11:** *The microscopic view of AM dot at 70% dot area*

| 100 lpi, Coated Paper (a) | 120 lpi, Coated Paper (b) | 140 lpi, Coated Paper (c) | 100 lpi, Uncoated Paper (d) | 120 lpi, Uncoated Paper (e) | 140 lpi, Uncoated Paper (f) |
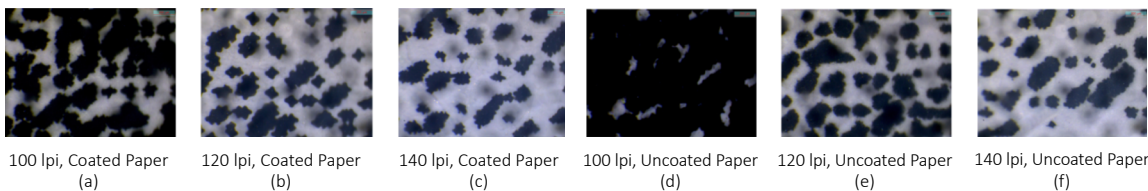
» **Figure 12:** *The microscopic view of FM dot at 30% dot area*

| 100 lpi, Coated Paper (a) | 120 lpi, Coated Paper (b) | 140 lpi, Coated Paper (c) | 100 lpi, Uncoated Paper (d) | 120 lpi, Uncoated Paper (e) | 140 lpi, Uncoated Paper (f) |
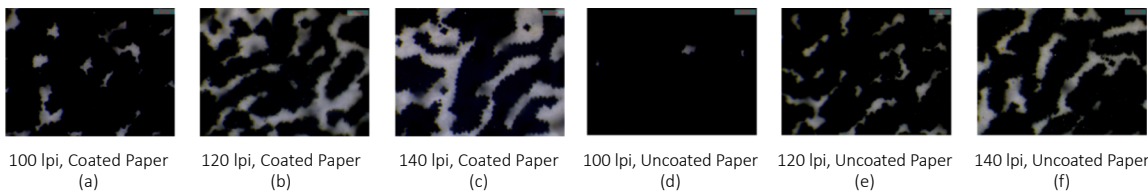
» **Figure 13:** *The microscopic view of FM dot at 50% dot area*

| 100 lpi, Coated Paper (a) | 120 lpi, Coated Paper (b) | 140 lpi, Coated Paper (c) | 100 lpi, Uncoated Paper (d) | 120 lpi, Uncoated Paper (e) | 140 lpi, Uncoated Paper (f) |
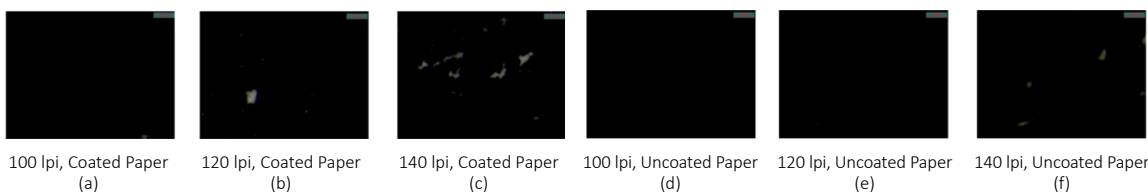
» **Figure 14:** *The microscopic view of FM dot at 70% dot area*

and print contrast. The tonal reproduction curve at 5% to 100% dot coverage is plotted for dot area, dot gain, hue error and the print contrast. Moreover, this research work employed the systematic implementation of Taguchi's Grey Relational Analysis Technique in the print quality assessment in a most reliable and meaningful way.

The results show that the screen printing quality is dependent on the screen mesh count. Printing with a high screen mesh counton smooth surface paper will give the best result in screen printing. The AM dots will work better in the middle tone region with a good tonal value transition from highlight to shadow region. Meanwhile, the FM dots are capable to give the vibrant color especially at the solid density regions than that of AM dots but fail to reproduce the middle tone densities with a smooth tonal transition. There is a huge shift of tonal value are obtained at the middle tones for FM dots. The accurate reproduction of FM dots in screen printing is dependent on the mesh count and some other crucial factors like adaptation with proper stencil making process, adhesion with screen mesh, squeegee pressure, ink parameters etc. The printing on uncoated paper with low mesh count will leads to high dot gain and it is a poor choice for high quality precision works.

Funding

References

Cazac, V., Cîrja, J., Balan, E. & Mohora, C. (2018) The study of the screen printing quality depending on the surface to be printed. In: *22nd International Conference on Innovative Manufacturing Engineering and Energy, IManE&E 2018, 31 May – 2 June 2018, Chisinau, Republic of Moldova*. Les Ulis, EDP Sciences- Web of Conferences. Available from: doi: 10.1051/matecconf/201817803015

Dharavath, N. H., Bensen, M. T. & Gaddam, B. (2005) Analysis of Print Attributes of Amplitude Modulated (AM) vs. Frequency Modulated (FM) Screening of Multicolor Offset Printing. *Journal of Industrial Technology*. 21 (3), 2-10.

Dina, R. B., Uddin, M. Z. & Fatema, U. K. (2020) Effect of mesh count on dot design and quality of screen printing in knit fabric. *Journal of Textile Engineering and Fashion Technology*. 6 (4), 122–131. Available from: doi: 10.15406/jteft.2020.06.00240

Kipphan, H. (2001) *Handbook of print media: technologies and production methods*. Berlin, Springer. Available from: doi: 10.1007/978-3-540-29900-4

Kumar, S. & Baral, A. K. (2023) Taguchi's Grey Relationship Analysis (GRA) for Comparing the Performance of Various Inkjet Printheads for Tone Value Increase on Uncoated Paper Substrates. *International Journal on Recent and Innovation Trends in Computing and Communication*. 11 (5s), 432-439. Available from: doi: 10.17762/ijritcc.v11i5s.7095

Kumar, V. (2020) Taguchi Method Experimental Design Technique. In: More, S. M. and Tyagi, N. (eds.) *International conference on Science, Technology and Management, ICSTM-2020, 15-16 February 2020, Nashik, India*. Modinagar, A.R. Research Publication. pp. 22-29.

Novaković, D., Kašiković, N., Vladić, G. & Pal, M. (2016) 15 – Screen Printing. In: Izdebska, J. and Thomas, S. (eds.) *Printing on Polymers*. Amsterdam, Elsevier, pp. 247-261. Available from: doi: 10.1016/B978-0-323-37468-2.00015-4

Poljacek Mahovic, S., Mandic, L., Agic, D. & Gojo, M. (2005) A Contribution to the AM and the FM screening in the graphic reproduction process. In: Katalinic, B. (ed.) *DAAAM International Scientific Book 2005*. Vienna, DAAAM International Vienna, pp. 395-404.

Roy, K. R. (2010) *A Primer on the Taguchi Method - 2nd Edition*. Southfield, Society of Manufacturing Engineers.

Revolution–bump mapping with texture function adjustment according to the geometry of the revolved object

ABSTRACT

Nowadays, 3D computer graphics are firmly anchored in our daily lives, extending across a multitude of distinct fields. Although each field follows its specific objectives, two major objectives are taken into consideration: realism and rendering speed. This is why image-based rendering (IBMR) techniques, such as revolution mapping, are gaining interest. Revolution-bump mapping is an image-based rendering that allows the creation of 3D objects in their entirety and without using polygonal meshes. The objective of the study presented in this paper is to improve the revolution-bump mapping technique as well as its extensions while ensuring that the application of textures on revolved surfaces is realized adequately. This development will allow the creation of pre-existing revolve models, while maintaining the essential rendering speed requirements for real-time rendering.

KEY WORDS

Computer graphics, Revolution mapping, Image-based modeling and rendering, Bump mapping, Ray-tracing

Anouar Ragragui [1] (ID)
Adnane Ouazzani Chahdi [2] (ID)
Amina Arbah [2] (ID)
Hicham El Moubtahij [3] (ID)
Akram Halli [4] (ID)
Khalid Satori [2] (ID)

[1] Abdelmalek Essaadi University, National School of Applied Sciences Al Hoceima (ENSAH), SOVIA Research Team, Tetouan, Morocco
[2] Sidi Mohamed Ben Abdellah University, Faculty of Science Dhar El Mahraz, LISAC Laboratory, Fez, Morocco
[3] Ibn Zohr University, High School of Technology, Agadir, Morocco
[4] Moulay Ismail University, Faculty of Law, Economics, and Social Sciences (FSJES), OMEGA-LERES Laboratory, Meknes, Morocco

Corresponding author:
Anouar Ragragui
e-mail:
a.ragragui@uae.ac.ma

Introduction

Based on traditional methods, real-time rendering still suffers from the number of vertices and polygons that the graphics cards need to handle, which affects the interactivity of rendering complex 3D scenes.

Furthermore, the appearance of the microreliefs constituted a problem in real-time rendering due to their diminutive size to be created by a mesh that requires a series of decomposition into a set of triangles, moreover, they represent a lot of details which make them difficult to simulate for shading functions and this because of

visual poverty. So, it is often necessary to make sacrifices by decreasing the number of polygons constituting the 3D scene so that it can maintain a reasonable display rate and consequently reduce the rendering quality.

The reason that pushed us to move towards alternative methods to polygonal mesh, namely image-based rendering and more precisely revolution mapping because it uses only a single RGBA texture to create 3D objects.

Revolution-bump mapping is a technique that combines two different approaches: revolution mapping and bump mapping (Ragragui et al., 2018). Revolution mapping is based on the use of a binary form stored in a 2D texture, which we call a shape map. During the rendering stage, the model to be revolved is represented by only the pixels with zero values. This method is based on the ray tracing algorithm to find the intersection point of the viewing ray and the revolved surface by using an empty space which is calculated using the Euclidean Distance Transform (EDT) computed from the binary form (Danielsson, 1980; Fabbri et al., 2008; Gustavson & Strand, 2011). On the other hand, bump mapping consists of adding more realism to 3D objects by simulating micro-reliefs during the shading phase. It uses a displacement map to disrupt the normals associated with the 3D surface to produce a microrelief effect.

Unfortunately, revolution mapping faces a recurring problem of poor texturing of revolved surfaces. Indeed, it has gaps in the ability to adequately apply textures to these surfaces due to the use of inappropriate texturing functions. This article aims to present an innovative solution that relies on the configuration of the revolution object to select the appropriate texturing function. Indeed, the two types of textures used for the revolved object, namely the color texture and the displacement map, prove insufficient to ensure optimal texturing of the surface of the 3D object, whether in terms of colorimetry or microreliefs.

As can be seen in Figure 1, the direct application of the texturing function presents problems in adapting texture to the shape of 3D objects. Looking at the object at the top of Figure 1a, it can be seen that spherical projection does not guarantee appropriate texturing, whereas the object at the bottom is adequately textured. On the other hand, in Figure 1b, the cylindrical projection guarantees perfect texturing of the object at the top, but the object at the bottom does not benefit from satisfactory texturing.

In this study, we propose an approach that uses the specific geometry of the revolved object to guide the choice of texturing method. This approach aims to solve the problems inherent in texturing the surfaces of a revolution, considering the coloring and rendering requirements of microreliefs.

By determining the texturing method based on the shape and characteristics of the revolved object, we aim to overcome the limitations of revolution bump mapping and enable the creation of 3D renderings that respect both visual realism and detail accuracy.

Related Work

One of the most popular techniques for real-time rendering is texture mapping. It allows to add realism to a computer-generated 3D object (Catmull, 1974; Heckbert, 1986; Blinn & Newell, 1976). Another use of texture mapping is presented by the authors Lim et al. (2023) and Kao, Chen & Ueng (2023). It is the oldest and simplest of the image-based techniques. Its goal is to determine the relationship between texture elements defined in 2D space and surfaces defined in 3D space. Bump mapping was introduced by Blinn (1978). This method reproduces microrelief on 3D surfaces without changing their geometry. A displacement value is calculated based on the partial derivatives of the applied texture, which is used to perturb the normal of a given surface.

Parallax mapping (Kaneko et al., 2001) is a technique similar to bump mapping, but based on different principles. It allows to significantly increase the detail of a textured surface, even if this detail is an illusion. It aims at displacing the texture coordinates to find approximately the intersection at which the height map's relief and the viewing ray, given in tangent space, cross. Further improvements are presented by the authors Welsh (2004) and McGuire & McGuire (2005).

To add detail, the height map's values are used in the displacement mapping (Cook, 1984; Lee, Moreton & Hoppe, 2000). It was able to hide almost all the defects of bump mapping by completely changing the surface geometry instead of just perturbing the normals. This approach is based on dividing the 3D surface into sub-polygons and displacing them along their normals using distances extracted from a displacement map. The method used is different from that described in the papers by Gumhold & Hüttner (1999) and Doggett & Hirche (2000), which significantly modified the geometry to reduce the number of triangles produced as a function of viewpoint. To reduce the polygon generation, they proposed the adoption of an adaptive subdivision based on the displacement map.

View-dependent displacement mapping is a technique suitable for real-time rendering. It relies on preprocessing to compute a texture (Wang et al., 2003). The goal is to move the surface by performing calculations at the texel level, thus optimizing performance. A significant improvement of this method is presented in Wang & Dana (2005), where the use of a compression method is introduced to meet high memory requirements.

Another interesting extension is discussed in Wang et al. (2004), which aims to generalize the displacement map approach under the name "GDM" (Generalized Displacement Maps).
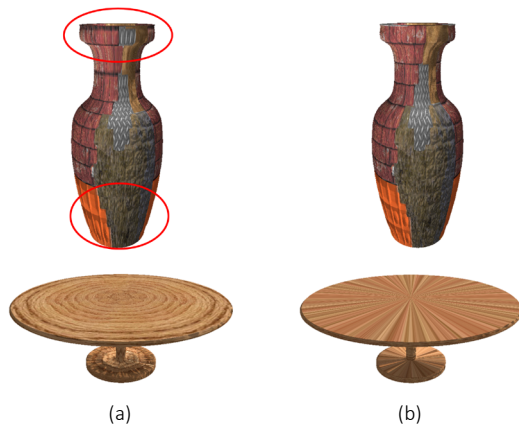
The ray tracing method aims to use the viewing ray to find the intersection point, sometimes referred to as linear search. It has only been used in the context of parallax mapping in the research by McGuire & McGuire (2005), and as a first step in the the papers of the authors Policarpo, Oliveira & Comba (2005) and Tatarchuk & Natalya (2006). Unfortunately, relying solely on linear search results in stair-step artifacts, unless very narrow intervals are used. This issue was resolved by the method suggested in Tatarchuk & Natalya (2006), which involved combining a secant step with a fine linear search (Wen, 2023; Yang & Jia, 2023; Wu et al., 2024; Zellmann et al., 2022). Unlike ray tracing, which follows light rays deterministically, path tracing uses a probabilistic approach to calculate light paths in the scene; This is a technique that uses the principle of ray tracing but in a different way (Chen, Chen & Yu, 2023; Wald & Parker, 2022; Wald, Jaroš & Zellmann, 2023).

The combination of secant and linear searches offers a solution for improving ray tracing (Yerex & Jagersand, 2004). A further improvement to this technique is introduced in Risser, Shah & Pattanaik (2006), where the secant method is repeated several times to accurately determine the intersection point.

The key advantage of per-pixel displacement mapping is its ability to enhance the reality of surfaces without adding complexity to the mesh structure, making it an exciting evolution of the per-vertex displacement mapping method previously described in Patterson, Hoggar & Logie (1991). This technique overcomes the bottleneck caused by the significant number of graphics primitives sent to the graphics processor as part of vertex displacement mapping.

Per-pixel displacement mapping relies on ray-tracing technology to accurately determine the texture coordinates for each pixel with respect to the displacement map.

Surfaces of revolution are commonly used in various sectors such as engineering, architecture and 3D modelling, as they can be used to generate refined and complex shapes (Li & Li, 2022). Several techniques are based on this approach, including extrusion mapping and revolution mapping, as discussed in Halli et al. (2009) and Halli et al. (2010).

Both methods use shape maps to create 3D surfaces. To increase the realism of the generated surfaces, various improvements have been made to both approaches, as shown in Ragragui et al. (2020), Ragragui et al. (2018), Ragragui et al. (2022) and Chahdi et al. (2021b).

To quickly converge to the intersection point, sphere tracing uses spheres to encode the empty space (Hart, 1996). It was subsequently adapted for the intersection point by using ray-tracing and the height map (Donnelly, 2005). Further improvements were presented in Fabbri et al. (2008) and Gustavson & Strand (2011), which aim at perfecting the algorithm for calculating distance maps.

Cone tracing determines the empty space around each pixel of the depth map in the pre-processing stage as an open cone at the top, and then stores its ratio in a cone map. During the rendering stage, the cone map is used to accelerate the convergence to the intersection point of the viewing ray and the surface, so that there is no chance of missing it. This approach comes in two flavors: a relaxed version (Policarpo & Oliveira, 2007) and a conservative version (Dummer, 2006). Both variants of cone mapping have been extended in Halli et al. (2008) and Chahdi et al. (2021a).

Due to its ability to speed up convergence to the point where the viewing ray intersects with the relief, relief mapping is one of the most popular methods for real-time rendering (Policarpo, Oliveira & Comba, 2005; Policarpo & Oliveira, 2006; Chahdi et al., 2018). This technique is an evolution of the relief texture mapping method introduced in Oliveira, Bishop & McAllister (2000).

Shadow mapping is a widely used technique that provides satisfactory results and is characterized by the fact that is relatively easy to implement, as suggested in Wang et al. (2003), Policarpo, Oliveira & Comba (2005) and Wang et al. (2017).

The idea behind shadow mapping is quite simple: it is based on the principle that the scene is illuminated according to the viewpoint of the light source.

A technique for interactive deformation and collision with reliefs was presented in Nykl, Mourning & Chelberg (2014). This technique can be seamlessly combined with existing relief rendering techniques, including parallax mapping, relief mapping, as well as applications using displacement mapping.

Bump mapping

Rendering microrelief was one of the main issues, particularly in real-time rendering. Blinn proposed bump mapping as a microrelief simulation technique (Blinn, 1978). As shown in Figure 2, this method involves adjusting the 3D surface's normals to create the appearance of microrelief. The principle is quite simple: it consists of displacing the normals to a surface to induce variations in shading, thus giving the illusion of relief without modifying the basic geometry of the 3D object. More concretely, it is based on the partial derivatives computed from a microrelief saved as a monochrome image known as a height map, which entails displacing the normal interpolated during the rasterization stage. Disturbed normals are calculated using the following formula:

$$\vec{N}'(u,v) = \vec{N}(u,v) + \frac{\left(\frac{\partial H(u,v)}{\partial u} \left(\vec{N} \wedge \frac{\partial \sigma(u,v)}{\partial v} \right) - \frac{\partial H(u,v)}{\partial v} \left(\vec{N} \wedge \frac{\partial \sigma(u,v)}{\partial u} \right) \right)}{\|\vec{N}\|} \quad (1)$$

By using the height map H(u, v) saved as a 2D grayscale image, we can calculate the disturbed normal $\vec{N}'(u,v)$ for each pixel by using the formula (1).

» **Figure 2:** *Comparison of a teapot rendered using texture mapping (top) and bump mapping (bottom)*

Revolution-bump mapping

Revolution mapping is a method for generating highly convincing 3D objects without resorting to polygonal meshes and presenting them interactively. The underlying concept is to use a shape map, which holds the geometric information of the basic form, to build virtual surfaces.

Figure 3 illustrates a geometric representation of the base form's revolution, positioned on a box (shape box), and highlights the process of searching the intersection point.

There are four essential components in the revolution mapping algorithm. Firstly, the shape map and displacement map are essential for precisely defining the geometry and displacement variations (microreliefs) associated with the basic form. Secondly, the ray-tracing algorithm plays a crucial role in visual creation by calculating the interactions between the viewing ray and the revolution surface. The last other components are the shading process that adds lighting and shadow effects, contributing to the realism of the final 3D object, and the shape box that provides a reference element for positioning the basic form and managing intersections.

Shape and displacement map

These two maps are obtained during the pre-processing phase. They contain the essential information for generating the surface of revolution (shape map) and for adding realism (displacement map).

Shape map: The data for the revolution mapping algorithm is contained in this map, which is an RGBA texture (Figure 4e). The alpha channel saves a binary image that represents the basic form (Figure 4a). The distance map is kept in the blue channel (Figure 4b).

Finally, the red and green channels contain the gradient values along x and y, which are used to calculate the normal coordinates (Figure 4c,d).
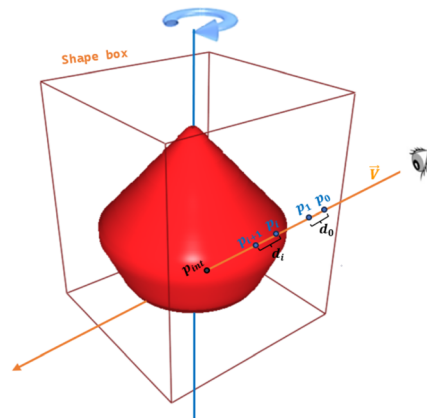

» **Figure 3:** *The shape of a piece of jewelry placed at the center of a box and the process of finding the point of intersection p_{int}*

Displacement map: the partial derivatives ∂H(u,v) are calculated as a function of u and v from the height map H(u,v) (Figure 5a), then saved in the red and green channels (Figure 5b and c) of a 2D texture called the displacement map (Figure 5d).

Before starting the rendering phase, the two maps; the shape and the displacement map; are transferred to the graphics card.

Basic shape
(a)

Distance map
(b)

The x and y values of normal
(c)   (d)
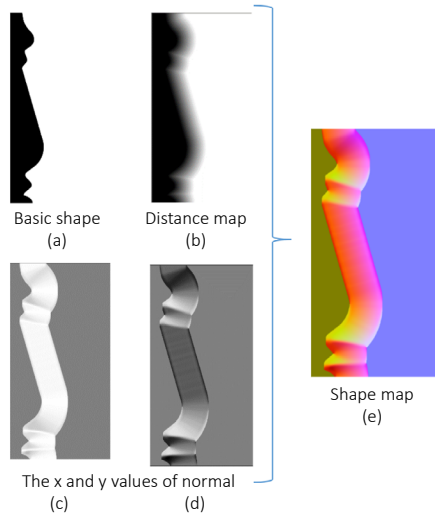
Shape map
(e)

» **Figure 4:** *Example of different data. (a) The alpha channel. (b) The blue channel. (c) Red and (d) green channels. (e) Shape map stores all this data*


Height map
H(u,v)

Red channel   Green channel
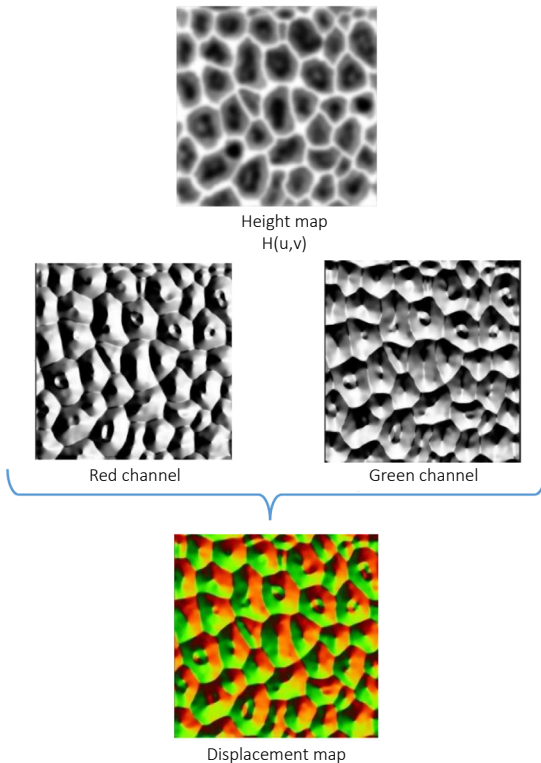
Displacement map

» **Figure 5:** *Example of displacement map ∂H(u,v) for which we store the partial derivatives of H(u,v)*

Ray tracing

Finding the intersection point is the first step in the revolution mapping algorithm. For this, the technique is

based on ray tracing, whose goal is to use the distances *d* recorded in the shape map to locate the intersection of the viewing ray and the revolved surface. The current pixel has coordinates (u,v), and the start point p_0 of the search has coordinates $(x_0, y_0, z_0)=(u,v,0)$. The normalized viewing ray is determined from the viewing point to the starting point p_0. The blue channel (figure 4b) is used, at each point p_i, to extract the distance d_i. The point p_{i+1} is calculated by the formula:

$$p_{i+1} = p_i + d_i \cdot \vec{V}_p \tag{2}$$
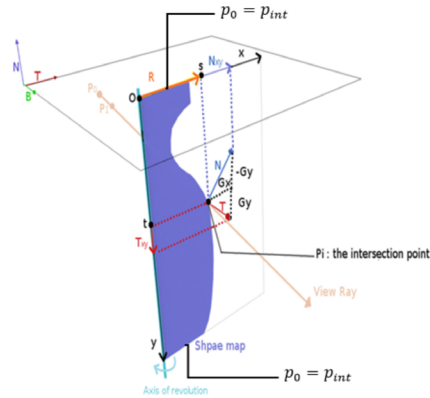
» **Figure 6:** *At the intersection point p_{int}, the process for computing the tangent and normal vectors*

To access the shape map and retrieve the distance d_i between the current point and the form, the revolution algorithm uses the coordinates (s_i, t_i) (Figure 6). Using the equation below:

$$\left(s_i, t_i\right) = (\|\vec{R}_i\|, z_i) \text{ with: } \vec{R}_i = (x_i - O_x, y_i - O_y) \tag{3}$$

Shading

For each intersection point found by the ray tracing algorithm, the next step is to identify the tangent space (TBN). This space will enable shading of the pixel correctly using the following equation:

$$\vec{N'}_{int}(u, v) = \frac{\vec{N}_{int}(u,v) + \vec{D}_{int}(u,v)}{\|\vec{N}_{int}(u,v) + \vec{D}_{int}(u,v)\|} \tag{4}$$

With

$$\vec{D}_{int}(u, v) = \left(\frac{a \cdot \partial H(u,v)}{\partial u} \left(\vec{N}_{int} \wedge \vec{B}_{int}\right) - \frac{a \cdot \partial H(u,v)}{\partial v} \left(\vec{N}_{int} \wedge \vec{T}_{int}\right)\right) \tag{5}$$

According to Figure 6, the normal is constituted by the components G_{intx} and G_{inty} of the gradient unit:

$$\vec{N}_{int} = \left(G_{int_x} \frac{R_{int_x}}{\|\vec{R}_{int}\|} , \quad G_{int_x} \frac{R_{int_y}}{\|\vec{R}_{int}\|} , \quad - G_{int_y}\right) \tag{6}$$

The tangent can be determined by the following equation:

$$\vec{T}_{int} = \left(G_{int_y} \frac{Rint_y}{\|\vec{R}_{int}\|} \, , \, - \, G_{int_y} \frac{Rint_x}{\|\vec{R}_{int}\|} \, , \, - \, G_{int_y} \right) \qquad (7)$$

The vector $\vec{B}_{int}$ is calculated by using the formula:

$$\vec{B}_{int} = \vec{T}_{int} \wedge \vec{N}_{int} \qquad (8)$$

Shape box

Applying the shape map to a simple polygonal mesh structure, such as a plane as shown in Figure 7a, will not completely render the 3D object created by revolution mapping. This is because the geometry is only visible from the textured surface of the polygons. To create and display complete 3D objects regardless of the viewing ray direction, this technique implements a solution that consists of enveloping the virtual volume in revolution with a shell space made of a single box. This envelope is called a shape box (Figure 7b).

(a)

(b)
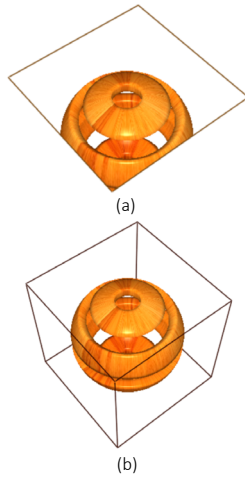
» **Figure 7:** *Highlighting the problem associated with applying the shape map to a simple plan (a) This problem is solved by using a shape box (b)*

Texturing function

In the context of our contribution, our goal is closely related to the precise determination of the color of a revolved object.

To achieve this, we rely on two fundamental elements: the color map and the displacement map. These elements are crucial for each intersection point p_{int}.

The process we've developed consists of several key steps. First, it is imperative to accurately calculate the texture coordinates, which we denote by (ξ_{int}, η_{int}). These coordinates are of paramount importance because they are used to access the information contained in the color map and the displacement map.

These maps meticulously wrap around the revolved object (Figure 8).
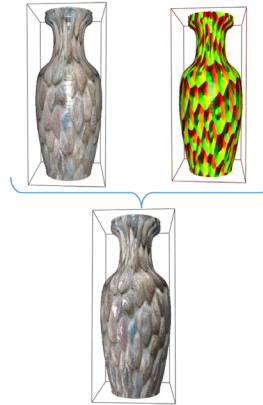
» **Figure 8:** *To properly texture the revolved object (below), we need to apply the color map to the object and the partial derivative map, using the appropriate projection for the object*

By accessing the color map, we can extract the information needed to determine the specific color of each intersection point. In addition, by consulting the displacement map, we have the elements we need to evaluate displacement variations as a function of position. This is crucial for our purpose, as it allows us to retrieve the desired values related to the color and displacement properties of the 3D object.

Direct use of the coordinates $(x_{int}, y_{int}, z_{in})$ allows only simple mapping with planar projection, which is well suited for a flat surface, but not for a revolved surface. The latter requires cylindrical or spherical projection, as shown in Figure 9. This distinction becomes clear when we look at Figure 9, where we can easily see that the use of a spherical or cylindrical projection must be adjusted according to the specific geometry of the revolved object. This adjustment is crucial to avoid visual errors, which are marked in Figure 9.

This problem also arises when revolution mapping is extended to variations such as revolution-bump mapping, extended, beveled, or chamfered mapping. Our fundamental goal is to give revolved objects a realistic texture that reflects their shape and appearance. To achieve this, we propose a two-step methodology. In the pre-processing stage, we propose to associate the appropriate projection type directly with the revolved object by integrating it with the name of the shape map. This approach greatly simplifies the management of different projections and ensures that each object receives the correct texture according to its unique geometry.

However, the key step is the rendering phase. This is where the information previously encoded in the name of the shape map comes into play.
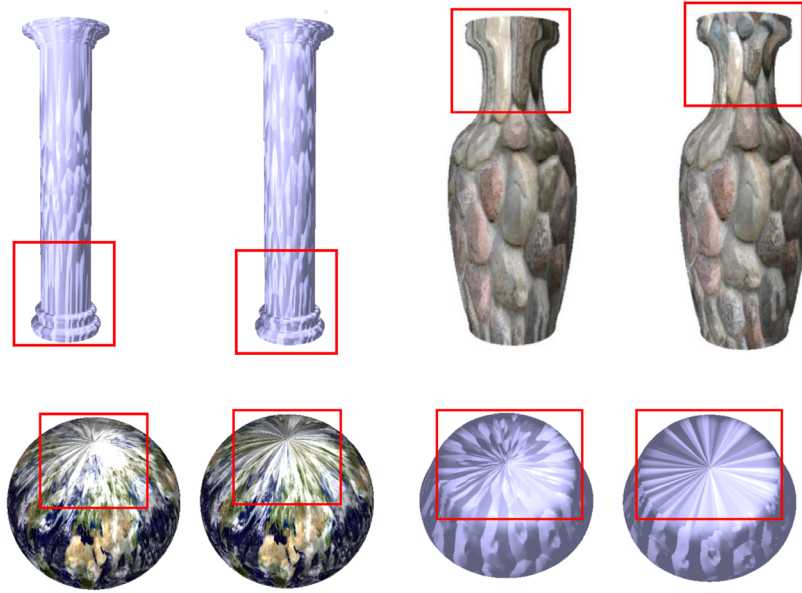
During the rendering stage, we extract this information to select the projection that perfectly matches the revolved object that we want to render.

By doing so, we succeed in transcending the constraints of simple projections and offering realistic textures, thus contributing to the visual quality and verisimilitude of revolution-generated objects, as shown in Figure 9.

To accurately ascertain the texture coordinates, and given that the texturing process must be applied to each replica, it is imperative to consider only the fractional portion of the intersection point coordinates:

$$\left(x'_i, y'_i, z'_i\right) = \left(x_i, y_i, z_i\right) - \left(E(x_i), E(y_i), E(z_i)\right) \quad (9)$$

Cylindrical projection

For cylindrical projection mapping, we use the cylindrical coordinates of the intersection point p_{int}, expressed with respect to an axis centered on the shape box:

$$\begin{cases} x_{int} - 0{,}5 = r\cos\ \varphi \\ y_{int} - 0{,}5 = r\sin\ \varphi \end{cases} \quad (10)$$

With:

$$r = \sqrt{(x_{int} - 0{,}5)^2 + (y_{int} - 0{,}5)^2} \quad (11)$$

We deduce the value of φ:

$$\varphi = atan2\left(y_{int} - 0.5, x_{int} - 0.5\right) \quad (12)$$

The texture coordinate η_{int} is equal to z'_{int}. As for ξ_{int}, it changes from 0 to 1 when φ changes from π to -π. We then have:

$$\left(\xi_{int}, \eta_{int}\right) = \left(\frac{\pi - \varphi}{2\pi}, z_{int}\right) \quad (13)$$

For revolution-bump mapping, use (O_x, O_y) instead of (0.5,0.5) if the axis of revolution is not centered on the shape box.

Spherical projection

Based on the intersection point's spherical coordinates, the spherical projection mapping is produced, expressed with respect to a reference frame placed at the centre of the shape box.

$$\begin{cases} x_{int} - 0{,}5 = r\sin\theta\ \cos\ \varphi \\ y_{int} - 0{,}5 = r\sin\theta\ \sin\ \varphi \\ z_{int} - 0{,}5 = r\cos\theta \end{cases} \quad (14)$$

With:

$$r = \sqrt{(x_{int} - 0{,}5)^2 + (y_{int} - 0{,}5)^2 + (z_{int} - 0{,}5)^2} \quad (15)$$

We deduce the values of φ and θ:

$$\begin{cases} \varphi = atan2(y_{int} - 0.5, x_{int} - 0.5) \\ \theta = \arccos \dfrac{z_{int} - 0{,}5}{r} \end{cases} \quad (16)$$

ξ_{int} varies in [0,1] when φ goes from π to π, and η_{int} int varies in [0,1] when θ goes from π to 0. Then we have:

$$\left(\xi_{int}, \eta_{int}\right) = \left(\frac{\pi - \varphi}{2\pi}, \frac{\pi - \theta}{\pi}\right) \quad (17)$$

Results and discussion

In the pre-processing stage, we implemented the algorithms using the C++ language to produce the displacement map and the shape map. During the rendering stage, we exploited OpenGL and its parallel processing language, GLSL, to create the vertex and fragment shaders.

During the rendering stage, in addition to the coordinates associated with the shape box, the two maps created during the preprocessing stage are transmitted to the graphics card. The analyses and illustrations were executed using an 8CPU Intel Core i7-11657G7 architecture at 2.80GHz, equipped with 8GB of RAM, and a GeForce MX330 graphics card with 4GB of dedicated memory. In this paper, the images provided were taken during a test in which the box occupies a significant part of the screen. We would like to note that the total number of iterations to find the intersection is 20, except for the beveled revolution mapping (35 iterations, of which 10 are for binary refinement), as well as the revolution mapping with chamfer (20 iterations, of which 35 are for the chamfer phase).

As shown in Figure 10, our approach correctly textures objects created by the revolution-bump mapping extensions: outward, beveled, and chamfered revolution-bump mapping. Our contribution perfectly adapts to the geometry of the rendered object.

Figure 11 shows additional examples of well-textured surfaces, using either cylindrical or spherical projection, depending on the object's geometry. These 3D objects are generated with revolution-bump mapping, using various shape and displacement maps. We can emphasize how many different kinds of objects can be made with this technique, as well as how many graphical primitives (polygons and vertices) can be avoided.

Figure 12 shows 3D objects rendered using revolution bump mapping with spherical projection (Figure 12a) and cylindrical projection (Figure 12b) by applying repetition to the texture and displacement map.

It should be noted that the improvement presented in this paper also applies to the other revolution mapping techniques, i.e. revolution with mirror and repetition (see Figure 13).


e = 0.25   b = 0.4   b = 0.6 c = 0.6
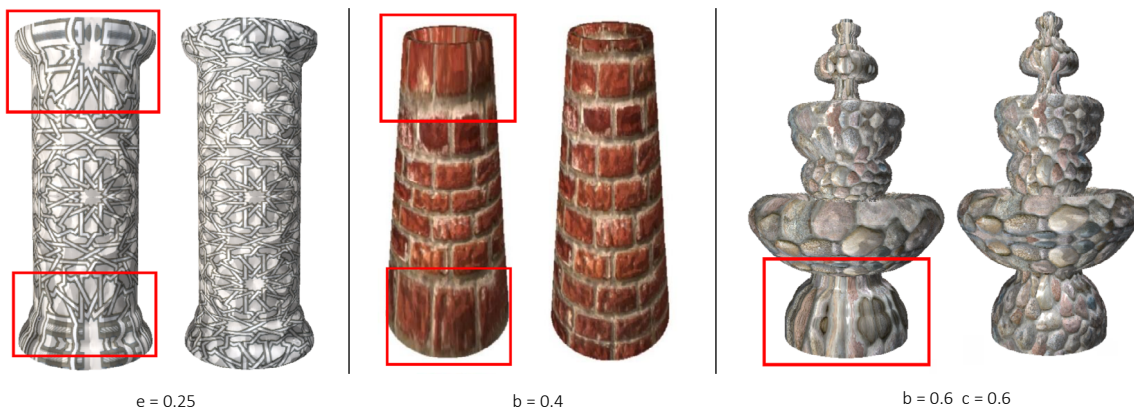
» **Figure 10:** *Extension of revolution-bump mapping. (a) Outward, (b) Beveled, and (c) Chamfered revolution-bump mapping. For each method, the spherical projection is on the left and the cylindrical one is on the right*
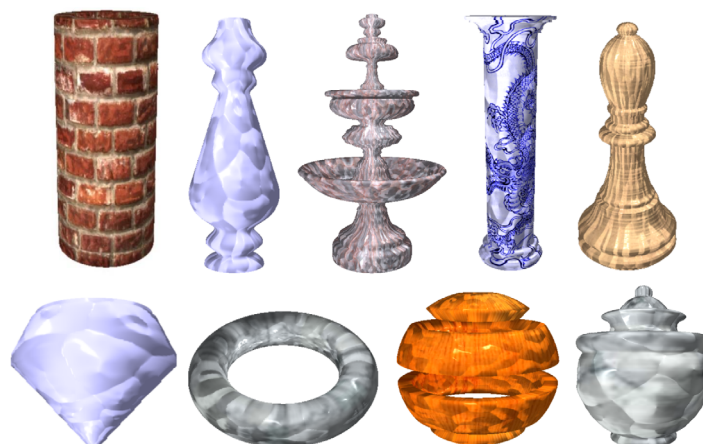
» **Figure 11:** *Various objects are rendered using revolution-bump mapping by adjusting the texturing function to the rendered surface. (Top) Cylindrical projection. (Bottom) Spherical projection*
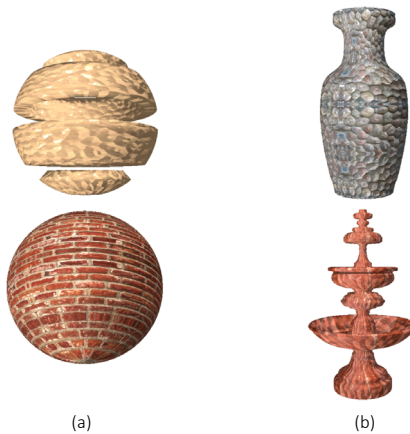
» **Figure 12:** *Various objects are rendered using revolution-bump mapping with adjustment of the texturing function and application of repetition to the texture and displacement map. (a) Spherical projection. (b) Cylindrical projection*
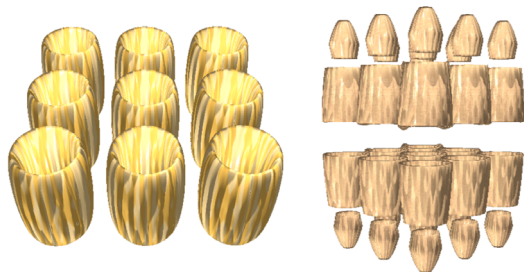
» **Figure 13:** *Various objects are rendered using revolution-bump mapping with adjustment of the texturing function and application of repetition to the texture and displacement map*

Note that our contribution has no impact on rendering speed. There is not much difference between revolution-bump mapping and revolution-bump mapping with texture function adjustment according to the geometry of the revolved object. Our improvement fully preserves all the features and properties of revolution-bump mapping and its extensions. In addition, we found that this improvement has no impact on the complexity of the raytracing algorithm since the revolution mapping algorithms always have linear complexity in O(n). As a result, the complexity of the algorithm is always linear. It's also worth noting that the memory used by the shape map does not exceed 10 MB, while the partial derivatives map does not exceed 4 MB. This ensures that the memory of the graphics card is not saturated, thus guaranteeing the continuous interactivity of the 3D scene.

Conclusion

This research presents an enhancement of revolution-bump mapping and its extensions. Our contribution makes it possible to adjust the texture of the revolution surface in real-time while enriching the visual quality of

the rendered objects. This improvement avoids overloading the graphics pipeline that can result from processing a large number of polygons and vertices. It focuses on determining the displacement and color values at each intersection point using the displacement map and color map.

This requires a careful determination of the texture coordinates and an adaptation of the texturing function to the geometry of the revolved object. for this, we have included the type of projection in the name of the shape map which will be appropriate to the object to be generated during the rendering phase. Our contribution relies only on the use of two different textures, a box, and the tangent space at each intersection point.

The first texture, or shape map, is used to generate the revolved surface, and the second texture, or displacement map, is used to integrate the microrelief effects. However, in the rendering stage, we adapt the rendering of the 3D object by using the appropriate texturing function. The improvements we propose are in line with the two goals we set out in the introduction: to meet rendering speed requirements and to present revolution models in a particularly convincing way.

Funding

References

Blinn, J. F. & Newell, M. E. (1976) Texture and reflection in computer generated images. *ACM SIGGRAPH Computer Graphics*. 10 (2), 266–266. Available from: doi: 10.1145/965143.563322

Blinn, J. F. (1978) Simulation of wrinkled surfaces. *ACM SIGGRAPH Computer Graphics*. 12 (3), 286–292. Available from : doi: 10.1145/965139.507101

Catmull, E. E. (1974) *A subdivision algorithm for computer display of curved surfaces*. PhD thesis. The University of Utah.

Chahdi, A. O., Ragragui, A., Halli, A. & Satori, K. (2018) Dynamic relief mapping[1]. In: *2018 International Conference on Intelligent Systems and Computer Vision, ISCV, 2-4 April 2018, Fez, Morocco*. Piscataway, IEEE. pp. 1-6. Available from: doi: 10.1109/ISACV.2018.8354053

Chahdi, A. O., Ragragui, A., Halli, A. & Satori, K. (2021a) Per-pixel displacement mapping using cone tracing with correct silhouette. *Journal of Graphic Engineering and Design*. 12 (4), 39–61. Available from: doi: 10.24867/JGED-2021-4-039

Chahdi, A. O., Ragragui, A., Halli, A. & Satori, K. (2021b) Per-Pixel Extrusion Mapping With Correct Silhouette.

Computer Science. 22 (3), 407–432. Available from: doi: 10.7494/csci.2021.22.3.3337

Chen, J., Chen, L. & Yu, Z. (2023) Accelerating path tracing rendering with Multi-GPU in Blender cycles. In: *25th International Conference on Advanced Communication Technology, ICACT, 19-22 February 2023, Pyeongchang, Republic of Korea*. Piscatawy, IEEE. pp. 314-318. Available from: doi: 10.23919/ICACT56868.2023.10079514

Cook, R. L. (1984) Shade trees. *ACM SIGGRAPH Computer Graphics*. 18 (3), 223-231. Available from: doi: 10.1145/964965.808602

Danielsson, P. E. (1980) Euclidean distance mapping. *Computer Graphics and Image Processing*. 14 (3), 227-248. Available from: doi: 10.1016/0146-664X(80)90054-4

Doggett, M. & Hirche, J. (2000) Adaptive view dependent tessellation of displacement maps. In: *Proceedings of the SIGGRAPH/Eurographics Workshop on Graphics Hardware, HWWS'00, 21-22 August 2000, Interlaken, Switzerland*. New York, Association for Computing Machinery. pp. 59-66. Available from: doi: 10.1145/346876.348220

Donnelly, W. (2005) Per-Pixel Displacement Mapping with Distance Functions. In: Pharr, M. and Randima, F. (eds.) *GPU Gems 2*. Boston, Addison-Wesley Professional, pp. 123-137.

Dummer, J. (2006) *Cone step mapping: An iterative ray-heightfield intersection algorithm*. Available from: https://www.scribd.com/document/57896129/Cone-Step-Mapping [Accessed 20th September 2024].

Fabbri, R., Costa, L. D. F., Torelli, J. C. & Bruno, O. M. (2008) 2D Euclidean distance transform algorithms. *ACM Computing Surveys*. 40 (1), 1–44. Available from: doi: 10.1145/1322432.1322434

Gumhold, S. & Hüttner, T. (1999) Multiresolution rendering with displacement mapping. In: *Proceedings of the ACM SIGGRAPH/EUROGRAPHICS workshop on Graphics hardware, HWWS'99, 8-9 August 1999, Los Angeles, California*. New York, Association for Computing Machinery. pp. 55–66. Available from: doi: 10.1145/311534.311578

Gustavson, S. & Strand, R. (2011) Anti-aliased Euclidean distance transform. *Pattern Recognition Letters*. 32 (2), 252–257. Available from: doi: 10.1016/j.patrec.2010.08.010

Halli, A., Saaidi, A., Satori, K. & Tairi, H. (2008) Per-Pixel Displacement Mapping Using Cone Tracing. *International Review on Computers and Software*. 3 (3), 1–11.

Halli, A., Saaidi, A., Satori, K. & Tairi, H. (2009) Per-Pixel Extrusion Mapping. *International Journal of Computer Science and Network Security*. 9 (3), 118-124.

Halli, A., Saaidi, A., Satori, K. & Tairi, H. (2010) Extrusion and revolution mapping. *ACM Transactions on Graphics*. 29 (5), 1–14. Available from: doi: 10.1145/1857907.1857908

Hart, J. C. (1996) Sphere tracing: A geometric method for the antialiased ray tracing of implicit surfaces. *Visual Computer*. 12 (10), 527–545. Available from: doi: 10.1007/s003710050084

Heckbert, P. S. (1986) Survey of Texture Mapping. *IEEE Computer Graphics and Applications*. 6 (11), 56–67. Available from: doi: 10.1109/MCG.1986.276672

Kaneko, T., Takahei, T., Inami, M., Kawakami, N., Yanagida, Y., Maeda, T. & Tachi, S. (2001) Detailed Shape Representation with Parallax Mapping. In: *Proceedings of the 11th International Conference on Artificial Reality and Telexistence, ICAT 2001, 5-7 December 2001, Tokyo, Japan*. pp. 205-208.

Kao, Y. C., Chen, W. H. & Ueng, S. K. (2023) Texture Mapping for Voxel Models Using SOM. In: *Proceedings - 2023 6th International Symposium on Computer, Consumer and Control, IS3C, 30 June – 3 July 2023, Taichung, Taiwan*. Piscataway, IEEE. pp. 99-102. Available from: doi: 10.1109/IS3C57901.2023.00035

Lee, A., Moreton, H. & Hoppe, H. (2000) Displaced subdivision surfaces. In: *Proceedings of the 27th annual conference on Computer graphics and interactive techniques, SIGGRAPH'00, 23-28 July 2000, New Orleans, Louisiana*. New York, ACM Press/Addison-Wesley Publishing. pp 85-94. Available from: doi: 10.1145/344779.344829

Li, H. & Li, M. (2022) Constant Winding Angle Curve on Revolution Surface and its Application. *CAD Computer Aided Design*. 144. Available from: doi: 10.1016/j.cad.2021.103160

Lim, A. X. W., Ng, L. H. X., Griffin, C., Kryer, N. & Baghernezhad, F. (2023) Reverse Projection: Real-Time Local Space Texture Mapping. In: *Proceedings – ACM SIGGRAPH 2023 Posters, SIGGRAPH'23, 6-10 August 2023, Los Angeles, California*. New York, Association for Computing Machinery. Available from: doi: 10.1145/3588028.3603653

McGuire, M. & McGuire, M. (2005) *Steep Parallax Mapping*. Available from: https://casual-effects.com/research/McGuire2005Parallax/index.html [Accessed 20th September 2024].

Nykl, S., Mourning, C. & Chelberg, D. (2014) Interactive mesostructures with volumetric collisions. *IEEE Transactions on Visualization and Computer Graphics*. 20 (7), 970–982. Available from: doi: 10.1109/TVCG.2014.2317700

Oliveira, M. M., Bishop, G. & McAllister, D. (2000) Relief texture mapping. In: *Proceedings of the 27th annual conference on Computer graphics and interactive techniques, SIGGRAPH'00, 23-28 July 2000, New Orleans, Louisiana*. New York, ACM Press/Addison-Wesley Publishing. pp. 359–368. Available from: doi: 10.1145/344779.344947

Patterson, J. W., Hoggar, S. G. & Logie, J. R. (1991) Inverse Displacement Mapping. *Computer Graphics Forum*. 10 (2), 129–139. Available from: doi: 10.1111/1467-8659.1020129

Policarpo, F. & Oliveira, M. M. (2006) Relief mapping of non-height-field surface details. In: *Proceedings of the 2006 symposium on Interactive*

3D graphics and games, I3D'06, 14-17 March 2006, Redwood City, California. New York, Association for Computing Machinery. pp. 55-62. Available from: doi: 10.1145/1111411.1111422

Policarpo, F. & Oliveira, M. M. (2007) Relaxed cone stepping for relief mapping. In: Nguyen, H. (ed.) *GPU Gems 3*. Boston, Addison-Wesley Professional, pp. 409–428.

Policarpo, F., Oliveira, M. M. & Comba, J. L. D. (2005) Real-time relief mapping on arbitrary polygonal surfaces. In: Gross, M. (ed.) *ACM SIGGRAPH 2005 Papers, SIGGRAPH'05, 31 July – 4 August 2005, Los Angeles, California*. New York, Association for Computing Machinery. p. 935. Available from: doi: 10.1145/1186822.1073292

Ragragui, A., Ouazzani Chahdi, A., Halli, A. & Satori, K. (2018) Revolution mapping with bump mapping support. *Graphical Models*. 100, 1–11. Available from: doi: 10.1016/j.gmod.2018.09.001

Ragragui, A., Ouazzani Chahdi, A., Halli, A. & Satori, K. (2020) Image-based extrusion with realistic surface wrinkles. *Journal of Computational Design and Engineering*. 7 (1), 30–43. Available from: doi: 10.1093/jcde/qwaa004

Ragragui, A., Ouazzani Chahdi, A., Halli, A., Satori, K. & El Moubtahij, H. (2022) The extensions of revolution-bump mapping. *Journal of Graphic Engineering and Design*. 13 (1), 21–31. Available from: doi: 10.24867/JGED-2022-1-021

Risser, E., Shah, M. A. & Pattanaik, S. (2006) *Interval Mapping*. Available from: https://www.semantic-scholar.org/paper/Interval-Mapping-Risser-Shah/d16d9da41ec53b604e15976b0615ad3993c67ed-c#citing-papers [Accessed 20th September 2024].

Tatarchuk, N. & Natalya (2006) Practical parallax occlusion mapping with approximate soft shadows for detailed surface rendering. In: *ACM SIGGRAPH 2006 Courses, SIGGRAPH'06, 30 July – 3 August 2006, Boston, Massachusetts*. New York, Association for Computing Machinery. pp. 81-112. Available from: doi: 10.1145/1185657.1185830

Wald, I. & Parker, S. G. (2022) Data Parallel Path Tracing with Object Hierarchies. *Proceedings of the ACM on Computer Graphics and Interactive Techniques*. 5 (3). Available from: doi: 10.1145/3543861

Wald, I., Jaroš, M. & Zellmann, S. (2023) Data Parallel Multi-GPU Path Tracing using Ray Queue Cycling. *Computer Graphics Forum*. 42 (8). Available from: doi: 10.1111/CGF.14873

Wang, J. & Dana, K. J. (2005) Compression of View Dependent Displacement Maps. In: Chantler, M. and Drbohlav, O. (eds.) *Proceedings of the 4th International Workshop on Texture Analysis and Synthesis, Texture 2005, 21 October 2005, Beijing, China*. pp. 143–148.

Wang, L., Wang, X., Tong, X., Lin, S., Hu, S., Guo, B. & Shum, H.-Y. (2003) View-dependent displacement mapping. In: *ACM SIGGRAPH 2003 Papers, SIGGRAPH'03, 27-31 July 2003, San Diego, California*.

New York, Association for Computing Machinery. pp. 334-339. Available from: doi: 10.1145/1201775.882272

Wang, L., Zhang, W., Li, N., Zhang, B. & Popescu, V. (2017) Intermediate shadow maps for interactive many-light rendering. *The Visual Computer: International Journal of Computer Graphics*. 34 (10), 1415-1426. Available from: doi: 10.1007/s00371-017-1449-7

Wang, X., Tong, X., Lin, S., Hu, S., Guo, B. & Shum, H.-Y. (2004) Generalized displacement maps. In: *Proceedings of the Fifteenth Eurographics conference on Rendering Techniques, EGSR04, 21-23 June 2004, Norrköping, Sweden*. Goslar, The Eurographics Association. pp. 227–233. Available from: doi: 10.2312/egwr/egsr04/227-233

Welsh, T. (2004) *Parallax mapping with offset limiting: A per-pixel approximation of uneven surfaces*. Infiscape Corporation. Available from: https://page.mi.fu-berlin.de/block/htw-lehre/wise2015_2016/bel_und_rend/skripte/welsh2004.pdf [Accessed 20th September 2024].

Wen, H. (2023) A Novel Ray Tracing Method Based on Unity Scriptable Render Pipeline and DirectX Raytracing. In: *2023 15th International Conference on Computer Research and Development, ICCRD, 10-12 January 2023, Hangzhou, China*. Piscataway, IEEE. pp. 156–160. Available from: doi: 10.1109/ICCRD56364.2023.10079997

Wu, C., Xia, Y., Xu, Z., Liu, L., Tang, X., Chen, Q. & Xu, F. (2024) Mathematical modelling for high precision ray tracing in optical design. *Applied Mathematical Modelling*. 128, 103–122. Available from: doi: 10.1016/j.apm.2024.01.012

Yang, M. & Jia, J. (2023) Implementation and Optimization of Hardware-Universal Ray-tracing Underlying Algorithm Based on GPU Programming. In: *2023 6th International Conference on Artificial Intelligence and Big Data, ICAIBD, 26-29 May 2023, Chengdu, China*. Piscataway, IEEE. pp. 171-178. Available from: doi: 10.1109/ICAIBD57115.2023.10206260

Yerex, K. & Jagersand, M. (2004) Displacement Mapping with Ray-casting in Hardware. In: Barzel, R. (ed.) *ACM Siggraph 2004 Sketches, SIGGRAPH'04, 8-12 August 2004, Los Angeles, California*. New York, Association for Computing Machinery. p. 149. Available from: doi: 10.1145/1186223.1186410

Zellmann, S., Wald, I., Barbosa, J., Dermici, S., Sahistan, A. & Güdükbay, U. (2022) Hybrid Image-/Data-Parallel Rendering Using Island Parallelism. In: *Proceedings - 2022 IEEE 12th Symposium on Large Data Analysis and Visualization, LDAV, 16 October 2022, Oklahoma City, Oklahoma*. Piscataway, IEEE. Available from: doi: 10.1109/LDAV57265.2022.9966396